The application of Free Electron Lasers to Biology: Playing with retinal proteins and GPCRs

Wir schaffen Wissen – heute für morgen

Gebhard F. X. Schertler

Head of Biology and Chemistry Department PSI
Professor for Structural Biology ETH Zürich
Laboratory of Biomolecular Research
Switzerland

Biology is Dynamic and has many Time Domains

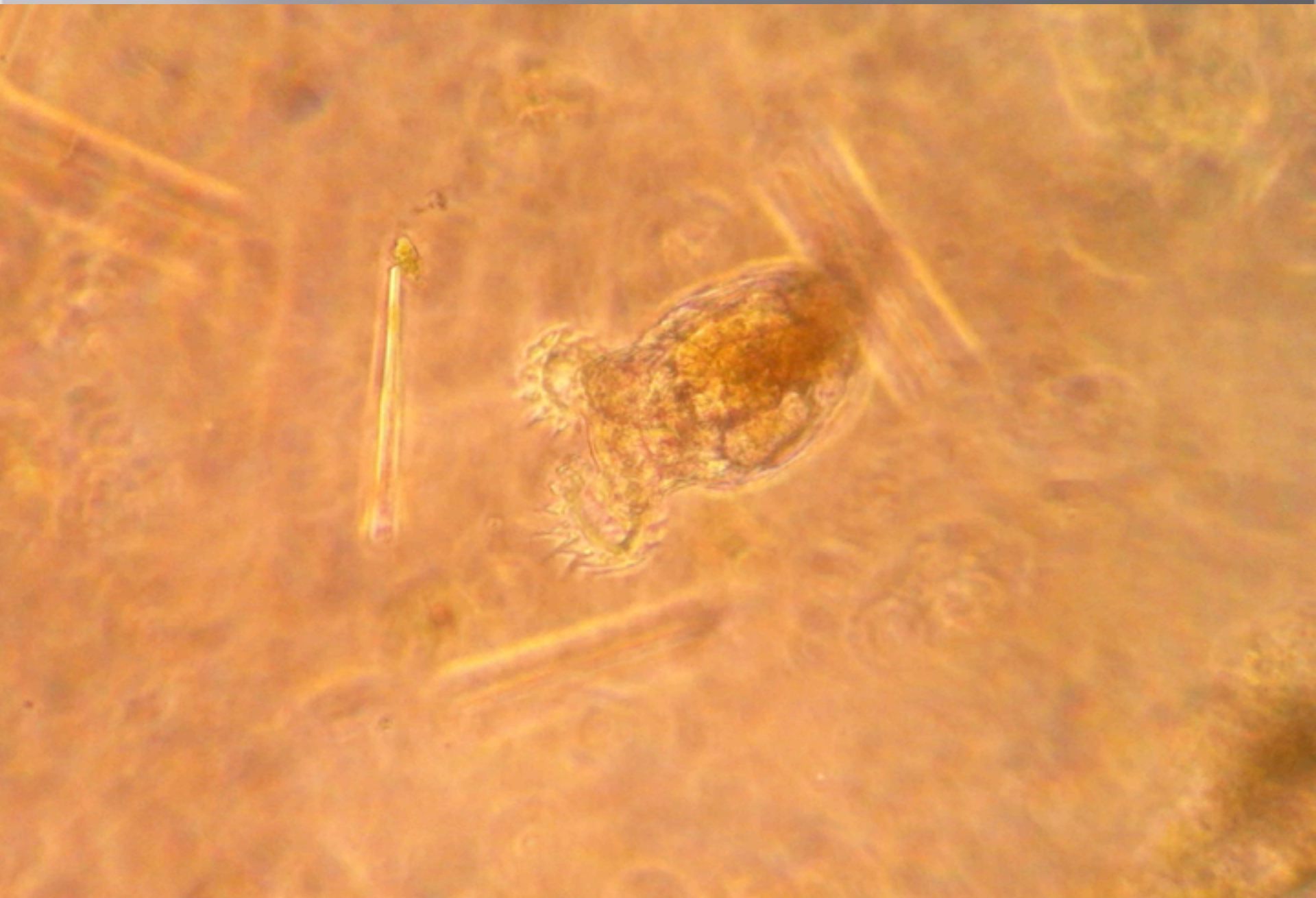

Dynamic X-ray tomography of a flying fly

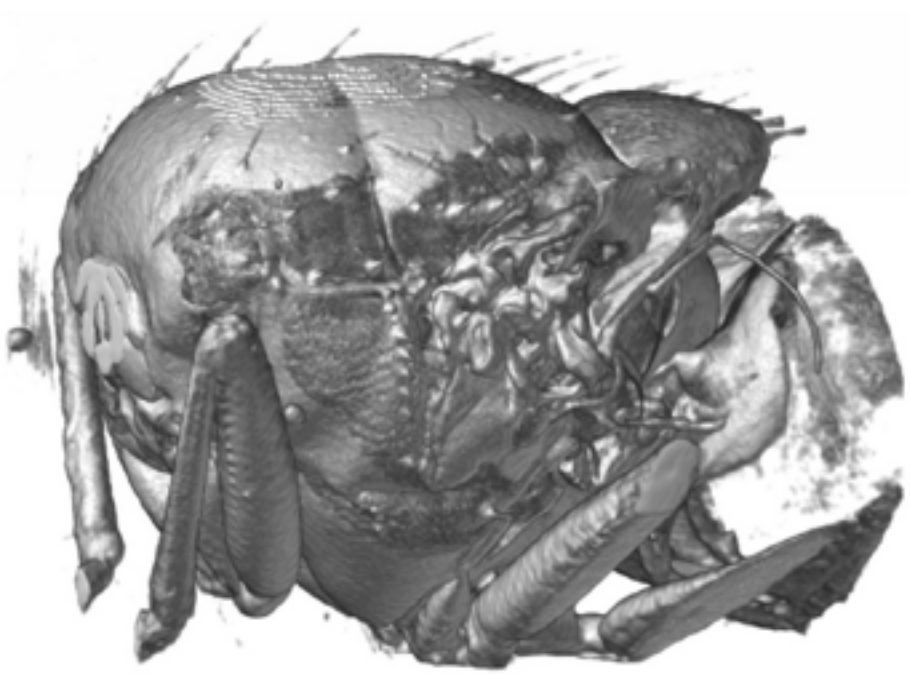

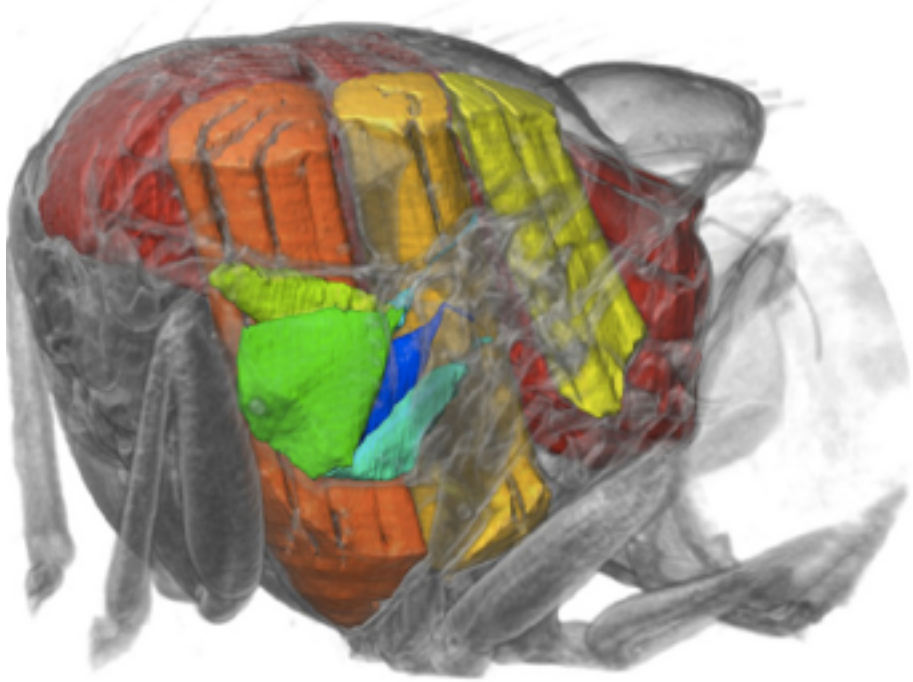

Dynamic image of a Flying insect in real time recorded

No sectioning no complicated sample manipulation!!

http://youtu.be/P6lBkK3J9wg

Time domains in Biology

Evolution million of years

Human life cycle 80 years

Circadian day night rhythm one day

Cell division hours

Enzyme activation milliseconds

Protein motion conformational change microseconds

Formation of early photoproduct in vision picoseconds

Retinal isomerization femtoseconds

Photon capture, orbital rearrangements attoseconds

PSI solves relevant Membrane Protein Structures

Understanding Drug Action in G-Protein Coupled Receptors: GPCRs

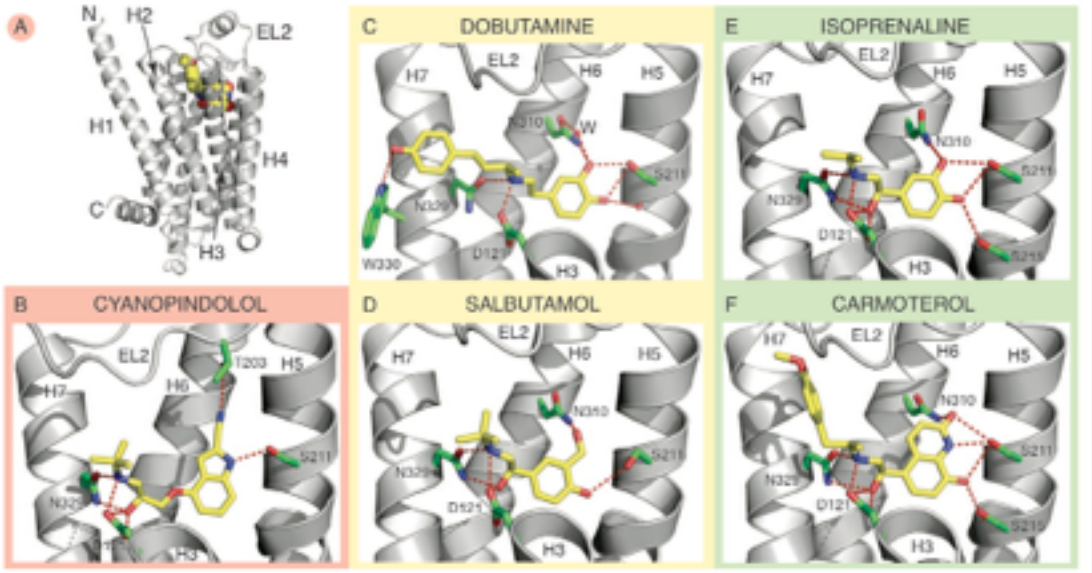

Agonists and Antagonists in
Adrenergic Receptor
Nature ***469, 241-244*** 2011

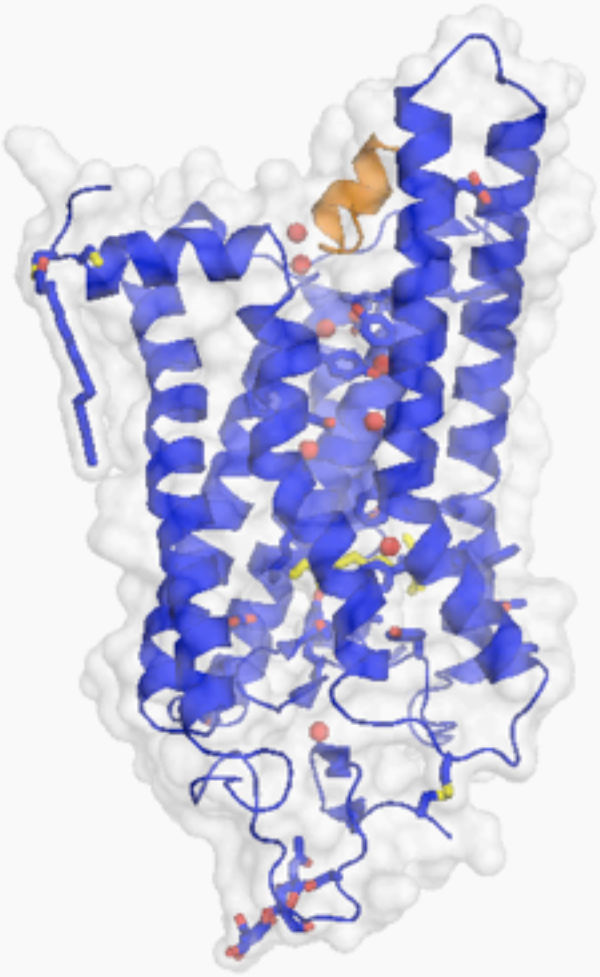

Visual Pigment Rhodopsin
Fully Active Conformation
Nature ***471, 656-660*** 2011

Paul Scherrer Institute PSI

Membrane proteins are key drug targets

EMBL-EBI | All Databases | Enter Text Here | Go | Reset | Advanced Search | Give us feedback

Databases | Tools | EBI Groups | Training | Industry | About Us | Help | Site Index

- Home
- local help
- Integr8 News
- Focal Point archive
- Latest Species
- Browse Species
- H.sapiens
  - Literature
  - Genome Statistics
  - Proteome Analysis
  - Downloads
  - Taxonomy
- Inquisitor
  - status
- BioMart
- Proteomes and Genomes FASTA
- About Integr8
- Publications
- Integr8 Web service

Genome Reviews

Curated versions of EMBL entries for complete genome sequences

IPI

A top-level guide to the main databases that describing higher eukaryotic proteomes

EBI › Databases › Integr8

Integr8 : Proteome analysis:

Search for species | Go! | Search for gene/protein | in H.sapiens | Go!

Selected species *H.sapiens* Change scope

InterPro | Comparative | CluSTr | GO | Structure

Select analysis: 15 most common families

InterPro

15 most common families for H.sapiens

InterPro	Proteins matched	Name
IPR000276	848	GPCR, rhodopsin-like
IPR017452	842	GPCR, rhodopsin-like superfamily
IPR000725	532	Olfactory receptor
IPR001806	169	
IPR013753	127	
IPR007114	105	
IPR001664	88	
IPR011701	86	
IPR001128	76	
IPR000832	69	
IPR002494	64	
IPR002198	64	
IPR003579	63	
IPR004000	59	
IPR001993	59	

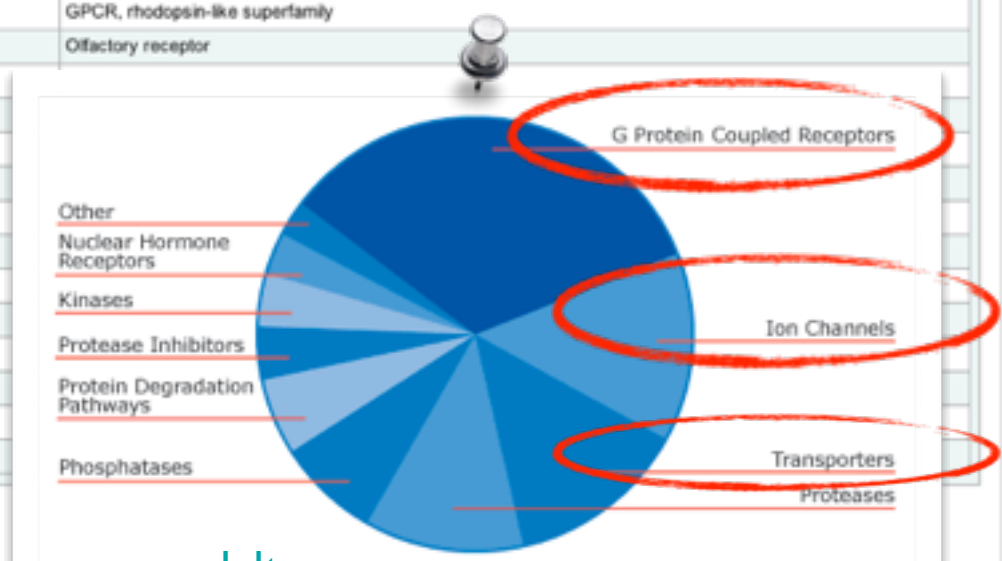

www.deltagen.com

G-ProteinCoupled Receptors GPCRs

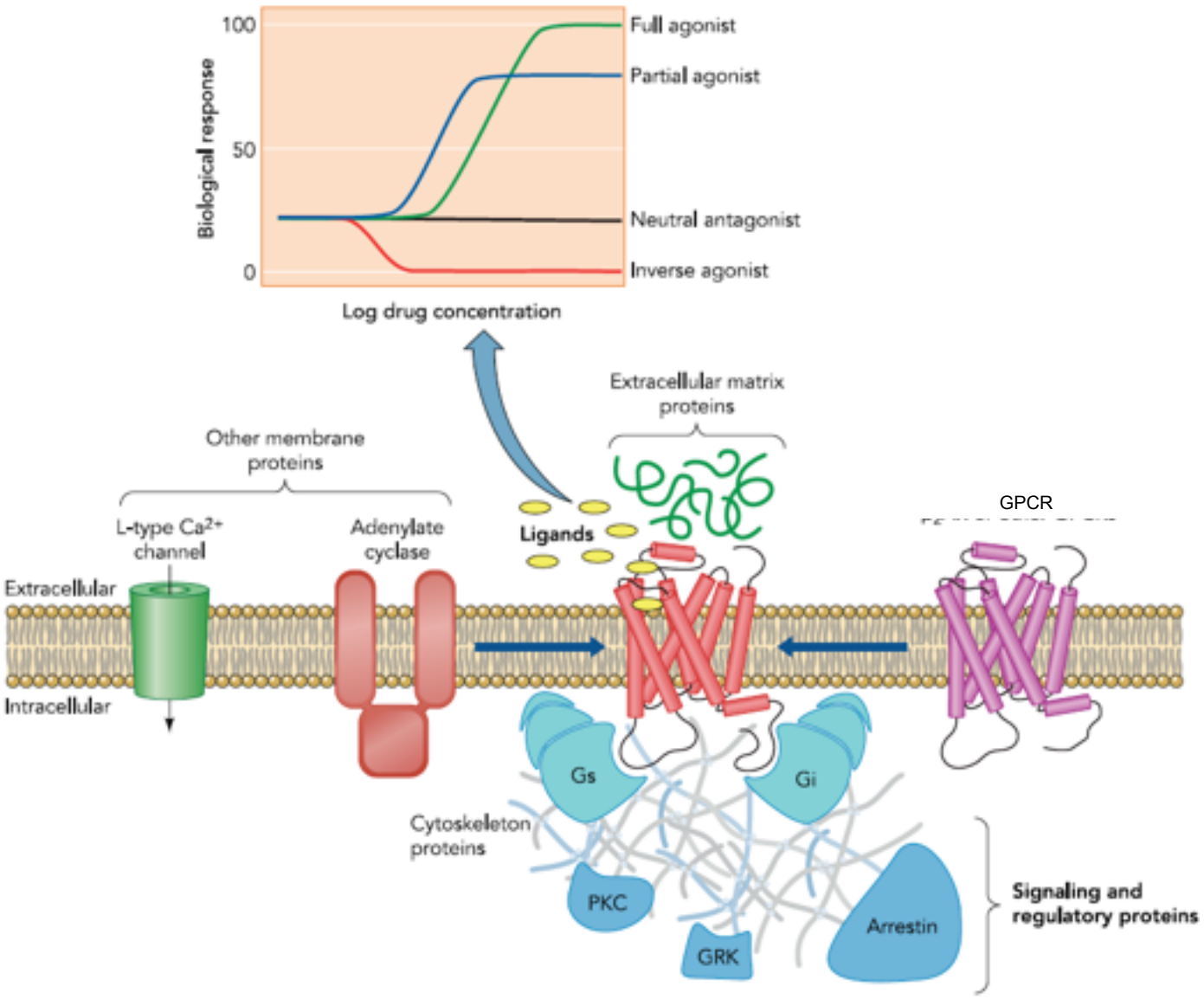

Deupi & Kobilka, 2010

Timeline of GPCR structures

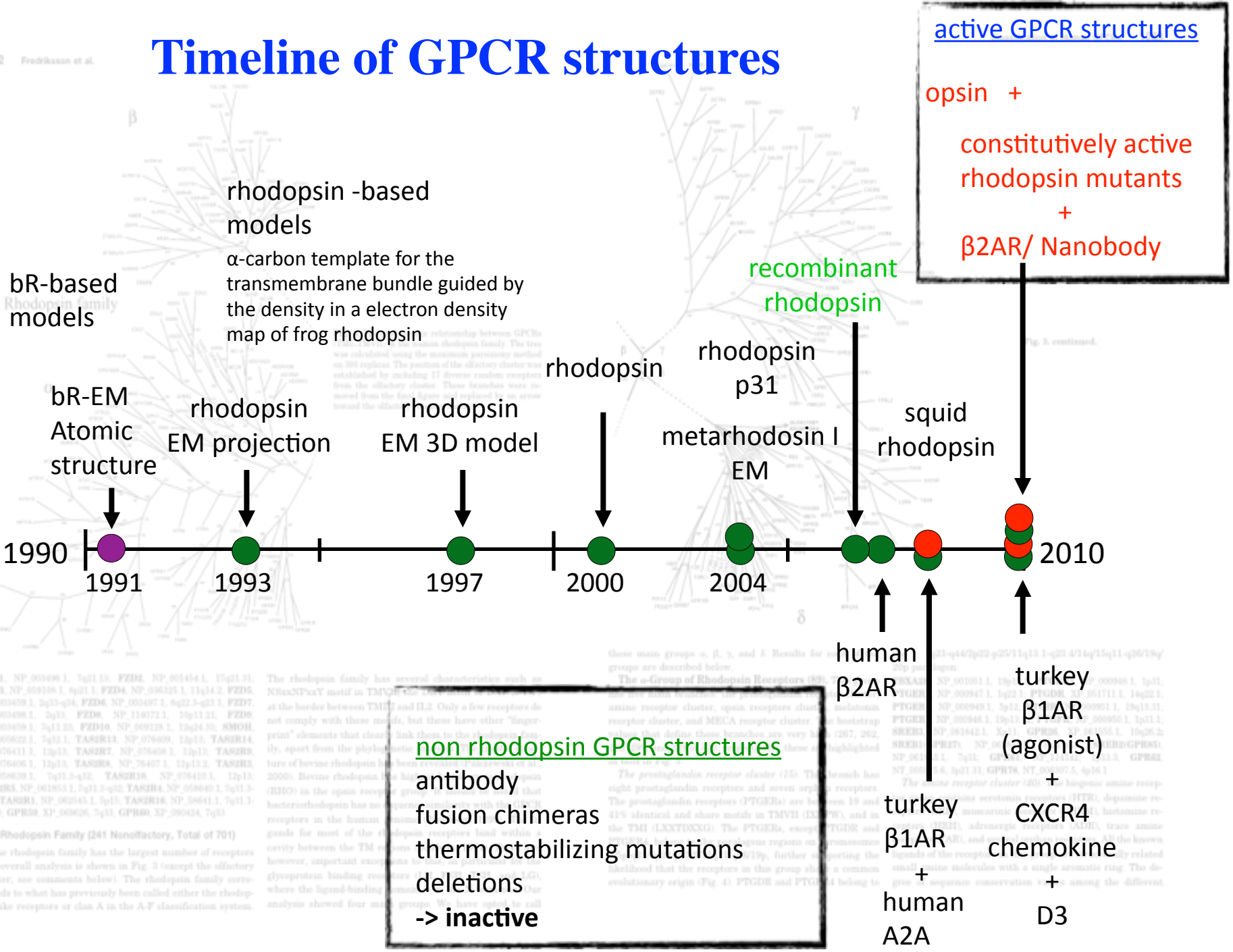

Receptor can be stabilised in a ground state and active conformations

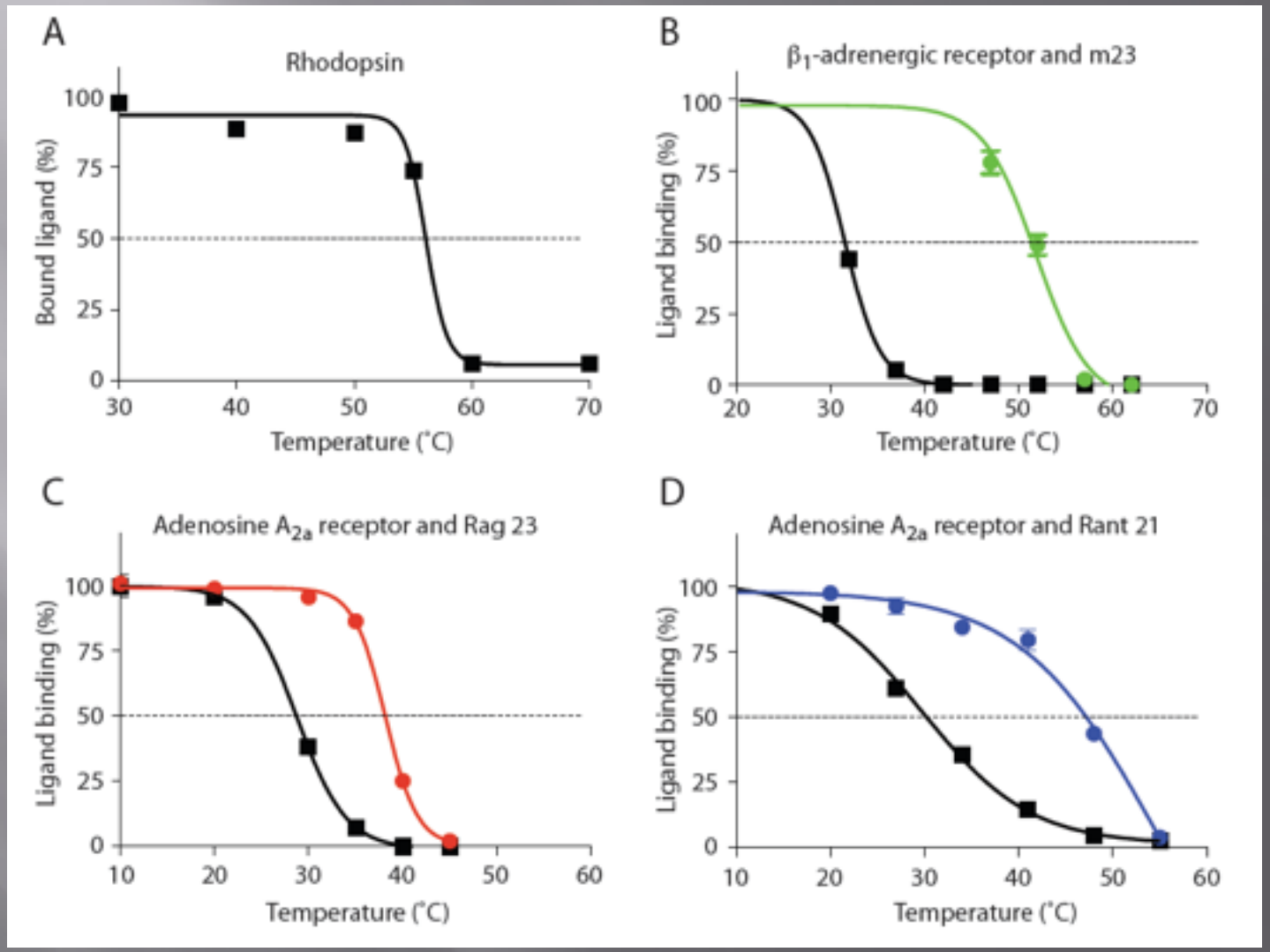

Micro crystallography data collection beta 1 adrenergic receptor

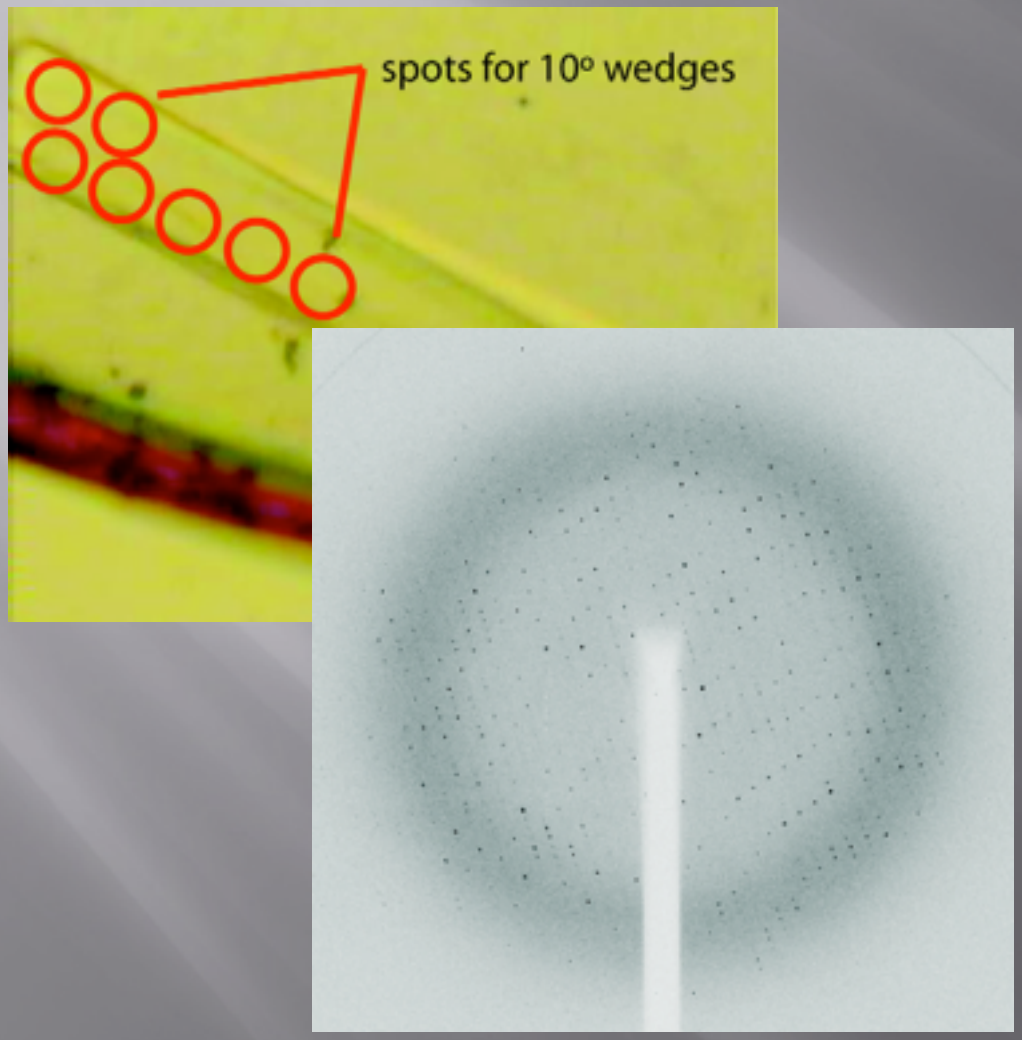

Relatively long exposures

Narrow wedges (10º)

1º oscillations

Recording from good positions only

At least 18 wedges (180º of data for 100% completeness due to monoclinic space group)

Diffraction quality over crystal very variable !!

Extended Arginine Rotamer Stabilised by Conserved Tyrosine in Helix 5

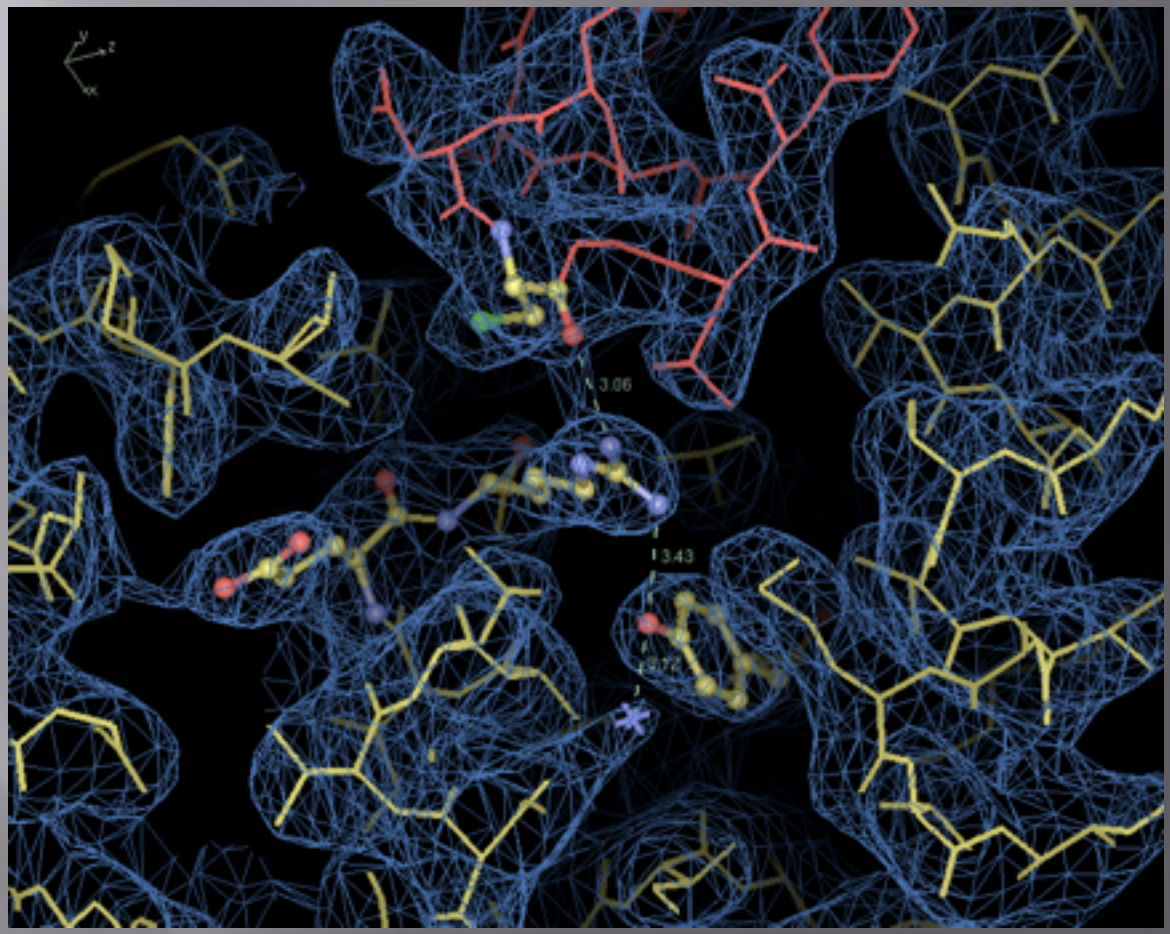

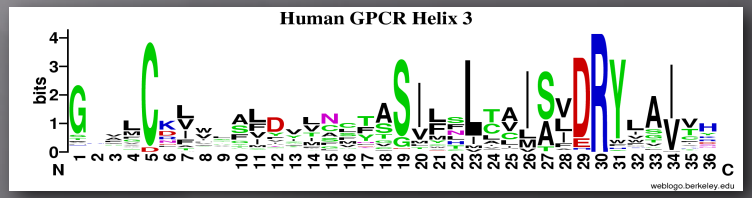

E 113Q Standfuss, Oprian and Schertler Nature 2011

How does a ligand bind to a GPCR?

Structure of stabilized beta 1 adrenergic receptor

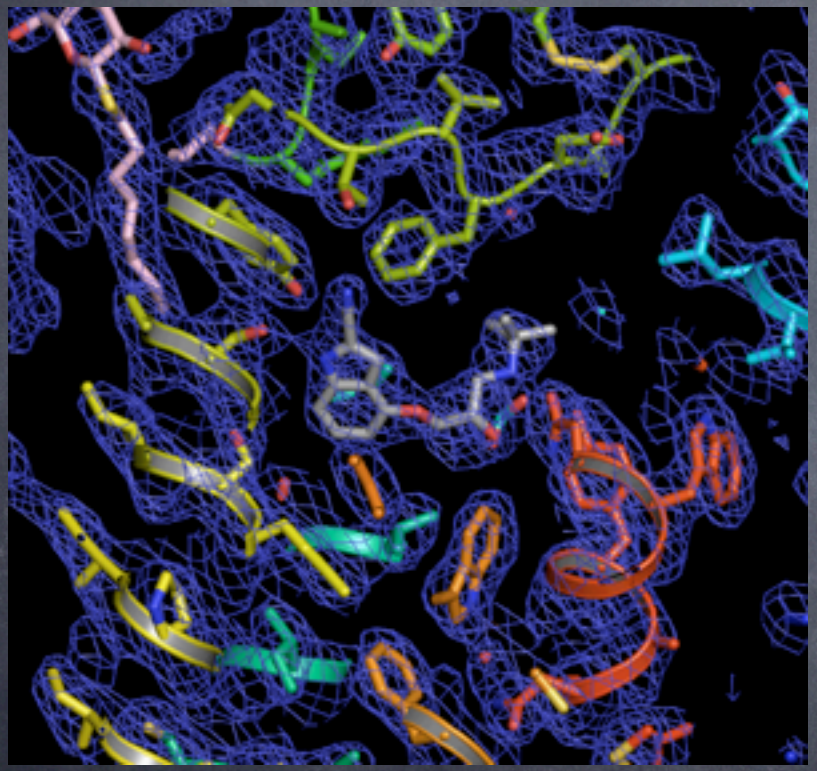

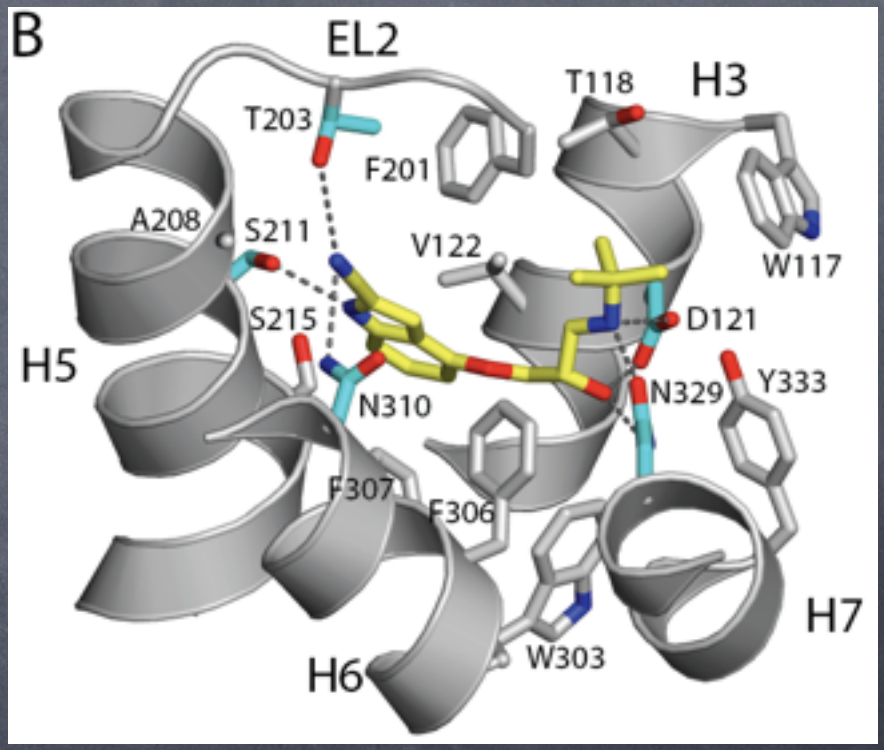

Warene, Tate and Schertler Nature 2008

Beta1 Adrenergic Receptor
C3 deletions and stabilising mutations

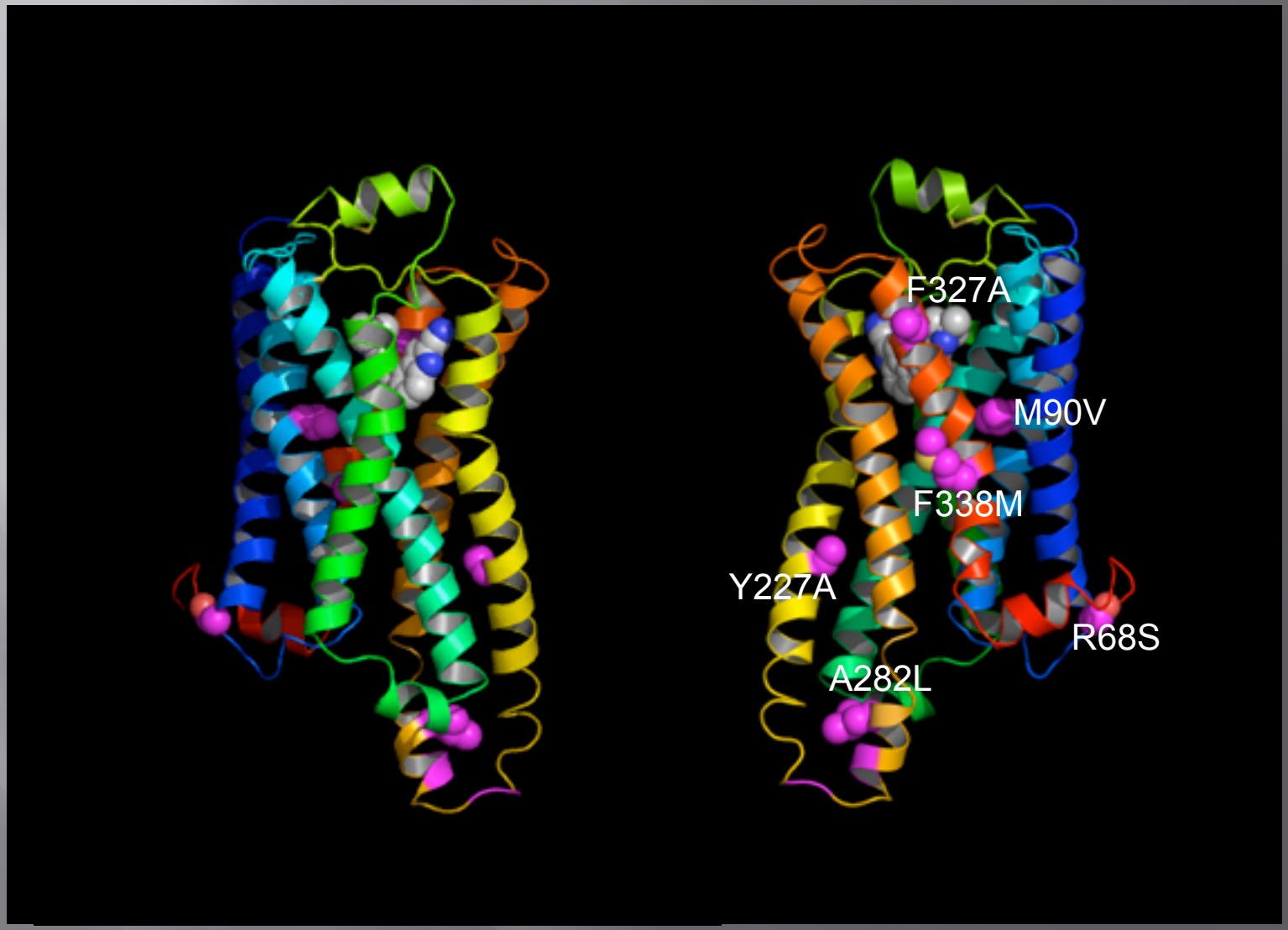

Moukhametzianov and Schertler PNAS 2011

A framework for G Protien Coupled Receptor signaling

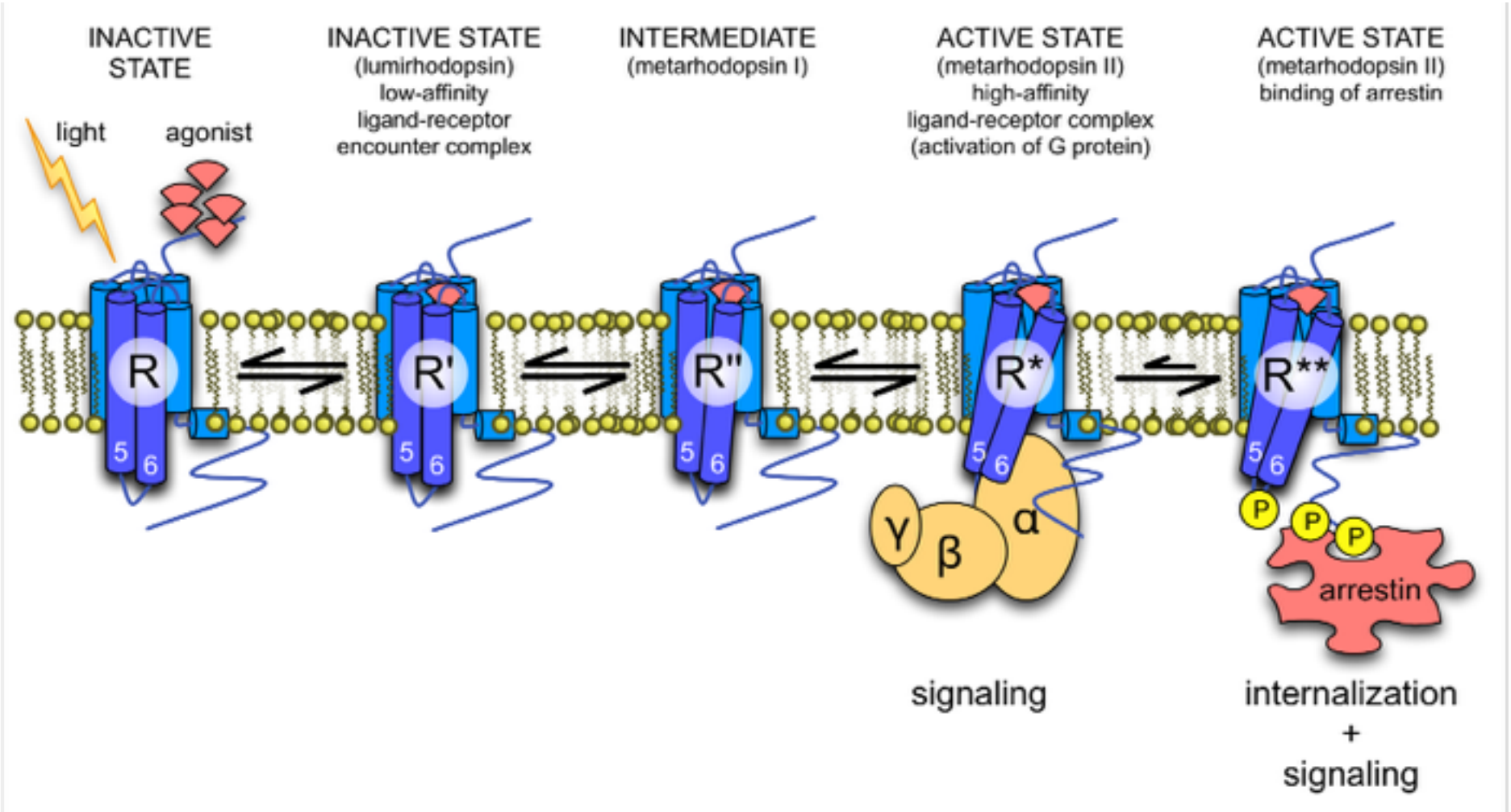

Deupi & Standfuss, *Curr. Opin. Struct. Biol.*, 2011

Mammalian visual system

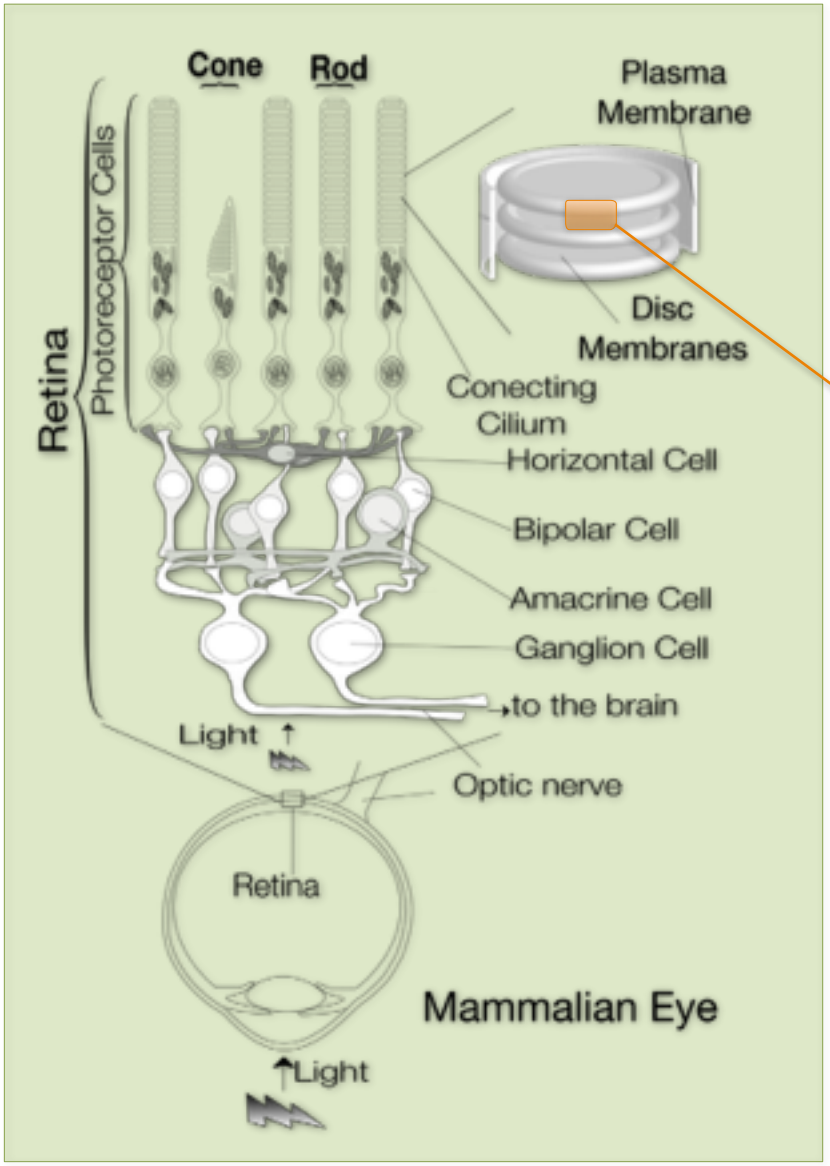

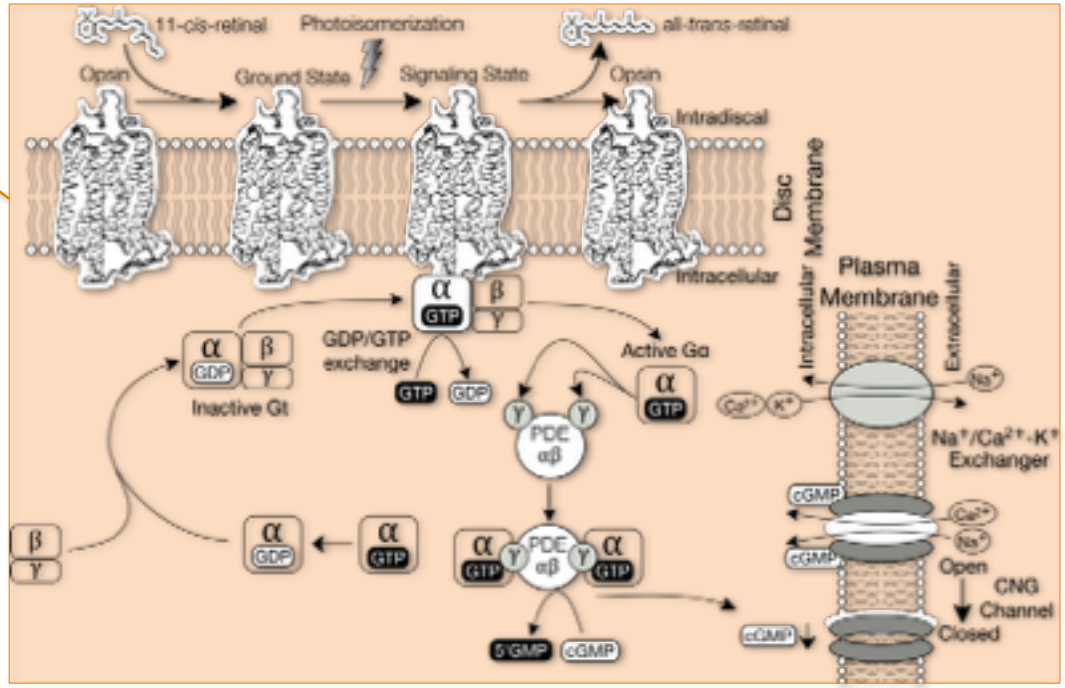

Large scale expression using HEK293 cells in a wave bag bioreactor

Wave bag bioreactor

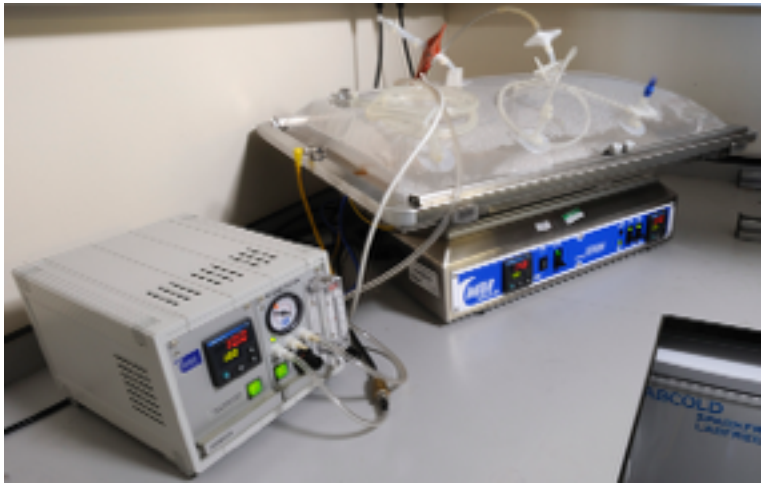

Growth curve

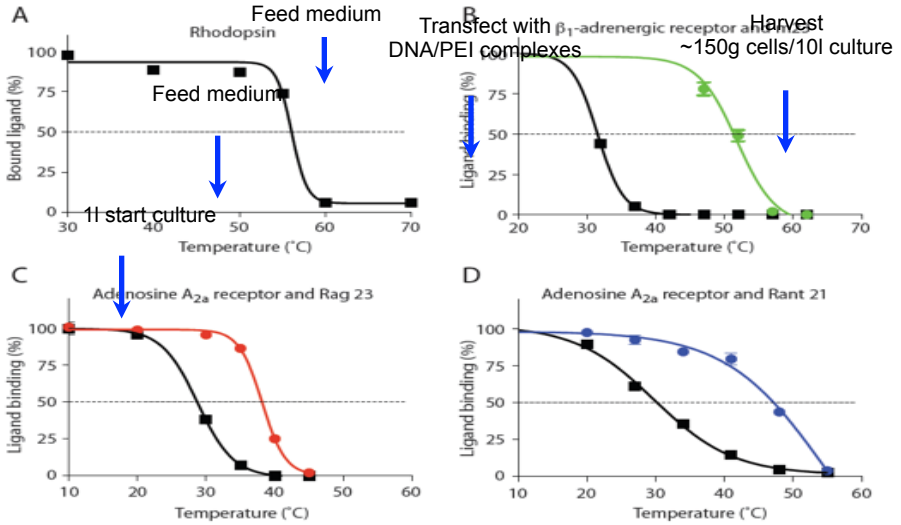

Effect of GnTI⁻ cells

Typical yields from 10l suspension culture:

Transient transfection:
4-5 mg

Stable Tetracycline inducible cell line:
7-8 mg

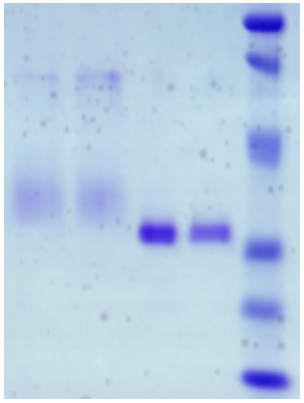

Free Style GnTI⁻

Purification of recombinant rhodopsin

- Expression in HEK293 GnTI- cells
- Solubilization of cell membranes
- Immuno affinity purification and reconstitution with retinal
- Gelfiltration to exchange detergent and remove residual retinal

Elution profile

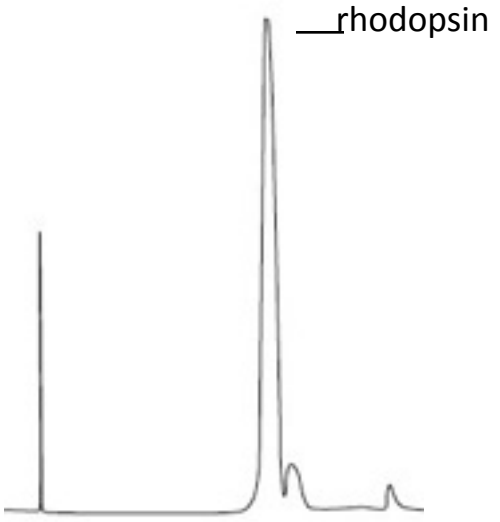

SDS-PAGE

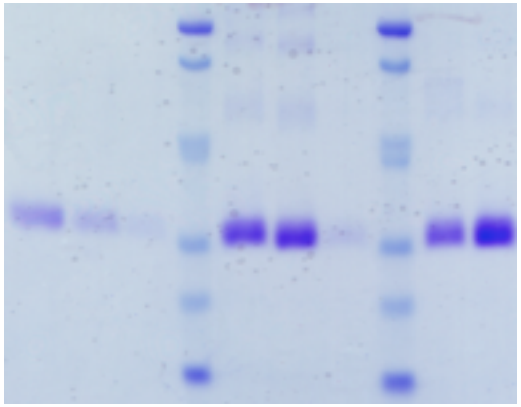

UV/Vis Spectrum

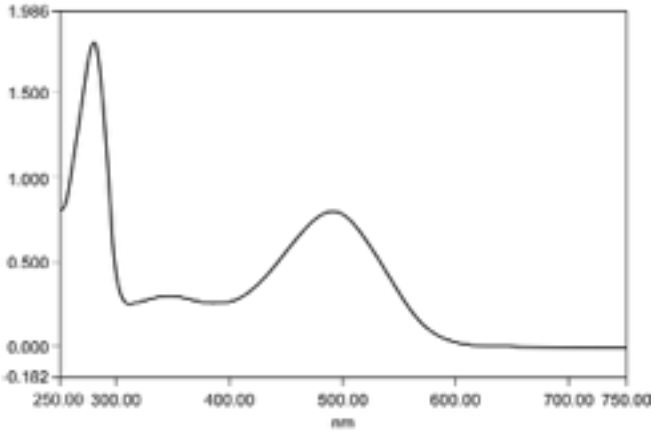

G protein activation

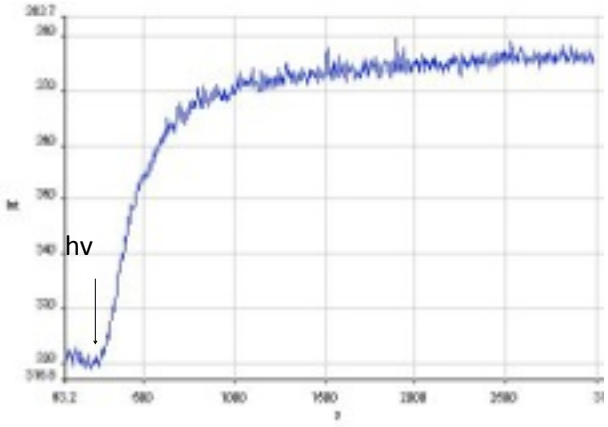

First structure of a recombinant GPCR

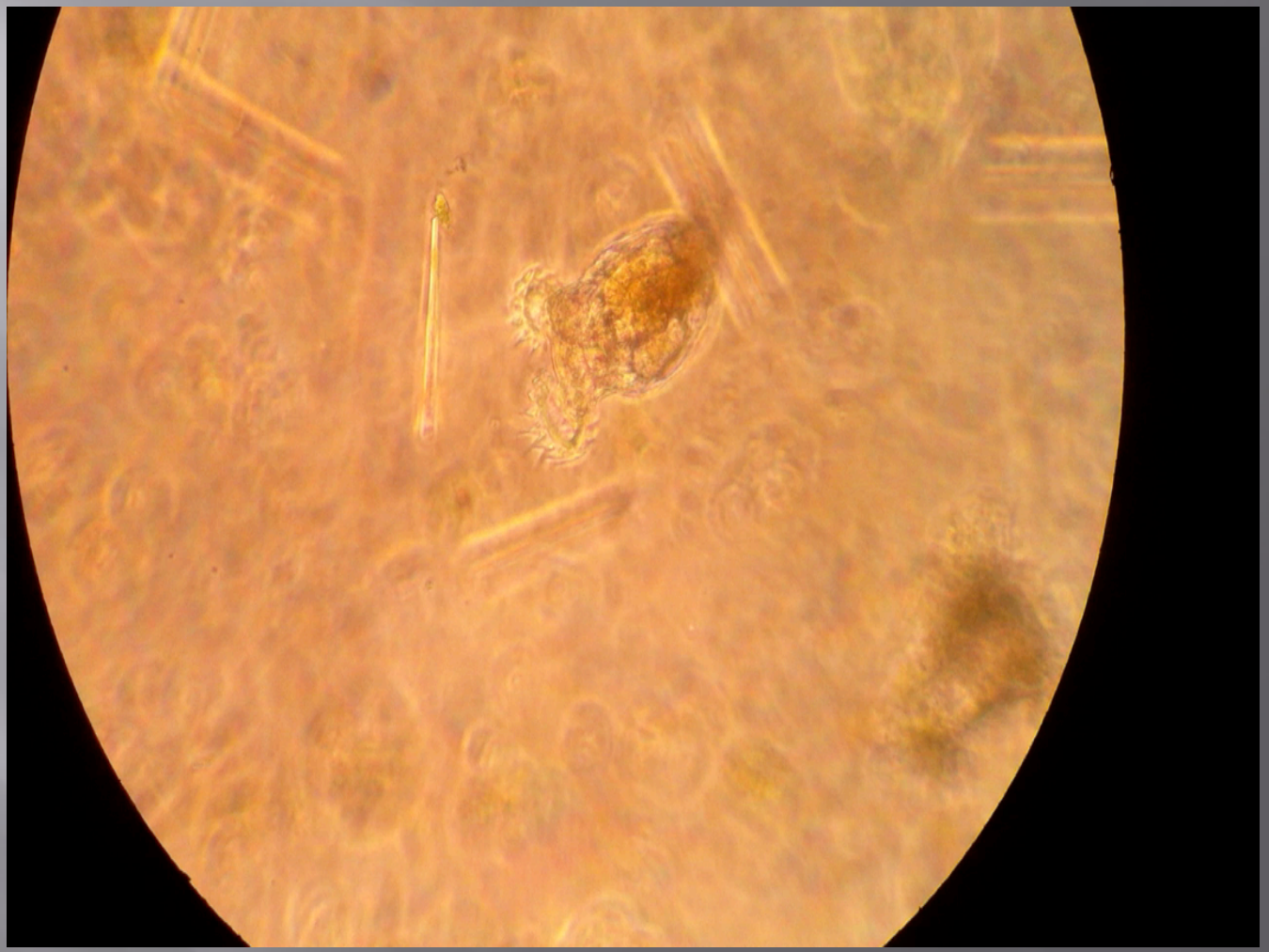

Opsin stabilising disulphide bond fixes the N-terminal Cap over the Lid

Standfuss et al JMB 2007

The constitutively active mutantS M257Y and E113Q

	Opsin (%)	all-*trans*	11-*cis*/light
Wt	1	14	100
M257L	1	17	112
M257A	10	112	102
E113A	21	58	100
M257N	23	93	72
E113Q	23	111	97
M257Y	**33**	**98**	**101**

Strongest known constitutively active single mutations

E113Q Removes the counterion and restraining salt bridge

M257Y Modifies the hydrophobic barrier between the retinal binding site and the ionic lock region

Activation data taken from Han & Sakmar, 2000

M257Y rhodopsin contains all-*trans* retinal covalently bound as in active Rhodopsin: Meta-rhodopsin II

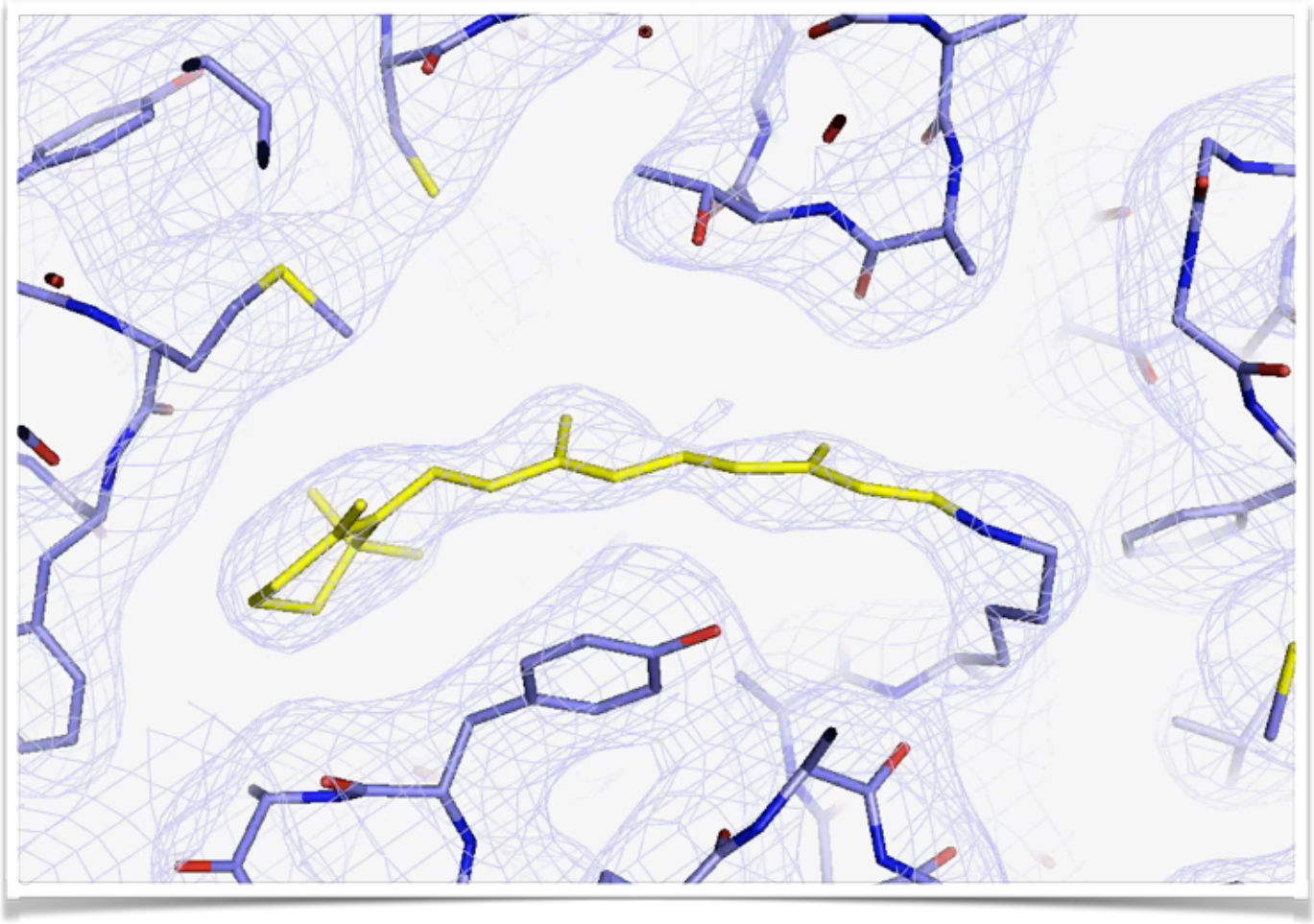

Deupi *et al., Proc. Natl. Acad. Sci.*, 2012

GPCR Activation: Rhodopsin

Retinal and CWxP

NPxxY

E(D)RY

GαCT

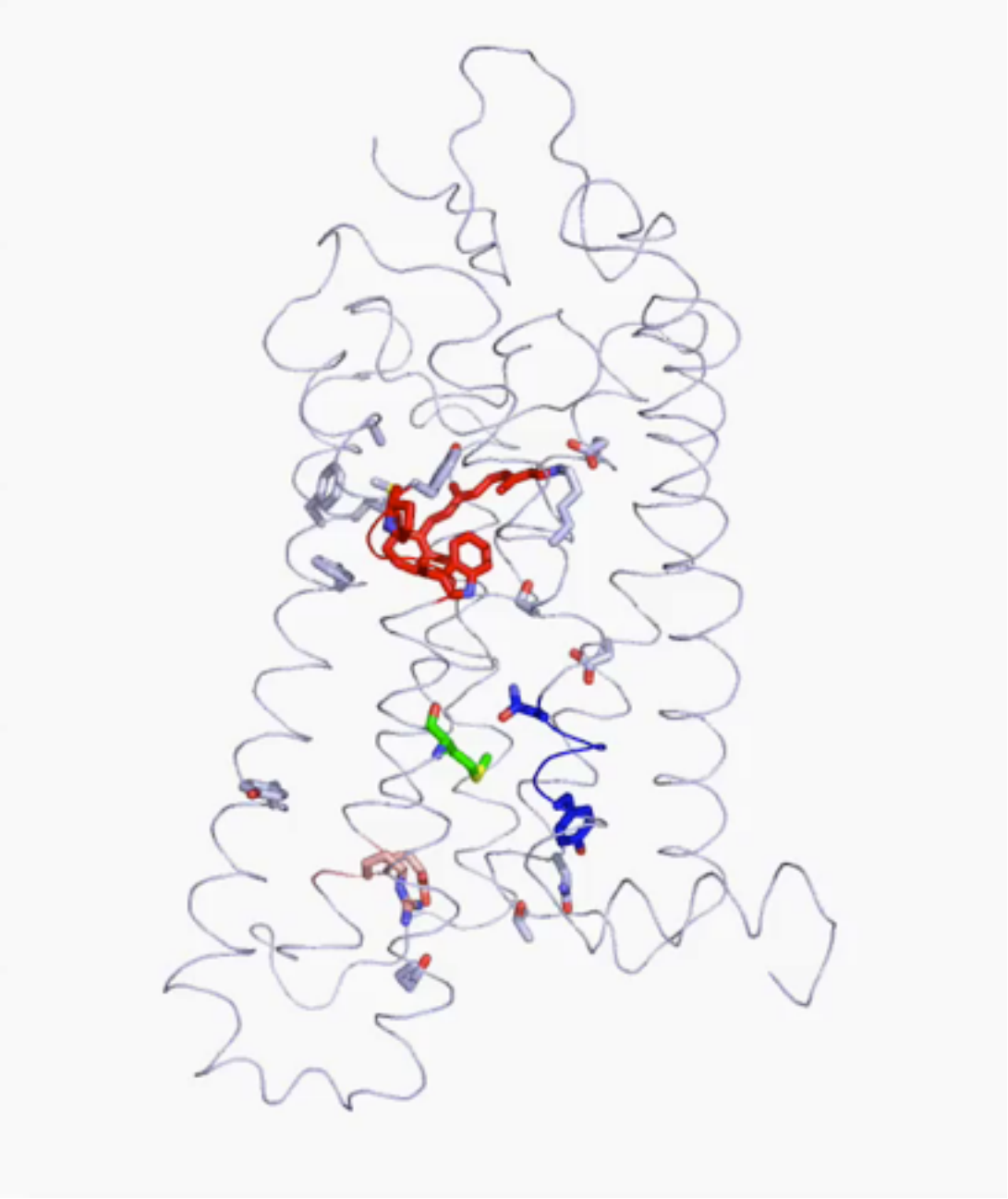

A structural basis for hereditary blindness

Normal Vision

Retinitis Pigmentosa (RP)

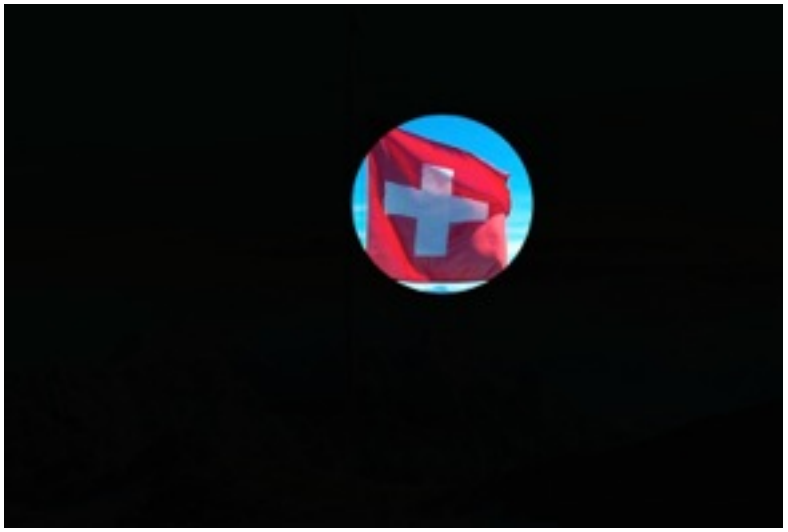

Retinitis pigmentosa (RP) is a hereditary disease leading to initial night blindness with slow progression towards complete loss of sight

- Occurrence 1:4000 at birth
- Rho gene disease origin for 25% of RP patients
- 90% of mutations are misfolding mutations
- Four mutations result in a non-progressive night blindness phenotype (CSNB)
- Oral application of small molecules (Vitamin A plamitate, Safranal) reduces retina degeneration in mice and human RP patients

Ankita Singhal

Insights into congenital stationary night blindness based on the structure of active G90D rhodopsin

Ankita Singhal[1], Martin K. Ostermaier[1], Sergey A. Vishnivetskiy[2], Valérie Panneels[1], Kristoff T. Homan[3], John J. G. Tesmer[3], Dmitry Veprintsev[1], Xavier Deupi[1,4], Vsevolod V. Gurevich[2], Gebhard F.X. Schertler[1,5] and Joerg Standfuss[1,*]

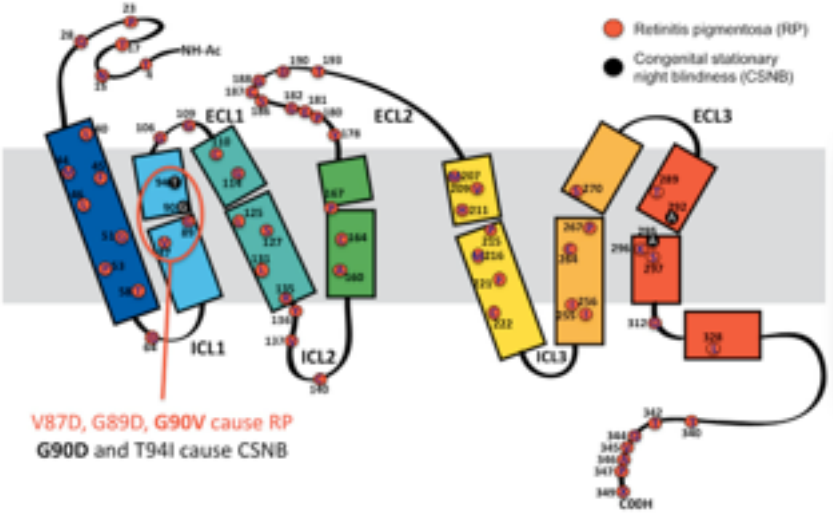

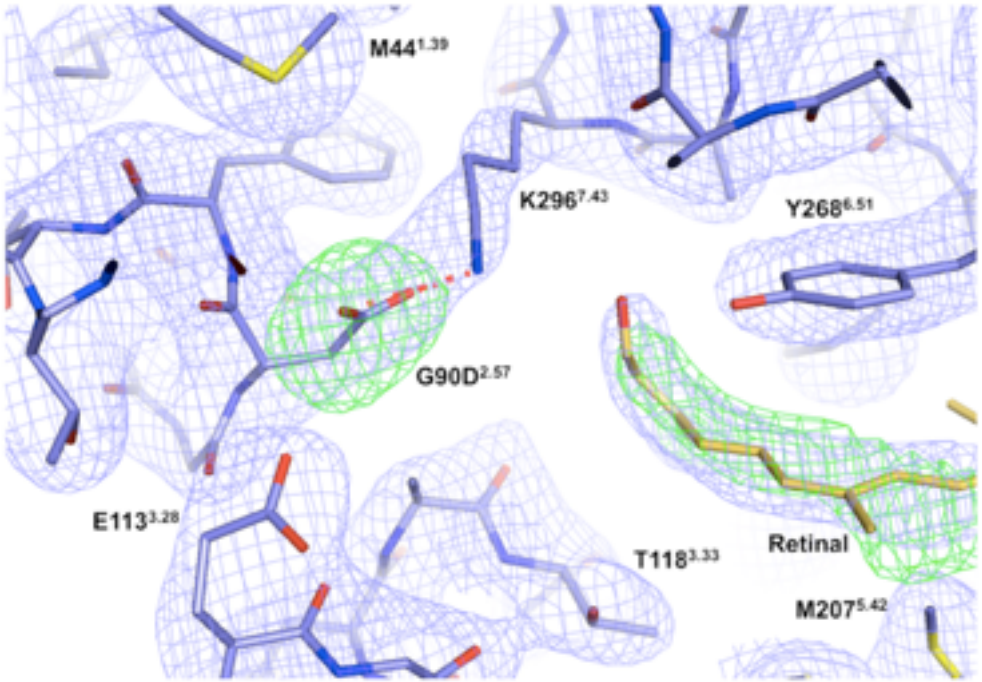

Singhal *et al., EMBO Rep. 2013*

ACTIVE GPCR WITH AGONIST

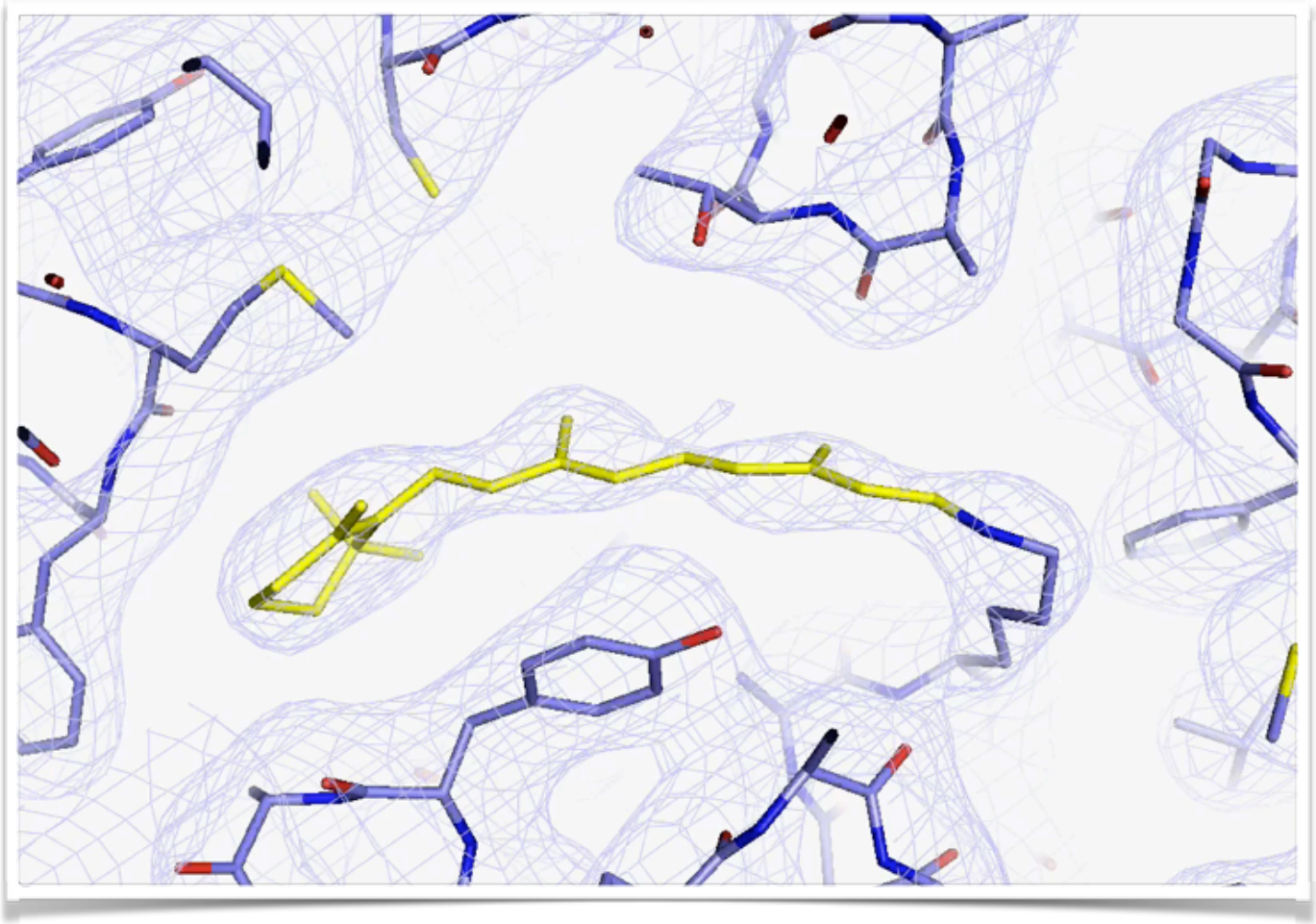

Deupi *et al., Proc. Natl. Acad. Sci.*, 2012

The catalytic step in vision

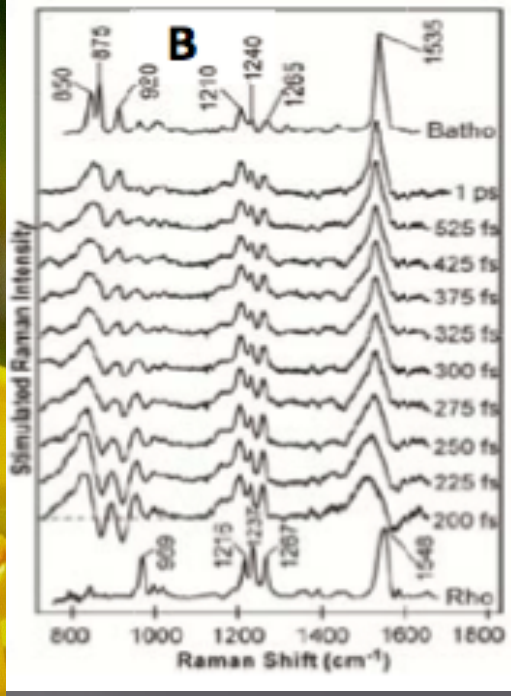

- The quantum yield and stereo selectivity
- is decided in 200 femtoseconds!!!

Paul Sherrer Institue PSI

- Neutronen Quelle PSI
- Synchrotron PSI
- Swiss FEL PSI
- Protonen Therapie PSI
- Biologie und Chemie Department PSI

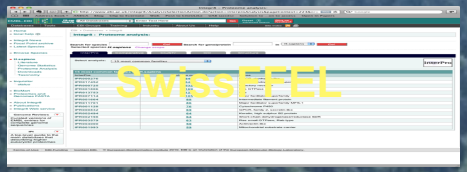

Grossanlagen der Schweiz
Paul Scherrer Institute
PSI

SwissFEL under construction

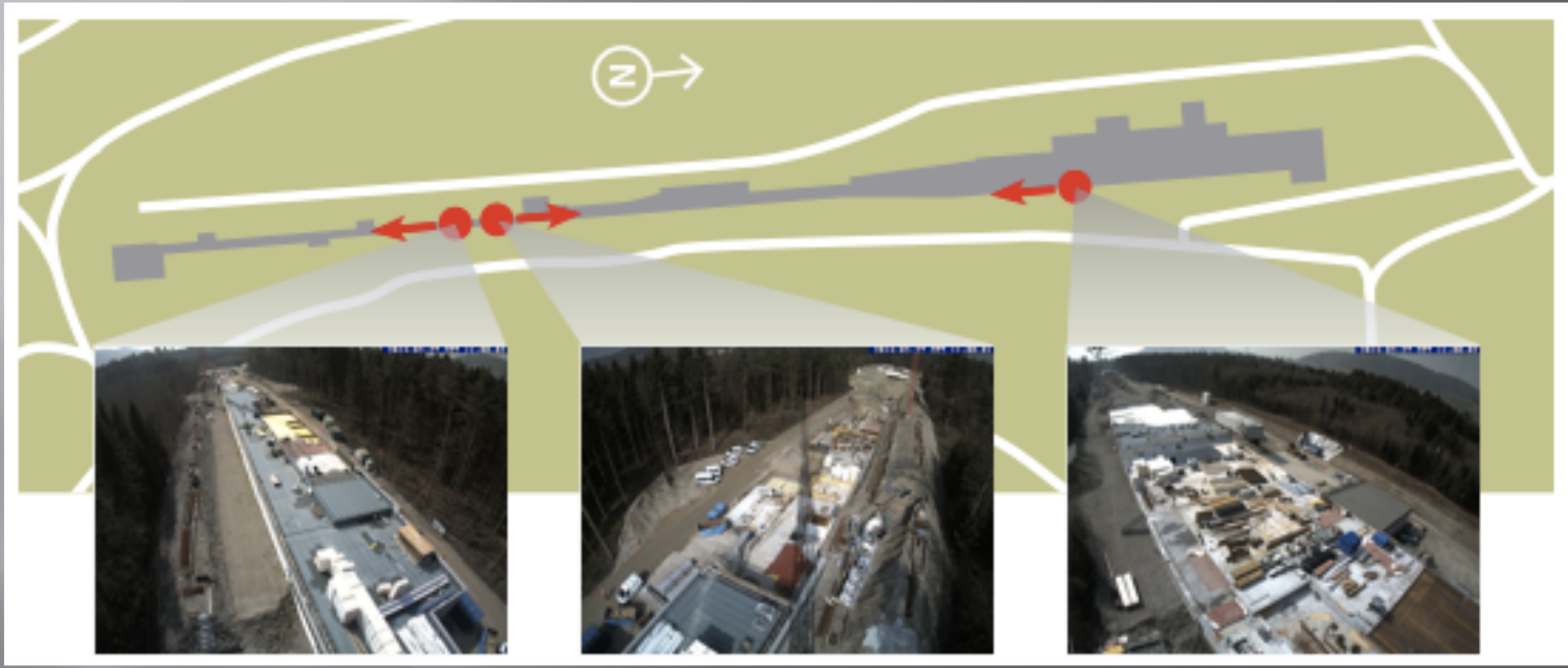

The development of X-ray sources

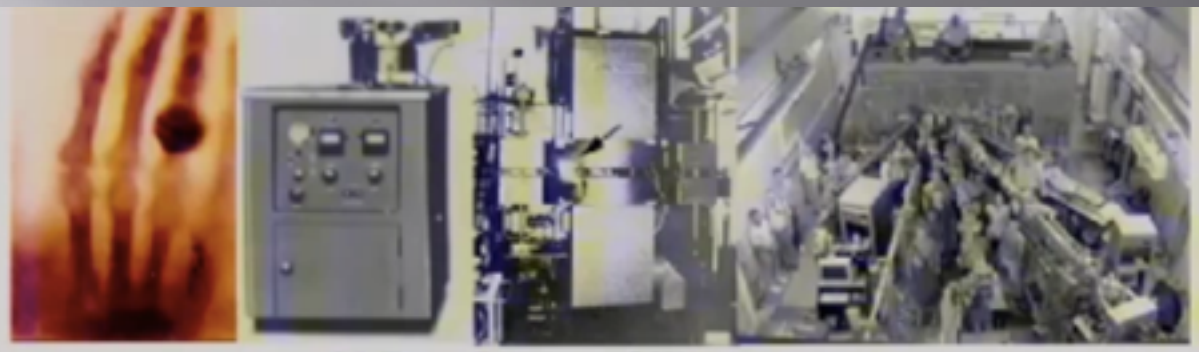

PAUL SCHERRER INSTITUT PSI

X-Ray Source Milestones

1895	Röntgen (Würzburg)
1953	Rotating-anode (Rigaku)
1947	Synchrotron radiation (GE)
1961	1st generation synchrotron (NBS) - parasitic
1981	2nd gen. (Daresbury) - dedicated to SR
1984	3rd gen. (Grenoble) - undulators
2001	3rd+ gen. (SLS, Villigen) - high-brightness
2009	4th gen. (Stanford) - X-ray Free Electron Laser

Taken from Bruce Patterson's presentation at EMPA
on the SwissFEL project

The development of X-ray sources

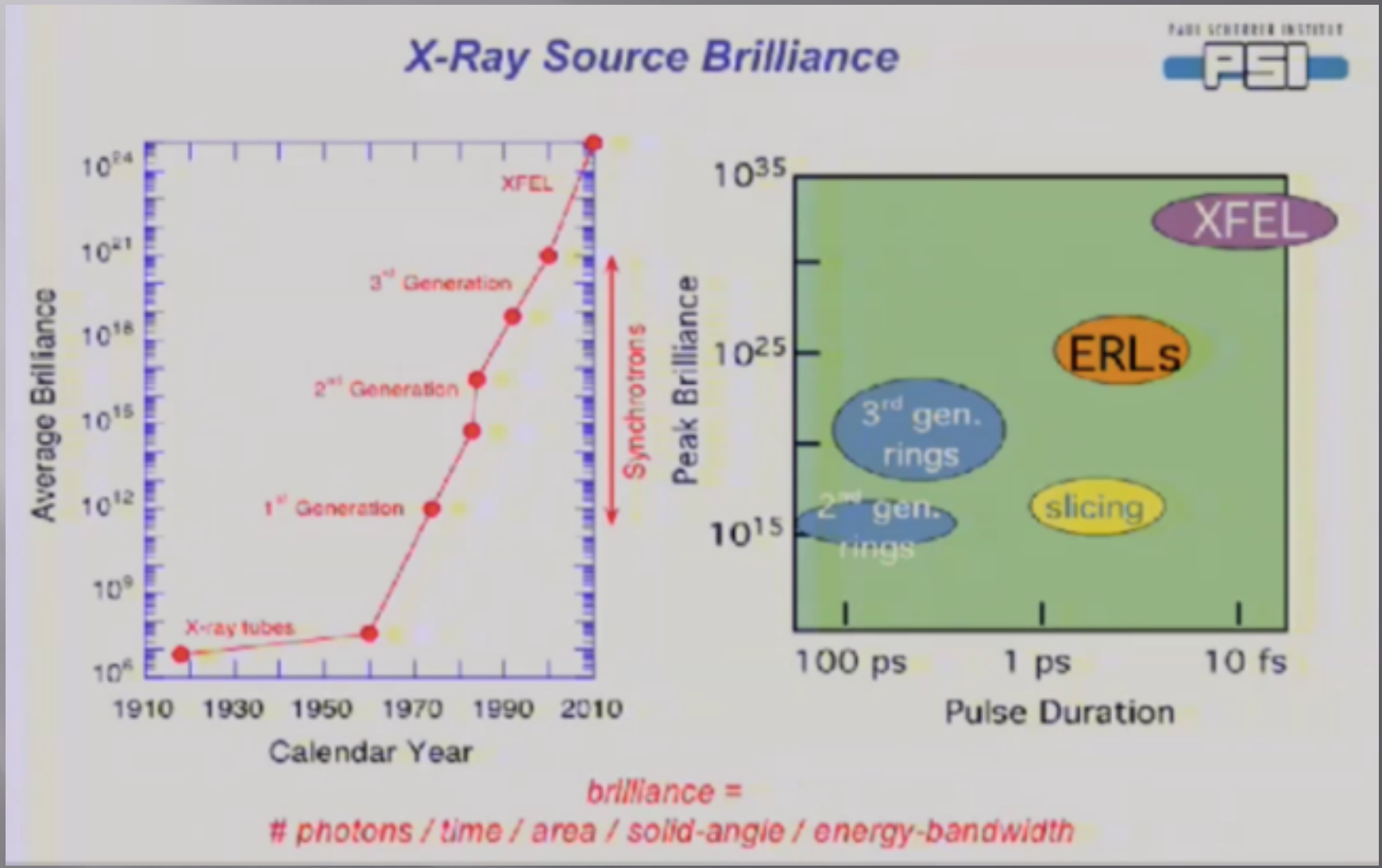

Taken from Bruce Patterson's presentation at EMPA
on the SwissFEL project

SwissFEL – A Scientific Opportunity

Synchrotron-Light

detailed, but too slow

Optical Laser-Light

very fast, but no spacial detail

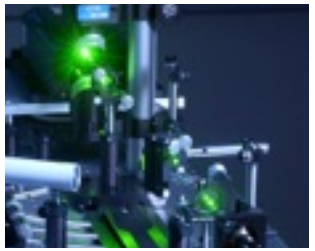

SwissFEL

detailed and fast and extremely intense

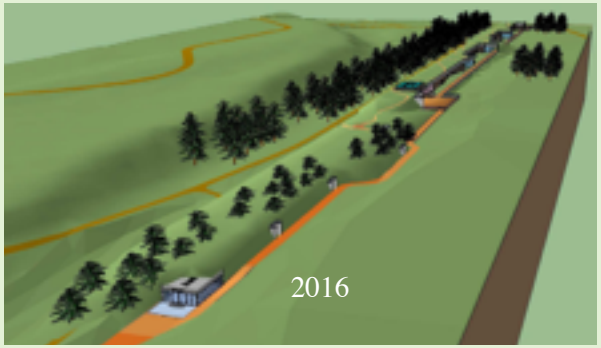

A free Electron Laser for Switzerland and Science

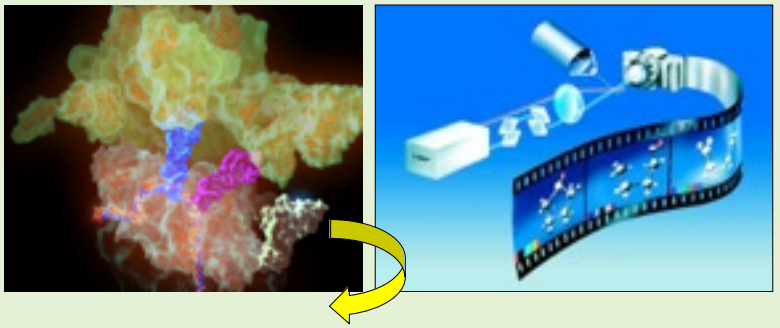

New and dynamic insight into matter:

With a X-ray video camera

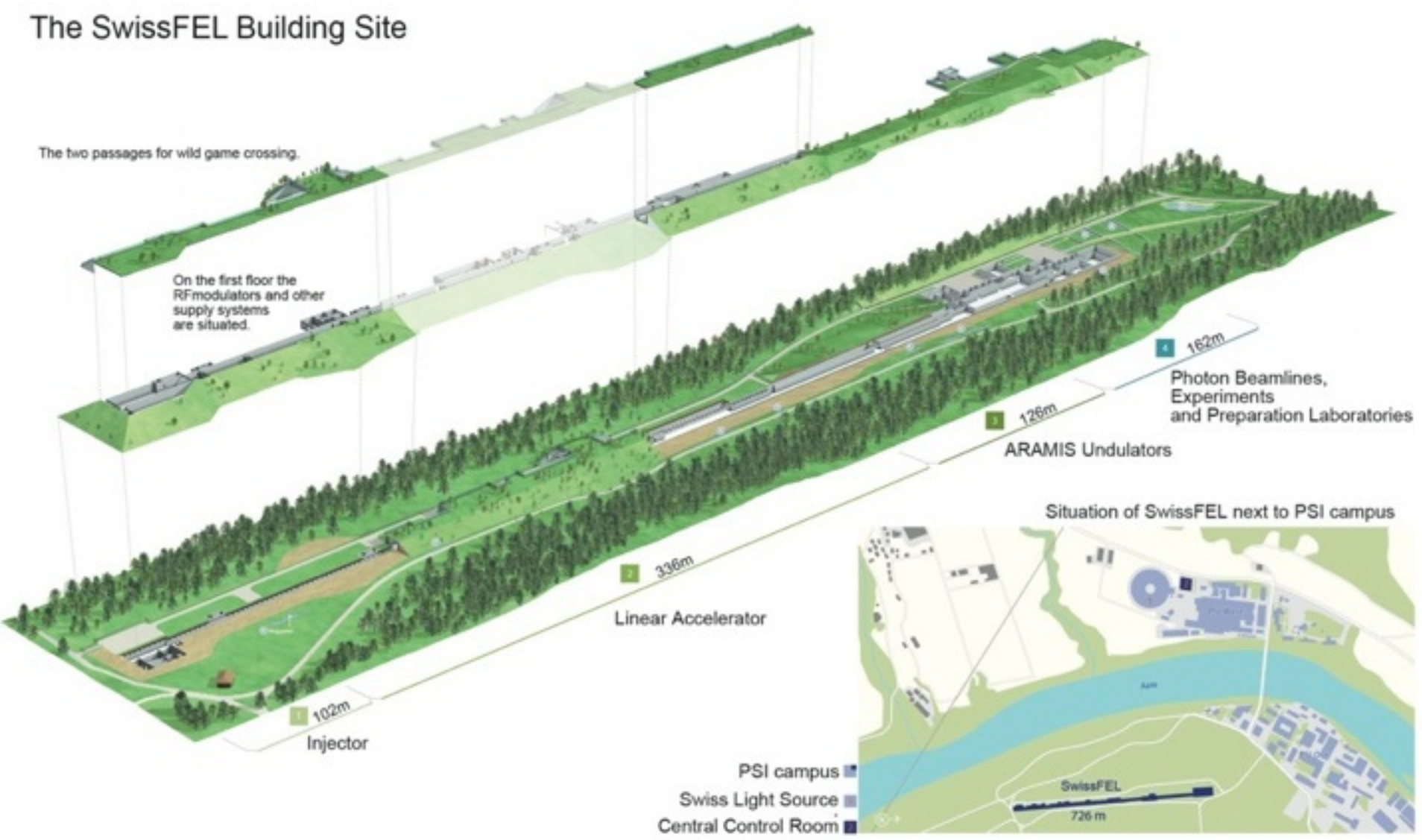
The SwissFEL Building Site
The two passages for wild game crossing.
On the first floor the RFmodulators and other supply systems are situated.
4 162m
Photon Beamlines, Experiments and Preparation Laboratories
3 126m
ARAMIS Undulators
2 336m
Linear Accelerator
1 102m
Injector
Situation of SwissFEL next to PSI campus
PSI campus
Swiss Light Source
Central Control Room
SwissFEL
726 m

Why Pharmacology needs SwissFEL

→Methods to look at unique structures on a wide range of length scales and time scales are necessary to obtain a building plan of biological signaling machines!

→Dynamic atomic information not static structure is necessary for understanding the pharmacology of drug targets!

→Understanding catalytic effect of proteins means to observe the changes to the dynamic energetic landscapes introduced by the the bound substrate or ligand.

→Quantification of the dynamic mixture of different conformations of Receptors, Channels and Transporters in solution can explain drug action in more precise detail.

→Using the right kind of experiments all these questions can be addressed with the Free Electron Laser SwissFEL in the future.

The SwissFEL

- 20 fs pulses
- 10^{11} ph/pulse
- $4x10^{-5}$ – $4x10^{-2}$ bandwidth
- 1.4 transverse modes

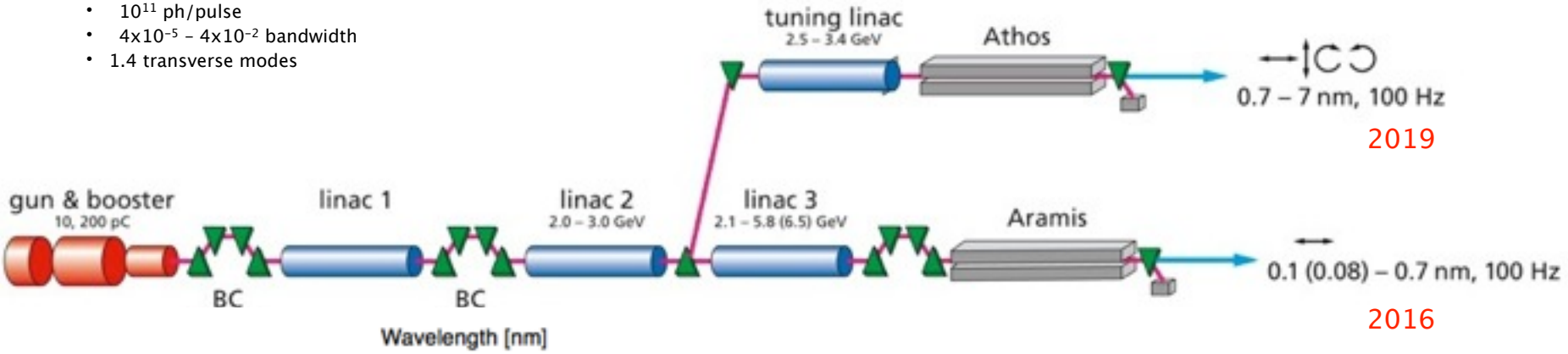

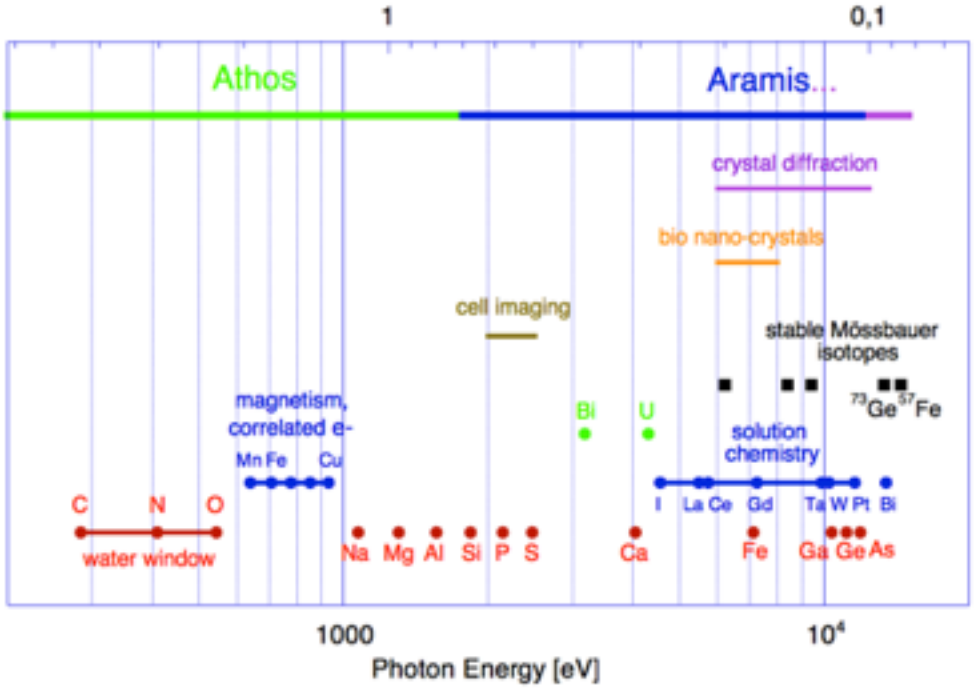

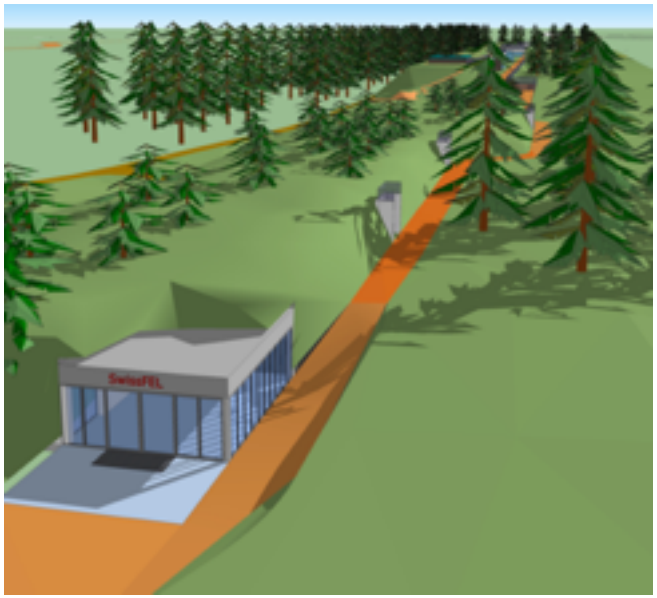

Soft X-ray imaging in waterwindow

3D Ultrastructural Organization of Whole *Chlamydomonas reinhardtii* Cells Studied by Nanoscale Soft X-Ray Tomography

Eric Hummel[1]*, Peter Guttmann[2], Stephan Werner[2], Basel Tarek[2], Gerd Schneider[2], Michael Kunz[3], Achilleas S. Frangakis[3], Benedikt Westermann[1]

1 Institut für Zellbiologie, Universität Bayreuth, Bayreuth, Germany, **2** Helmholtz-Zentrum für Materialien und Energie GmbH, Institute for Soft Matter and Functional Materials, Berlin, Germany, **3** Frankfurt Institute for Molecular Life Sciences and Institute of Biophysics, Goethe University Frankfurt, Frankfurt am Main, Germany

Abstract

The complex architecture of their structural elements and compartments is a hallmark of eukaryotic cells. The creation of high resolution models of whole cells has been limited by the relatively low resolution of conventional light microscopes and the requirement for ultrathin sections in transmission electron microscopy. We used soft x-ray tomography to study the 3D ultrastructural organization of whole cells of the unicellular green alga *Chlamydomonas reinhardtii* at unprecedented spatial resolution. Intact frozen hydrated cells were imaged using the natural x-ray absorption contrast of the sample without any staining. We applied different fiducial-based and fiducial-less alignment procedures for the 3D reconstructions. The reconstructed 3D volumes of the cells show features down to 30 nm in size. The whole cell tomograms reveal ultrastructural details such as nuclear envelope membranes, thylakoids, basal apparatus, and flagellar microtubule doublets. In addition, the x-ray tomograms provide quantitative data from the cell architecture. Therefore, nanoscale soft x-ray tomography is a new valuable tool for numerous qualitative and quantitative applications in plant cell biology.

Chlamydomonas
(Green Algae)

3D Soft X-ray images from Bessi Berlin

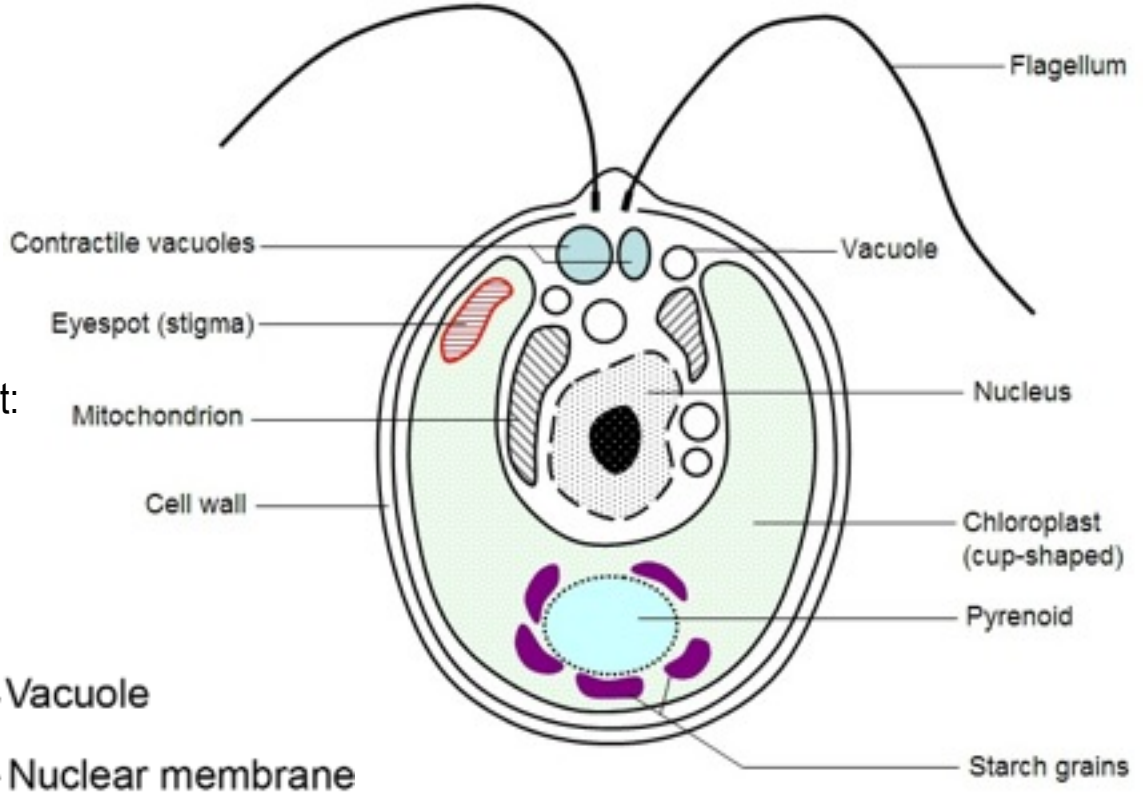

Slice of a cell from soft X-ray measurement:
Hummel *et al*. (2012) PLOS one

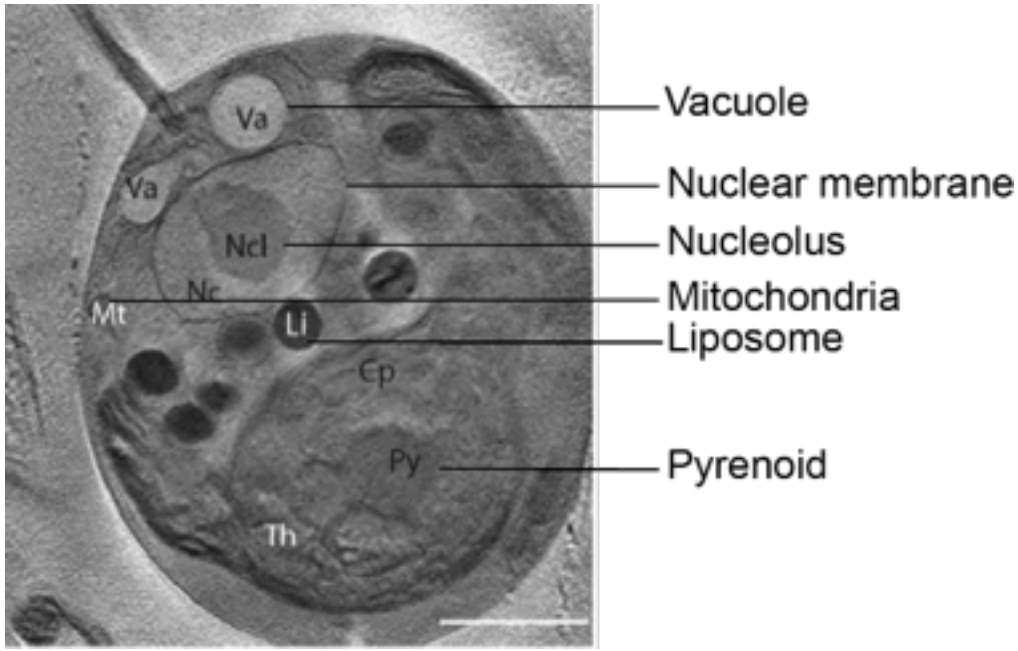

Chlamydomonas
(Green Algae)

Aramis Optical Layout

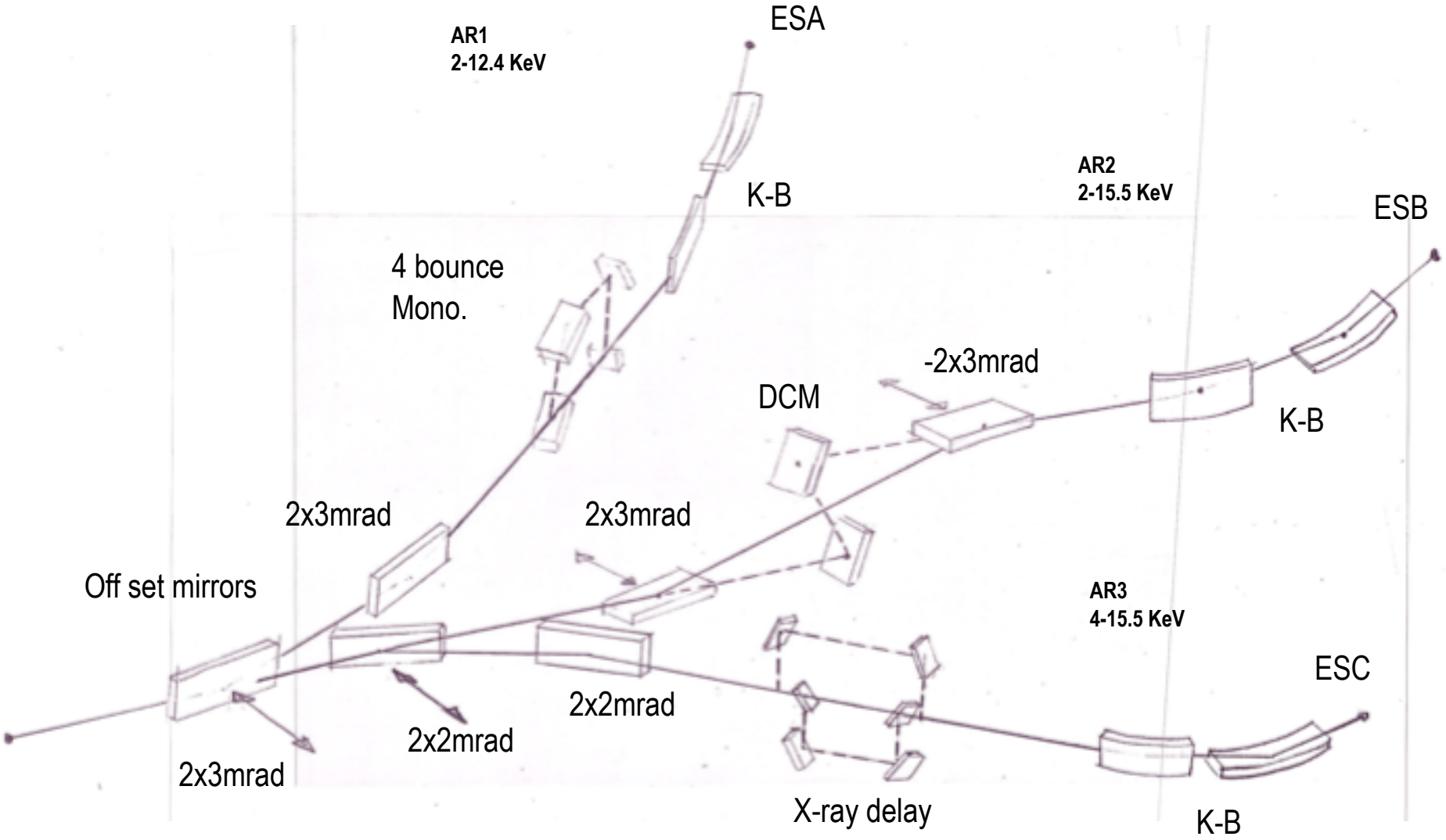

Phase-I ARAMIS Endstations (2016-2018)

ESA:
Multi-purpose pump-probe

ESB:
Pump-probe crystallography

ESC:
Coherent diffraction

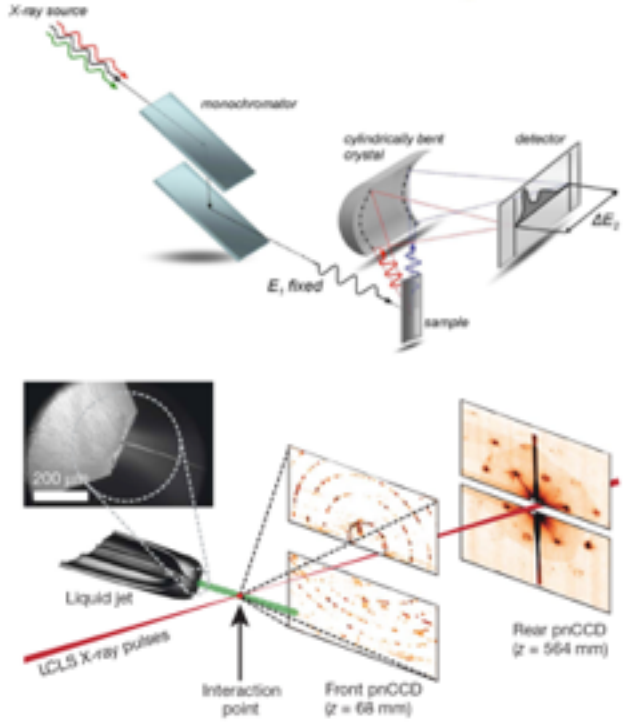

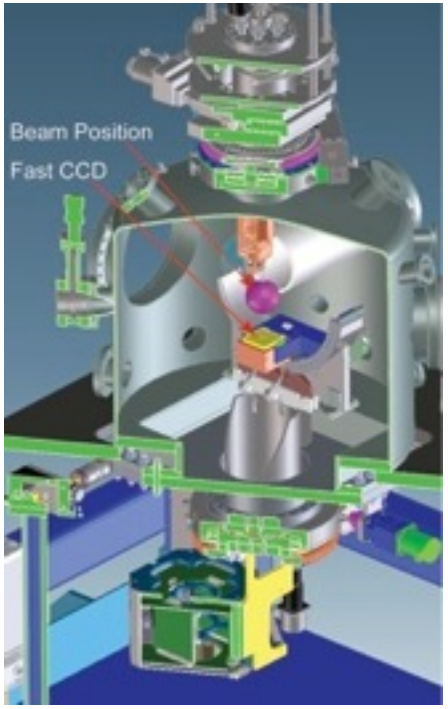

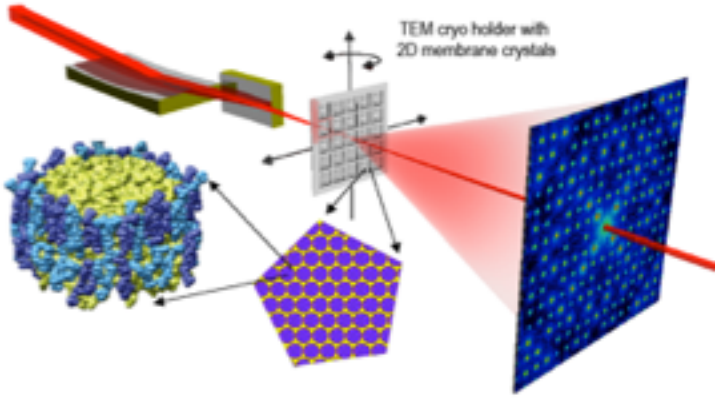

A Strategy for FEL Biology

Samples generated from live systems from biologists:

Suspensions:

3D nano and microcrystals
Large protein assemblies:
Virus particles, Virus shells
Protein/RNA assemblies:
Spliceosome, Signalosome, Ribosome
Protein solutions and Membrane proteins in detergent:

WAXS experiments
Ultrafast photochemistry and photobiology
Serial femtosecond crystallography (SFX)

Jet sample injectors:

Fast Jet system:
Fast pump-probe, WAXS and SFX
Slow Jet injector:
For viscous and jelly samples
LCP-Jet membrane protein SFX

Supported 2D sections:

Tissue sections
2D Membrane protein crystals
Tubular protein assemblies
Tubulin and helically arranged membrane protein tubes
3D Nanocrystals on a support

Nano-beam with cryo-2D scanning stage:

2D crystallography
Element selective topography
Helical 3D reconstruction
Characterization of nanocrystals
Crystallography with very small amounts

3D Blocks of tissues:

Retina
Bone
Muscle
Brain tissue
Block of frozen yeast
3D-printed cell assemblies

Nano-beam with cryo-3D scanning stage:

3D element selective topography
Element selective imaging
Direct or holographic imaging
Tomography

Radation Damage in X-Ray Diffraction and EM is limiting Structural Biology

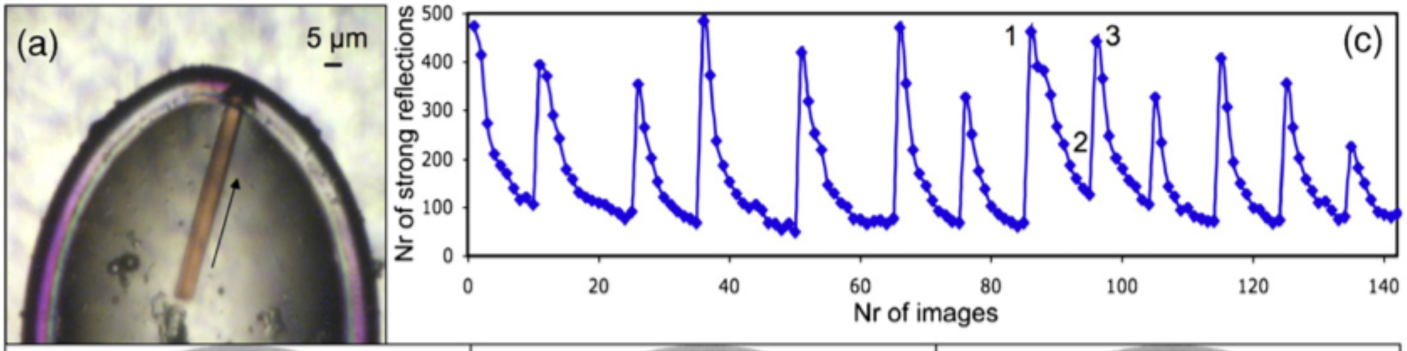

Outrunning Radiation Damage in Crystallography

Simulation of the Explosion dynamics of biomolecules (C,N,O):

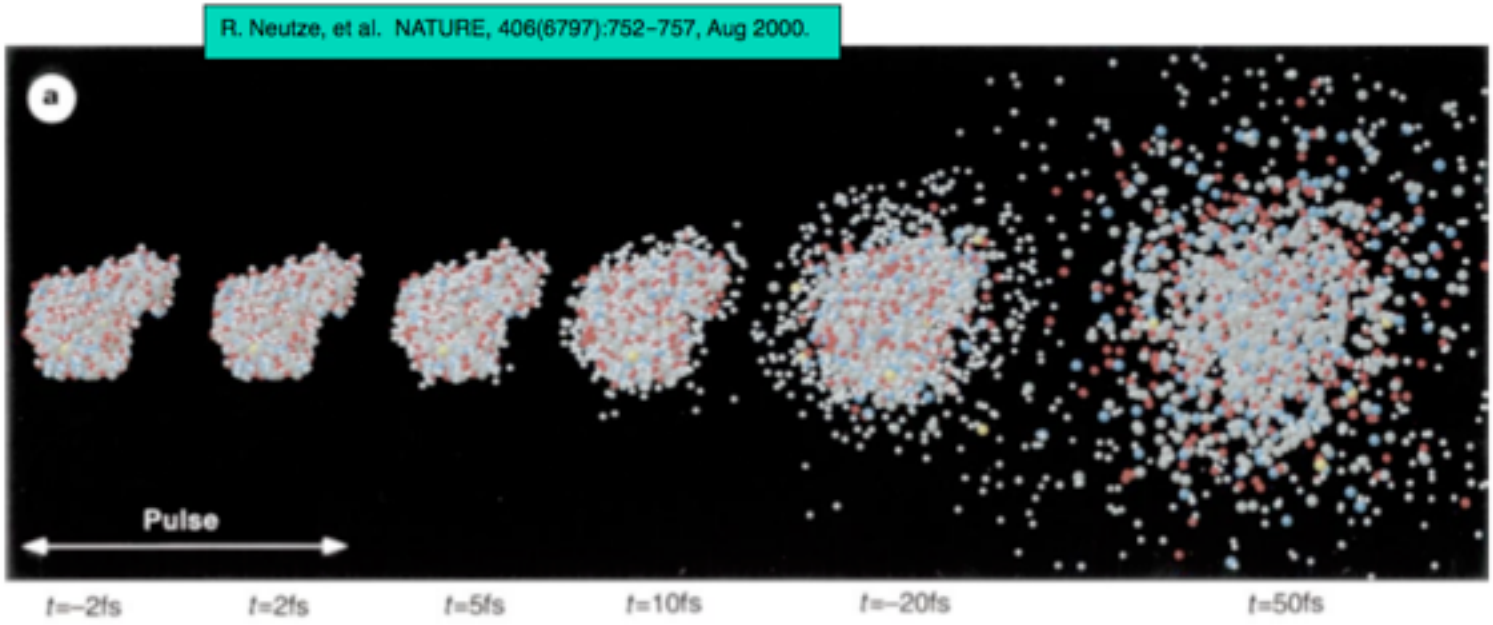

Tricks:

1) When the light is not on then we can not see what is happening

2) Only crystalline ordered material has enough average signal to be detected

The XFEL How it Works

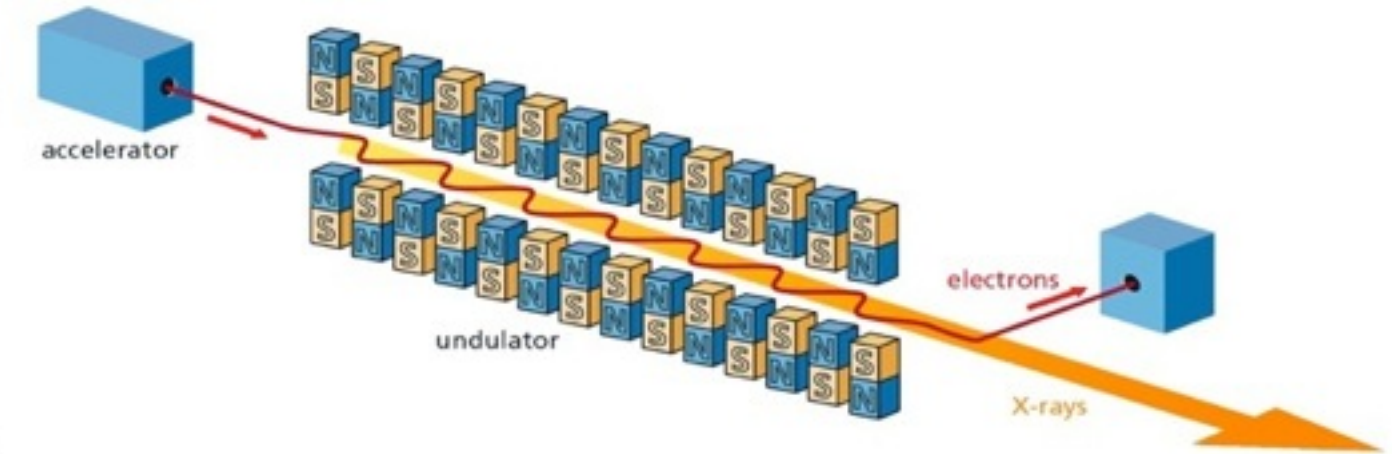

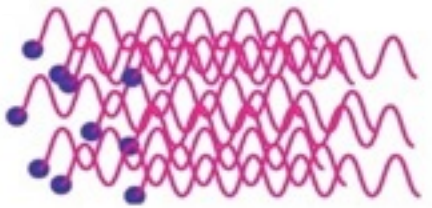

$$P = N\,P_1$$

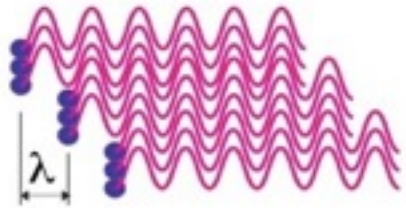

$$E = N\,E_1$$
$$P = N^2\,P_1$$

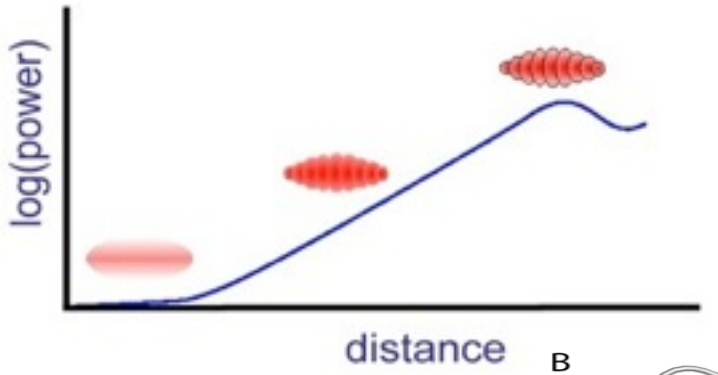

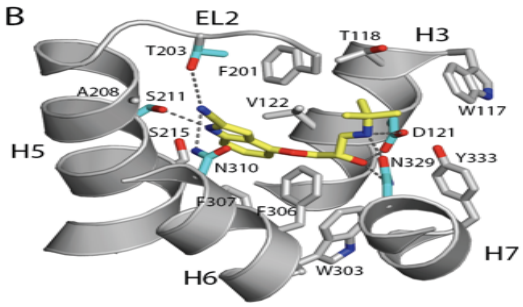

SASE: "self amplified spontaneous emission"

The LCLS is the world's first hard X-ray laser

First lasing in April 2009. The LCLS at Stanford is the world's first hard X-ray laser. It produces 9 kV X-rays (1.4 Ang) in 5 - 200 fs pulses, about 1E12 photons per pulse.

X-FEL how it works

Micro-bunching and coherent emission

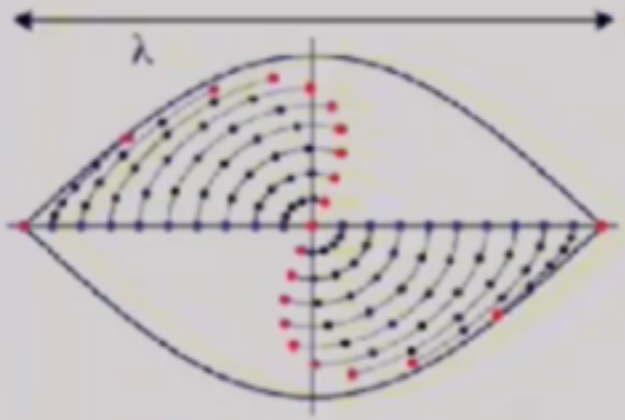

Initially uniform e⁻ distribution (blue) evolves into microbunches (red).

Micro-bunches radiate coherently.

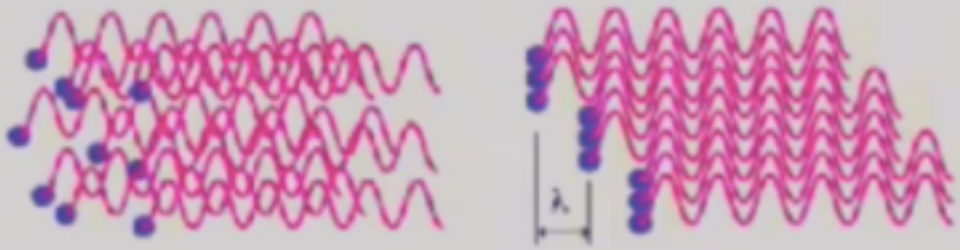

$$P_{incoh} = NP_1$$

$$E = NE_1$$

$$P_{coh} = N^2 E_1^2 = NP_{incoh}$$

$$N = 10^9 \text{ !!}$$

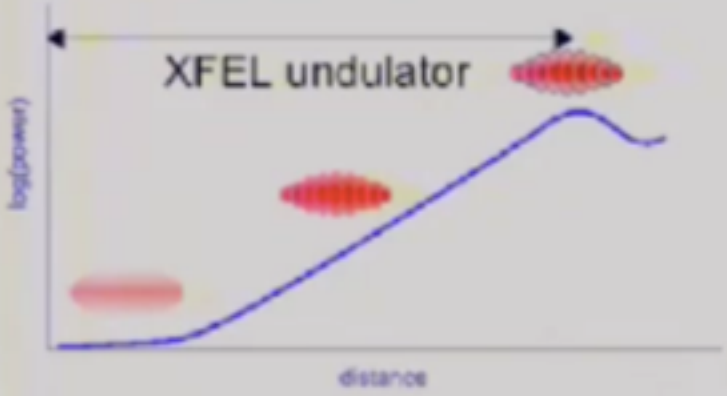

„Self-amplifying spontaneous emission" (SASE)

Taken from Bruce Patterson's presentation at EMPA on the SwissFEL project

X-ray Detector Development

Synchrotron detectors

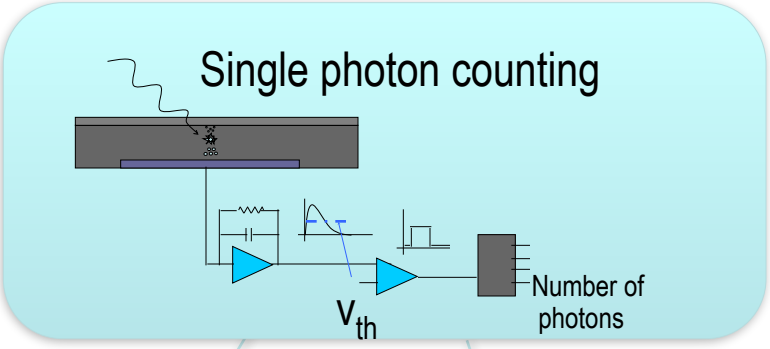

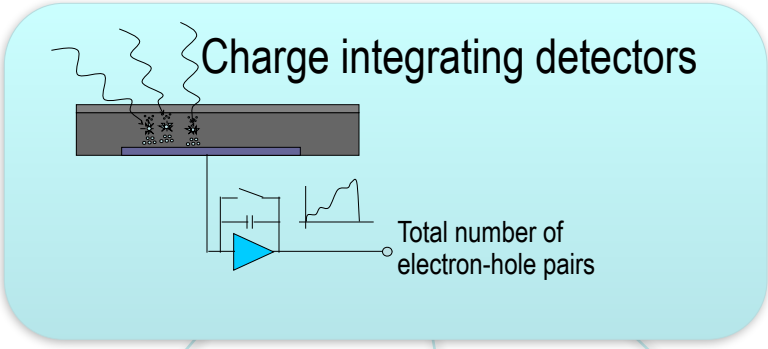

Mythen II

Eiger

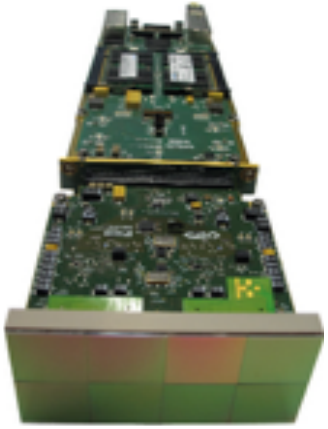

EU-XFEL, SwissFEL: Gotthard

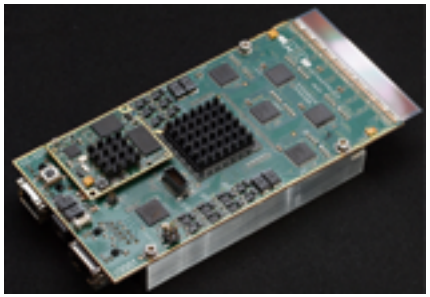

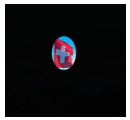

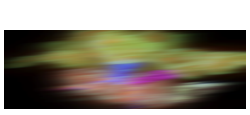

EU-XFEL: AGIPD

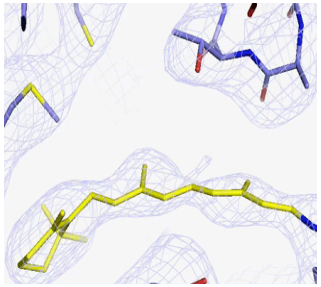

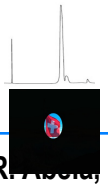

SwissFEL: Jungfrau

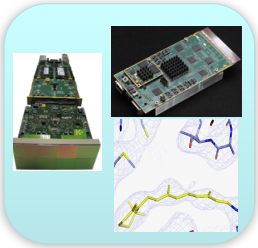

Newly Commissioned CXI Hutch Optimized

Cornell-SLAC Pixel Area Detector

- 10 micron pixels
- 1.5 megapixels
- tiled design

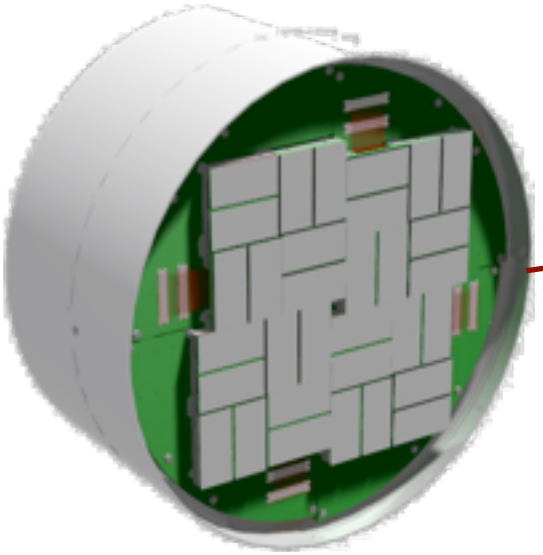

Detector Housing

Sample Chamber
1 micron beam

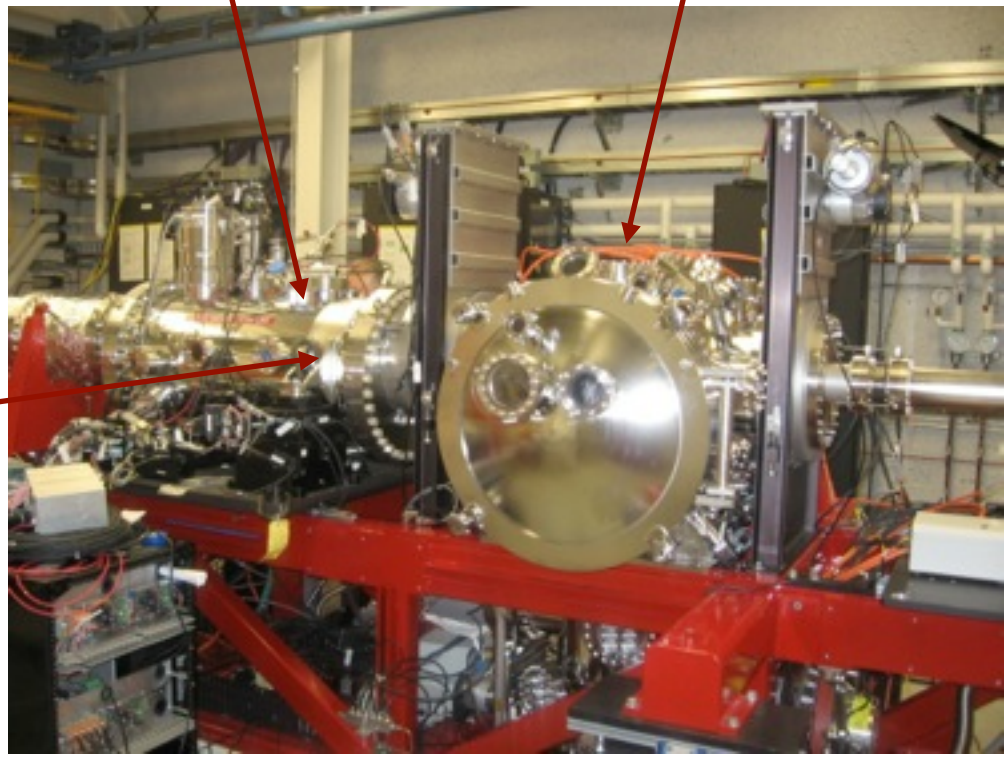

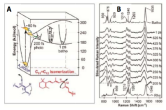

Fig.1. Femtosecond-photoisomerisation of retinal during the first event of vision. **A.** Multidimensional representation of the isomerization coordinate of retinal analyzed by coherent Raman vibrational spectroscopy[1]. The cis-retina photo-rhodopsin and the all-trans retinal bathorhodopsin states are reached after 200fs and 1ps, respectively. **B.** Time-resolved femtosecond stimulated Raman spectra of rhodopsin[17] in the ground-state (Rho) and in the trapped bathorhodopsin (Batho) state.

SwissFEL: making a incredibly intense Femtosecond Puls

PAUL SCHERRER INSTITUTE

Incredibly short and
intens and coherent X-ray puls

Basic XFEL design

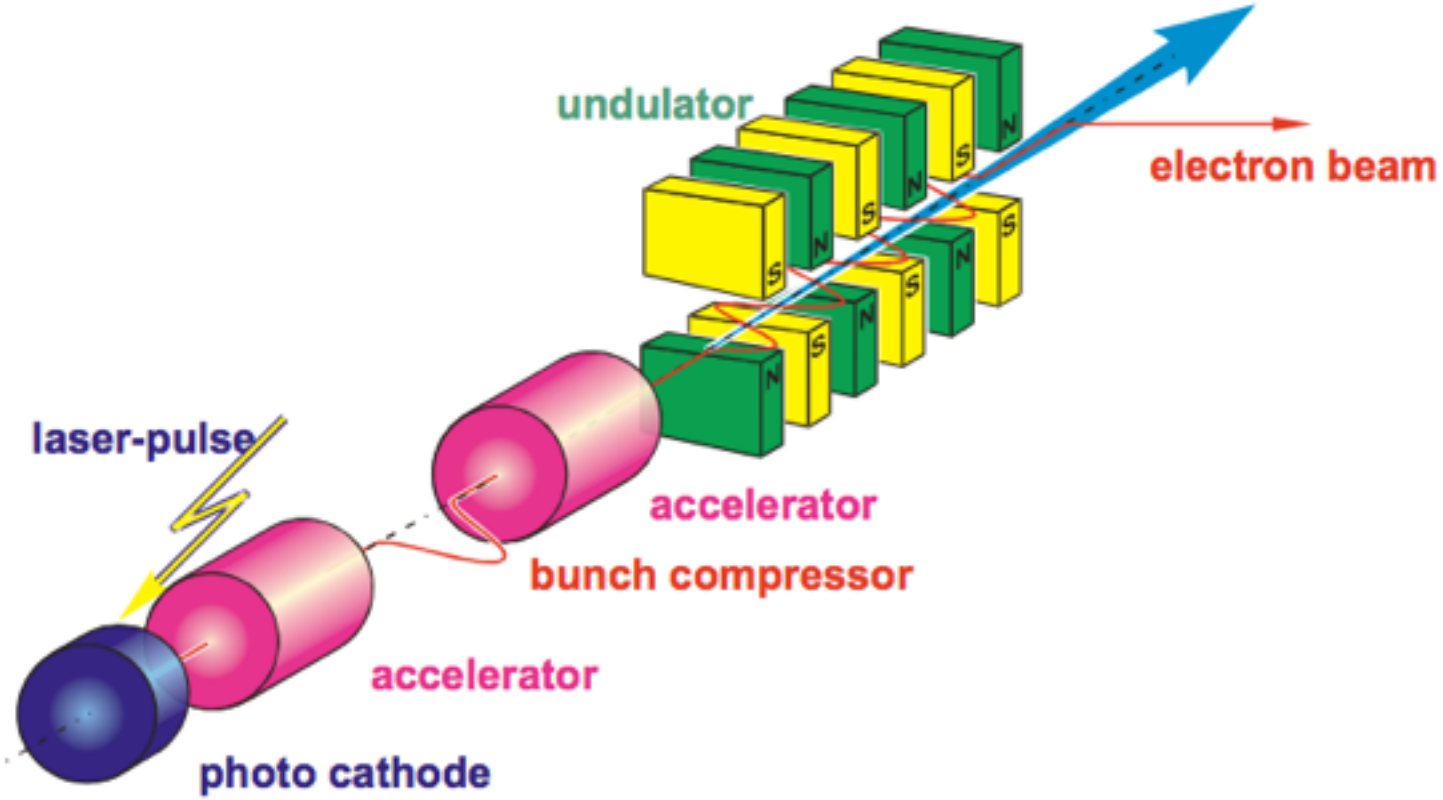

Radation Damage in X-Ray Diffraction and EM is limiting Structural Biology

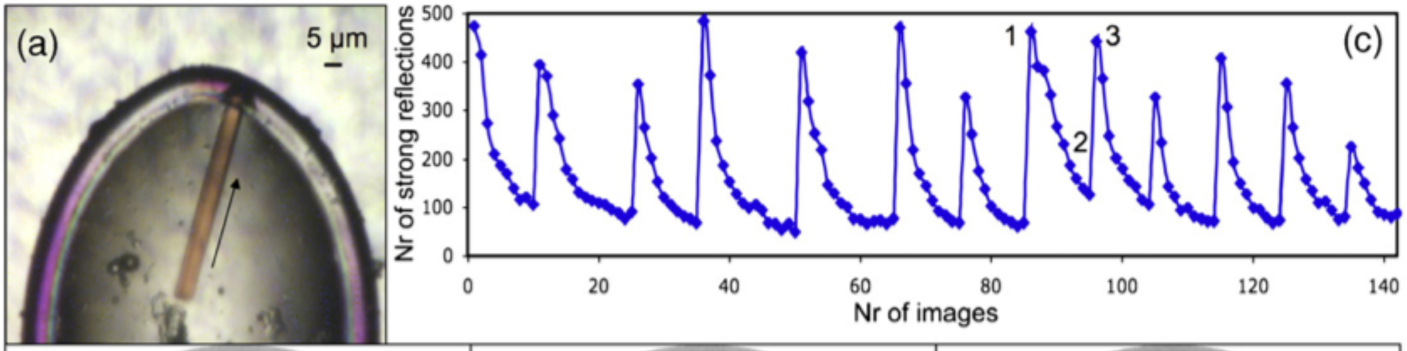

Outrunning Radiation Damage in Crystallography

Simulation of the Explosion dynamics of biomolecules (C,N,O):

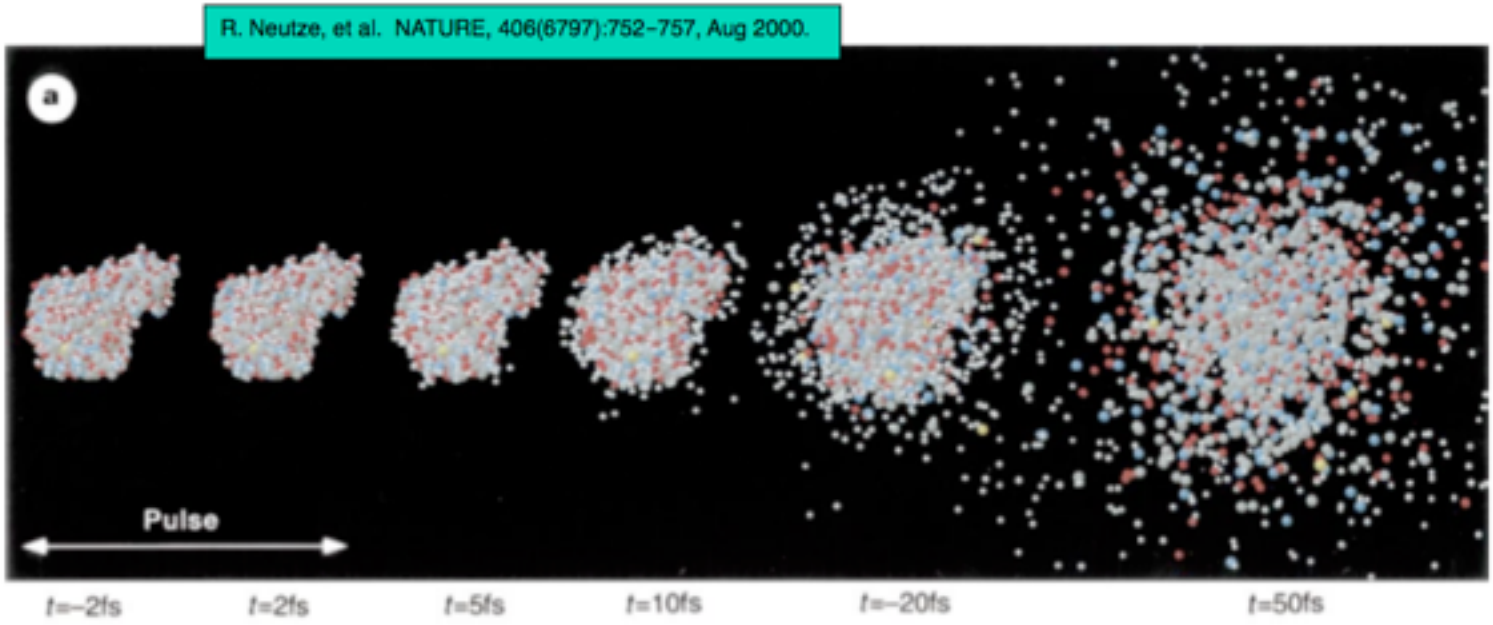

Tricks:

1) When the light is not on then we can not see what is happening

2) Only crystalline ordered material has enough average signal to be detected

3D CRYSTALLOGRAPHY WITH FELS

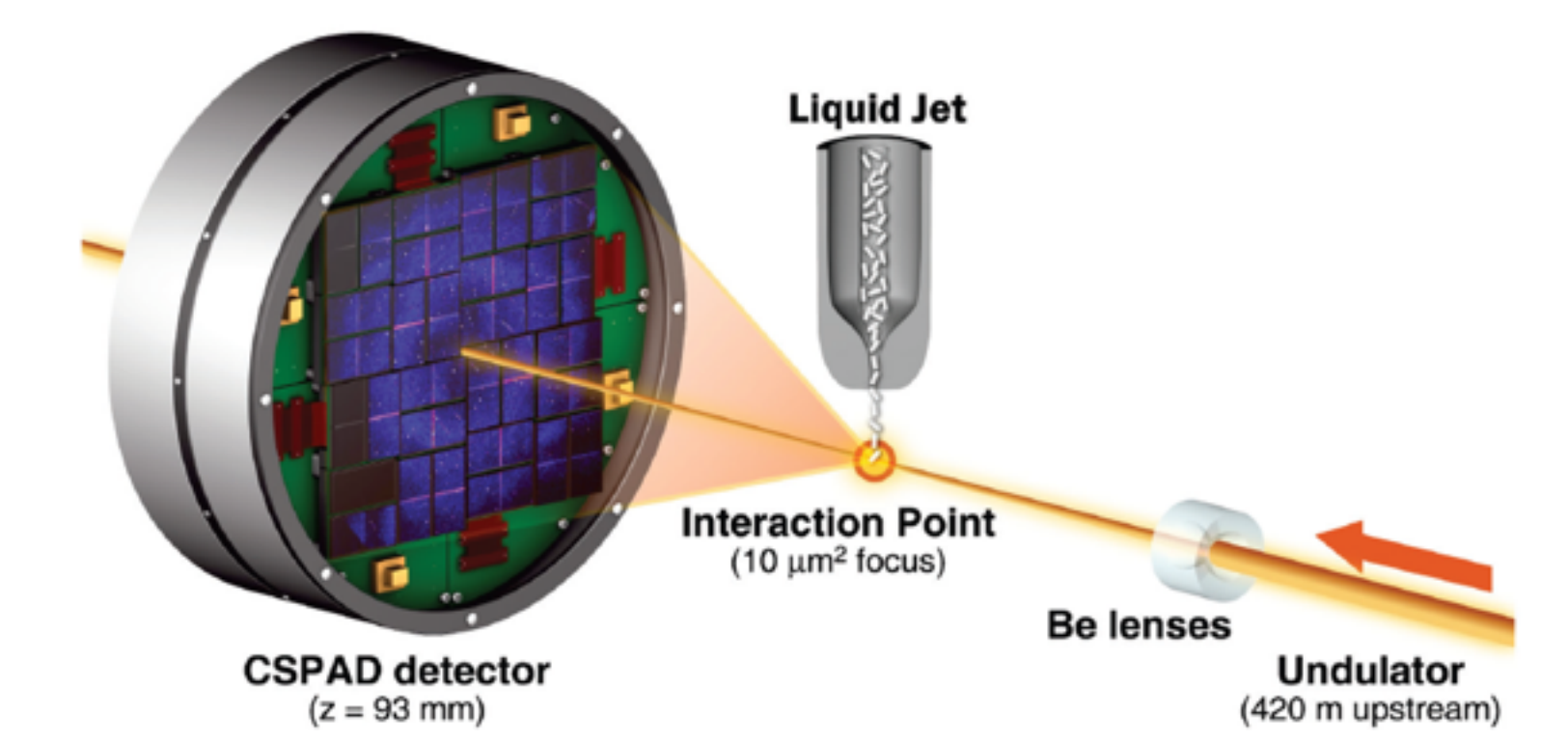

Boutet et al, 2012

Droplet Injector for Biological Suspensions

The new Aerojet technique provides very fine liquid stream of micrometer size

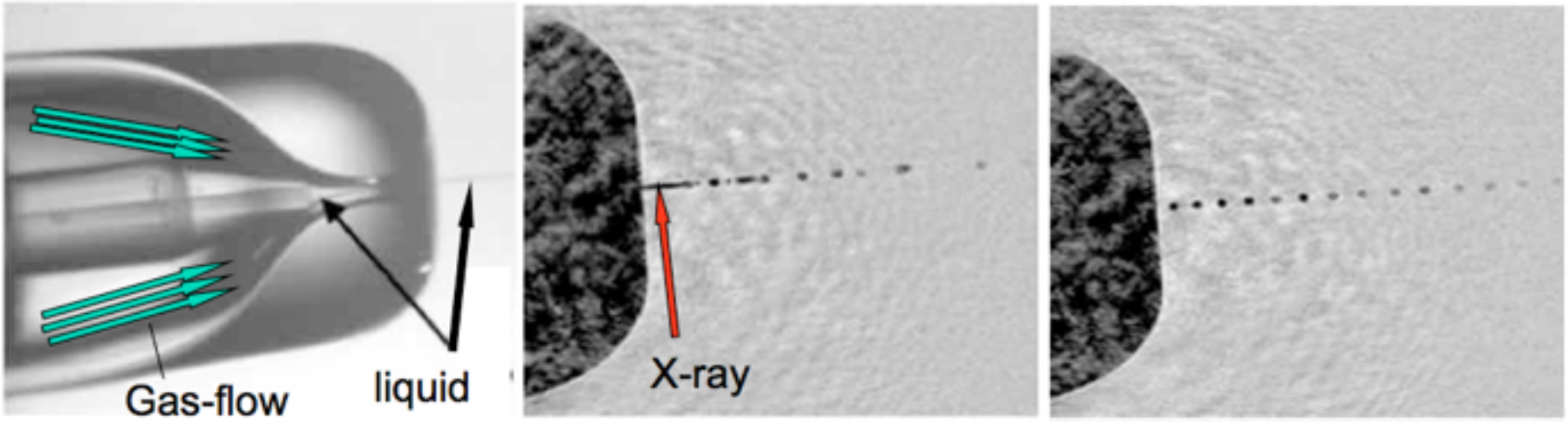

Aerojet source. Left: Liquid cone visible generated by converging gas flow.

Middle: Untriggered breakup into droplets.

Right: Triggered breakup into droplets.

Droplet speed about 10m/sec. Trigger frequency: 170kHz.

From John Spence

Femtosecond nano crystallography

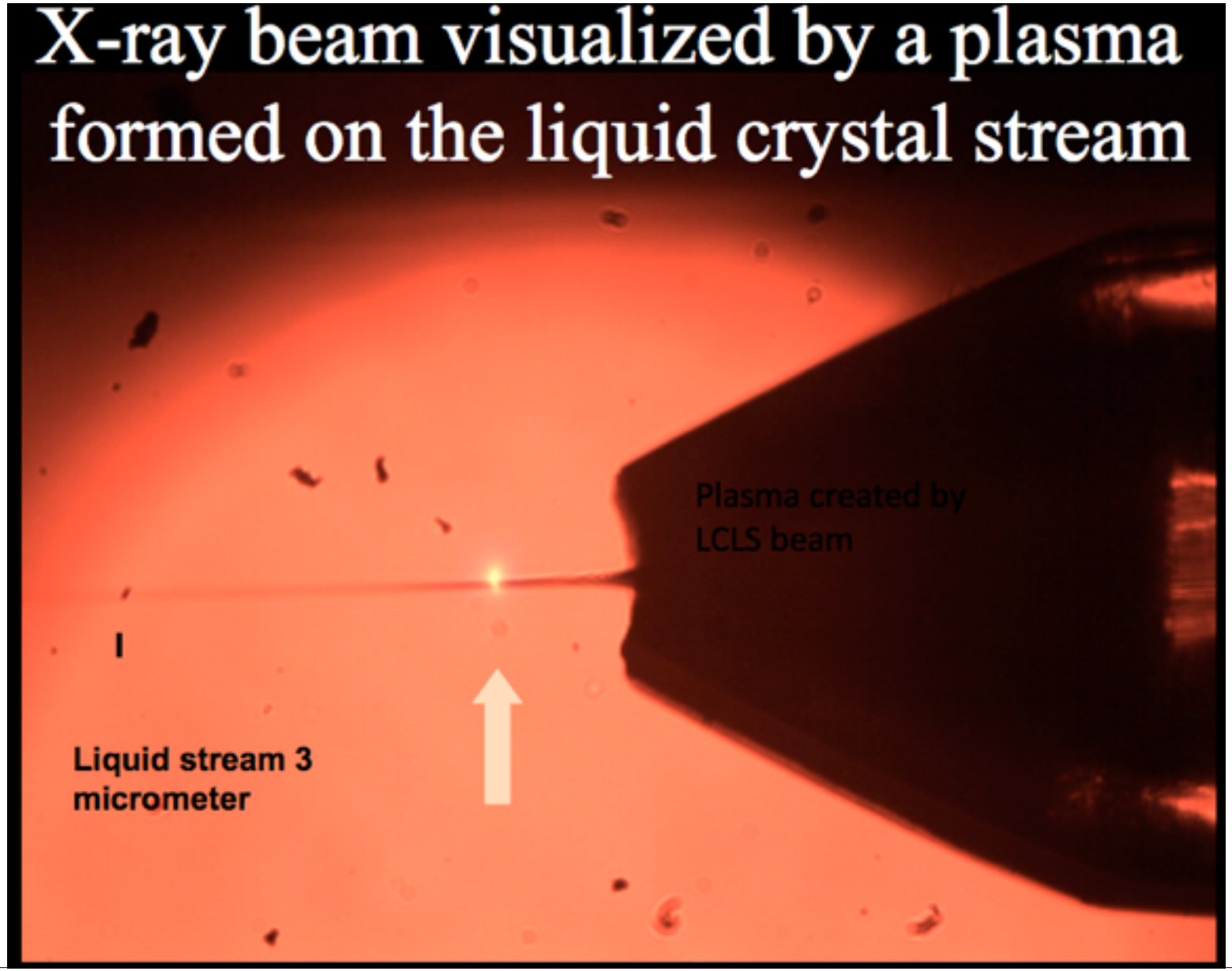

The Max Plank CAMP Chamber

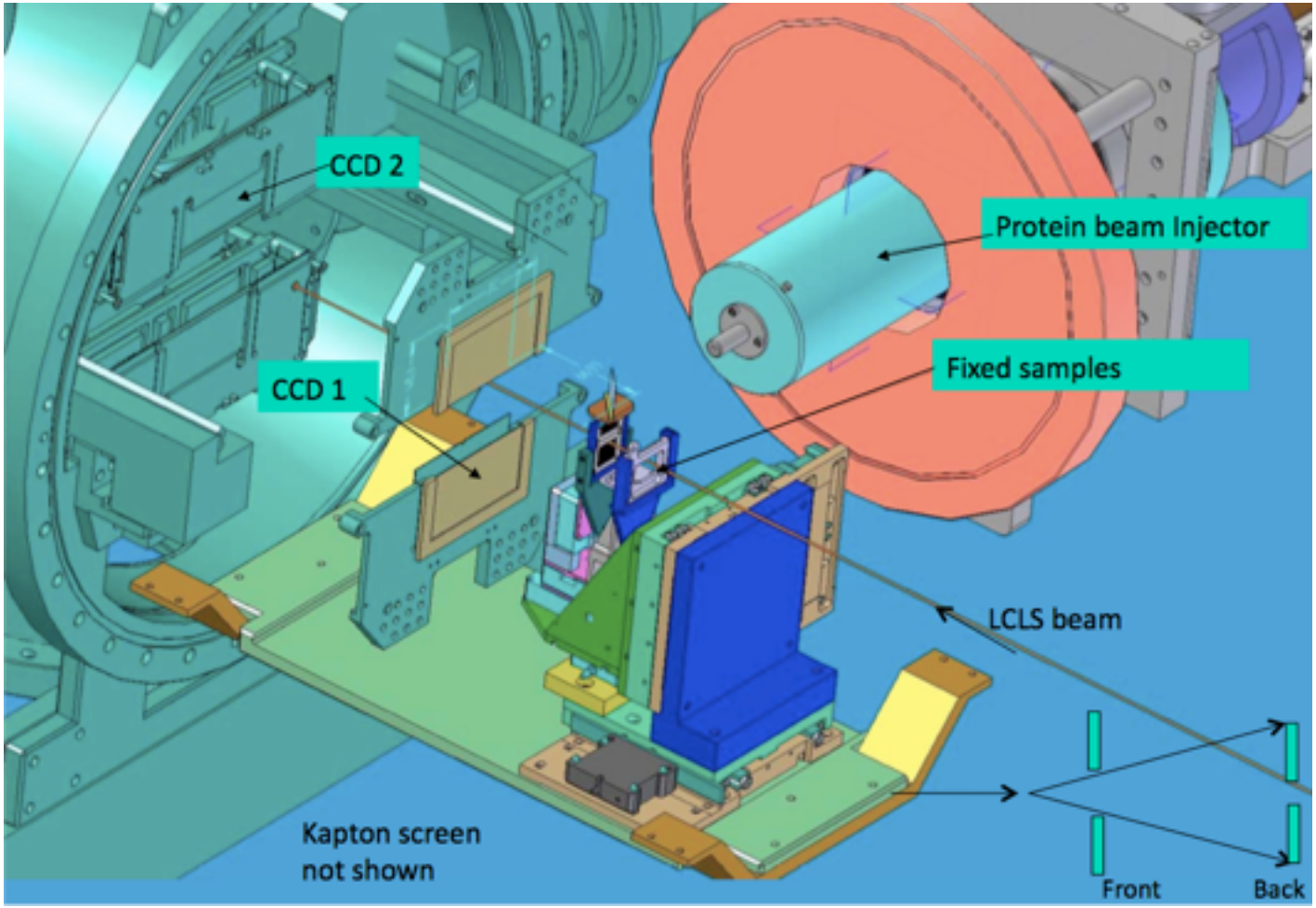

Endstation used for LCLS experiments

Femtosecond nano crystallography

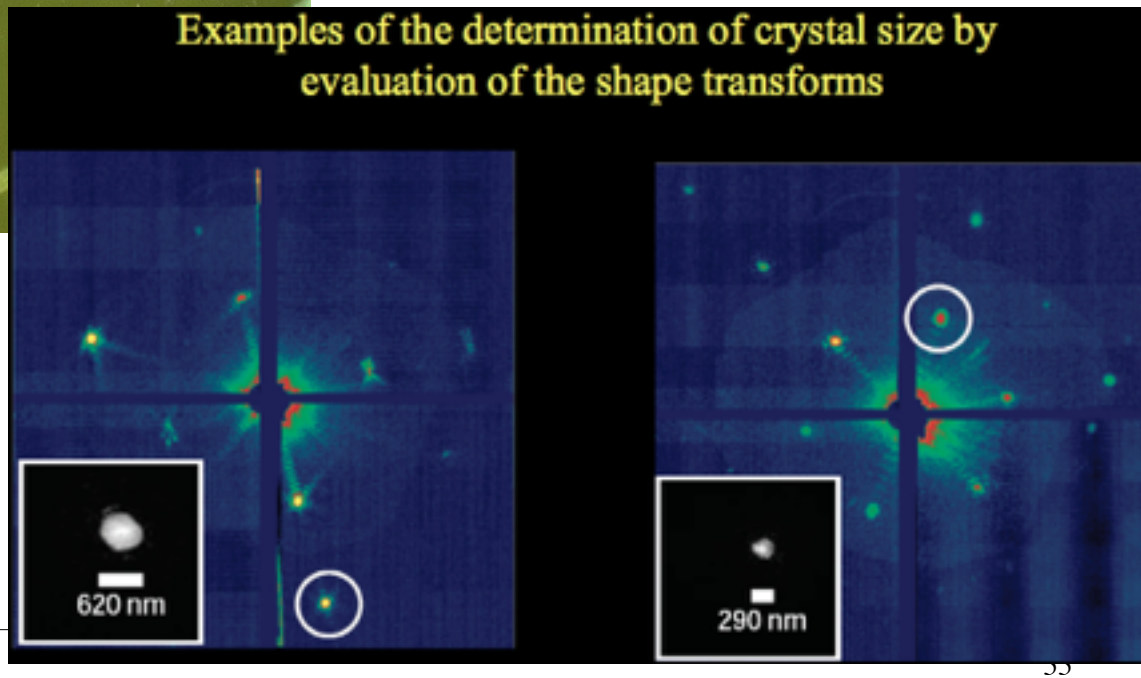

From
Petra Fromme

Structure of Photosystem I from XFEL Data

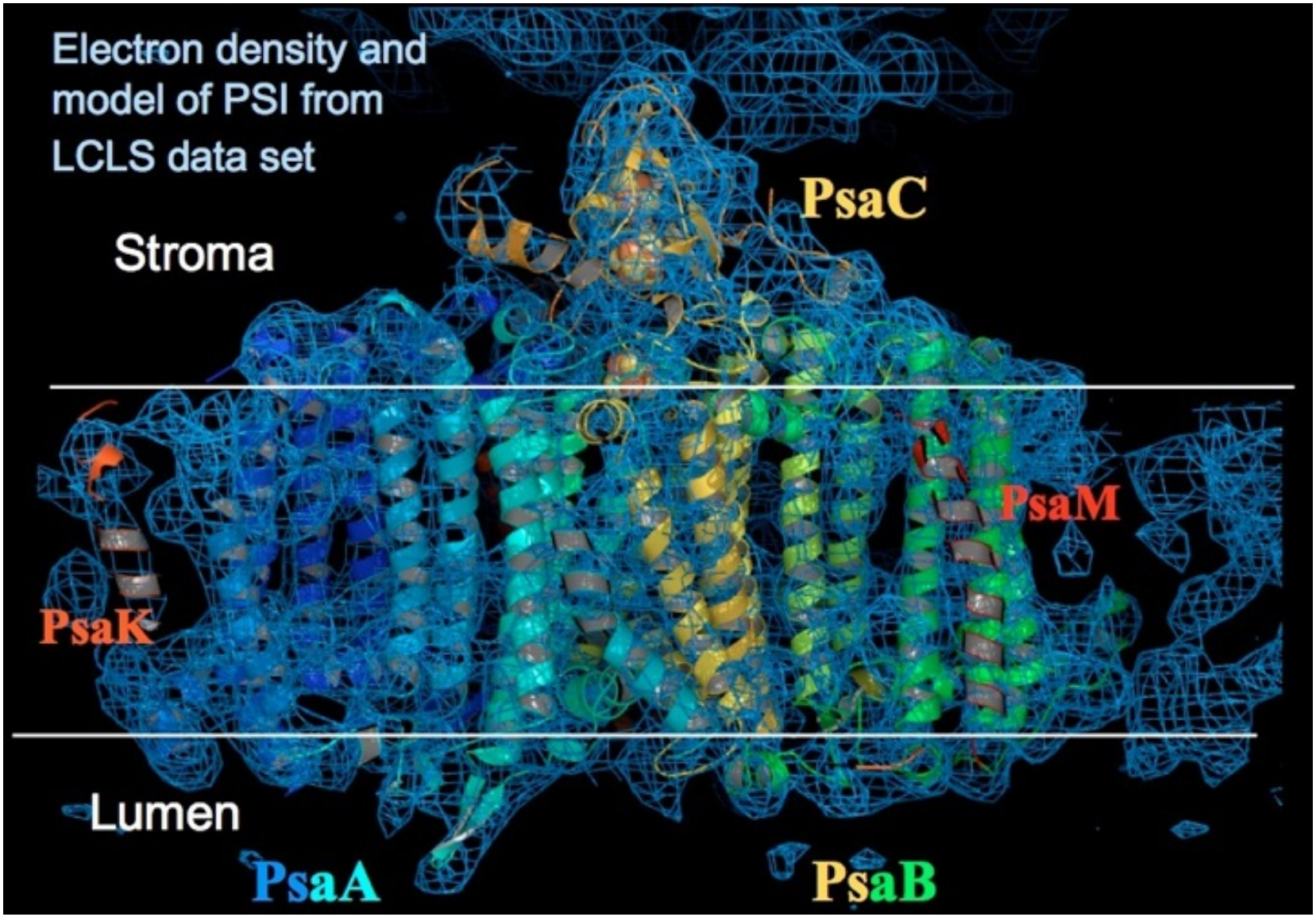

From Petra Fromme and John Spence

Serial Femtosecond Crystallography (SFX)

Lysozyme Nanocrystallisation

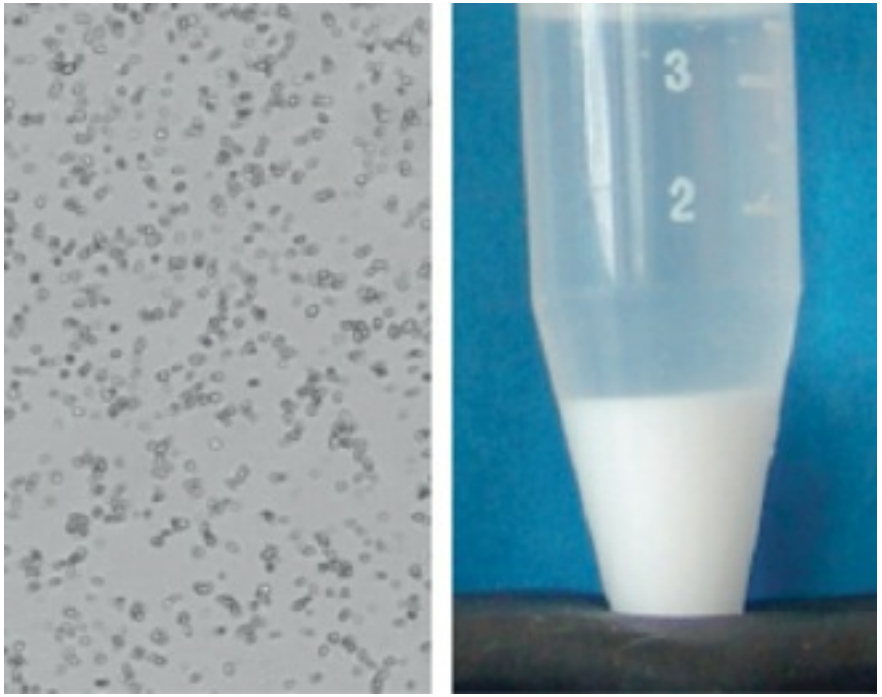

Schlichting et al, Curr.Op.Strcut.Biol. 2012

“about 1.5 million individual “snapshot” diffraction patterns.
About 4.5% of the patterns classified as crystal hits, 18.4% of which were indexed.”

Ilme Schlichting MPI Heidelberg

Boutet et al, 2012

Working with micro and nano crystals

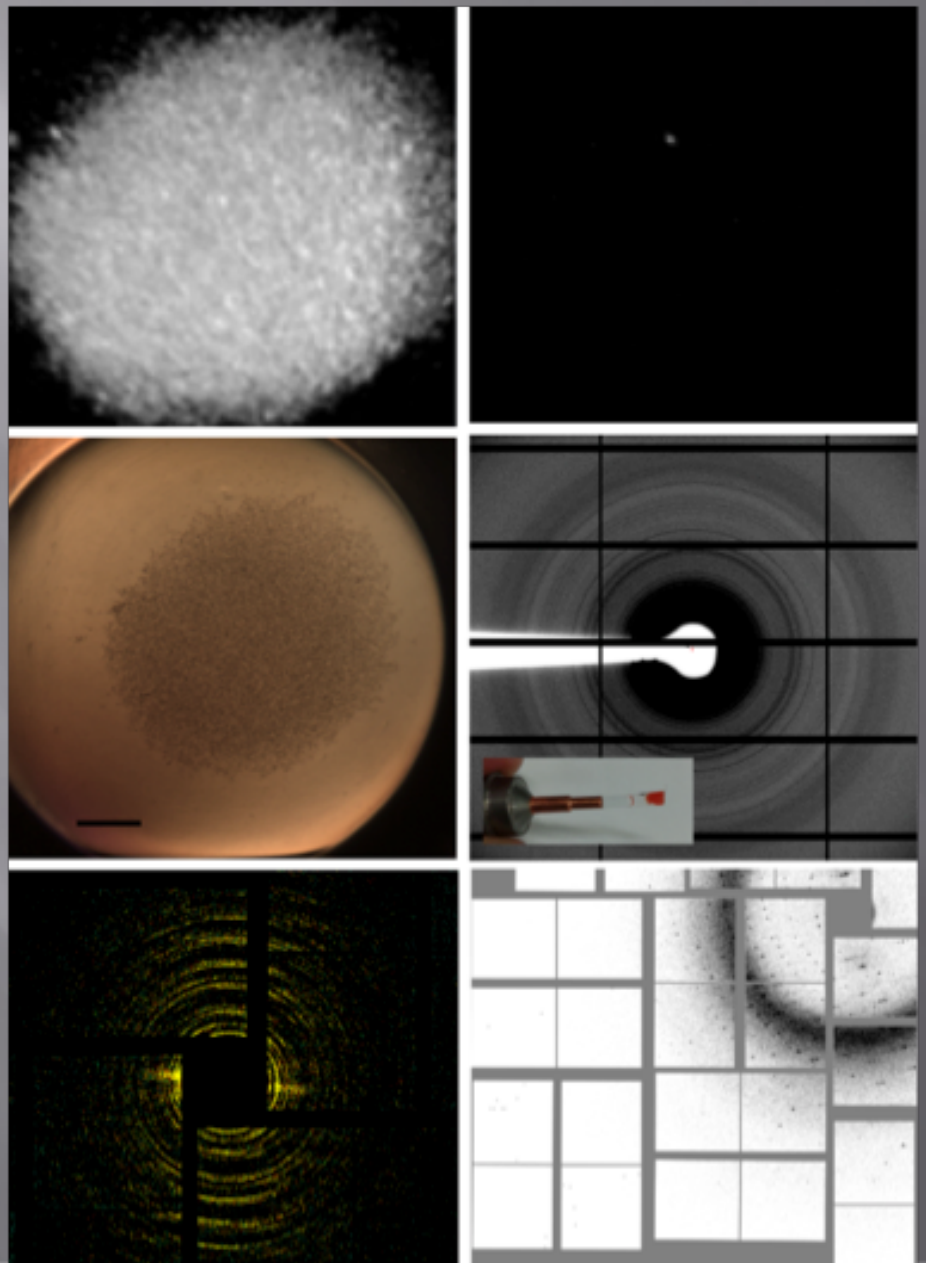

Serial Femtosecond Crystallography (SFX)

Parameter	40-fs pulses	5-fs pulses	SLS RT data 3
Wavelength	1.32 Å	1.32 Å	0.9997 Å
X-ray focus (μm^2)	~10	~10	~100 × 100
Pulse energy/fluence at sample	600 μJ/4 × 10^{11} photons per pulse	53 μJ/3.5 ×10^{10} photons per pulse	n.a./2.5 × 10^{10} photons/s
Dose (MGy)	33.0 per crystal	2.9 per crystal	0.024 total
Dose rate (Gy/s)	8.3 × 10^{20}	5.8 × 10^{20}	9.6 × 10^{2}
Space group	$P4_32_12$	$P4_32_12$	$P4_32_12$
Unit cell length (Å), α = β = γ = 90°	$a = b$ =79, c = 38	$a = b$ = 79, c = 38	$a = b$ = 79.2, c = 38.1
Oscillation range/exposure time	Still exp./40 fs*	Still exp./5 fs*	1.0°/0.25 s
No. collected diffraction images	1,471,615	1,997,712	100
No. of hits/indexed images	66,442/12,247	40,115/10,575	n.a./100
Number of reflections	n.a.	n.a.	70,960
Number of unique reflections	9921	9743	9297
Resolution limits (Å)	35.3–1.9	35.3–1.9	35.4–1.9
Completeness	98.3% (96.6%)	98.2% (91.2%)	92.6% (95.1%)
$I/\sigma(I)$	7.4 (2.8)	7.3 (3.1)	18.24 (5.3)
R_{split}	0.158	0.159	n.a.
R_{merge}	n.a.	n.a.	0.075 (0.332)
Wilson B factor	28.3 $Å^2$	28.5 $Å^2$	19.4 $Å^2$
R-factor/R-free	0.196/0.229	0.189/0.227	0.166/0.200
Rmsd bonds, Rmsd angles	0.006 Å, 1.00°	0.006 Å, 1.03°	0.007 Å, 1.05°
PDB code	4ET8	4ET9	4ETC

*Electron bunch length

Boutet et al, 2012

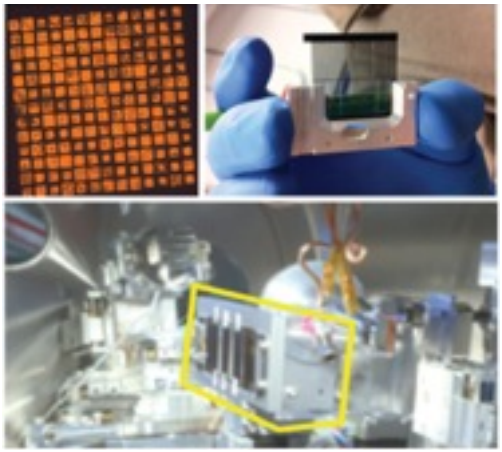

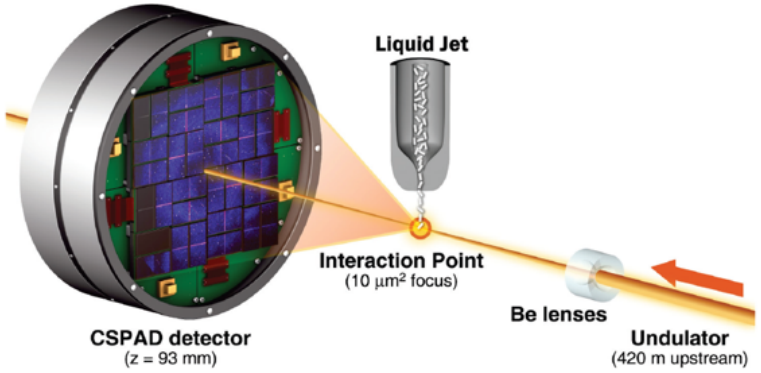

Femtosecond Nano Crystallography

→Fully hydrated nanocrystals gave excellent diffraction patterns at room temperature

→Pulses from 2 to 60 Femtoseconds were useful to outrun radiation damage and no degradation of patterns was detectable when nanocrystals were used

→The method of Femtosecond X-ray crystallography will revolutionise structural biology and atomic structure information can be extracted

→Difficult but medically very interesting targets like membrane proteins are very well suited for femtosecond nano crystallography

Coherent X-ray Diffraction Imaging: CXI

Structural C
Primary Isome
Femtosecond

Philipp Kukura, David W. McCamant,* Sangwoon Yoon, Daniel B. Wandschneider, Richard A. Mathies†

The primary event that initiates vision is the light-induced 11-cis to all-trans isomerization of retinal in the visual pigment rhodopsin. Despite decades of study with the traditional tools of chemical reaction dynamics, both the timing and nature of the atomic motions that lead to photoproduct production remain unknown. We used femtosecond-stimulated Raman spectroscopy to obtain time-resolved vibrational spectra of the molecular structures formed along the reaction coordinate. The spectral evolution of the vibrational features from 200 femtoseconds to 1 picosecond after photon absorption reveals the temporal sequencing of the geometric changes in the retinal backbone that activate this receptor.

Diffraction from 2D crystals on a

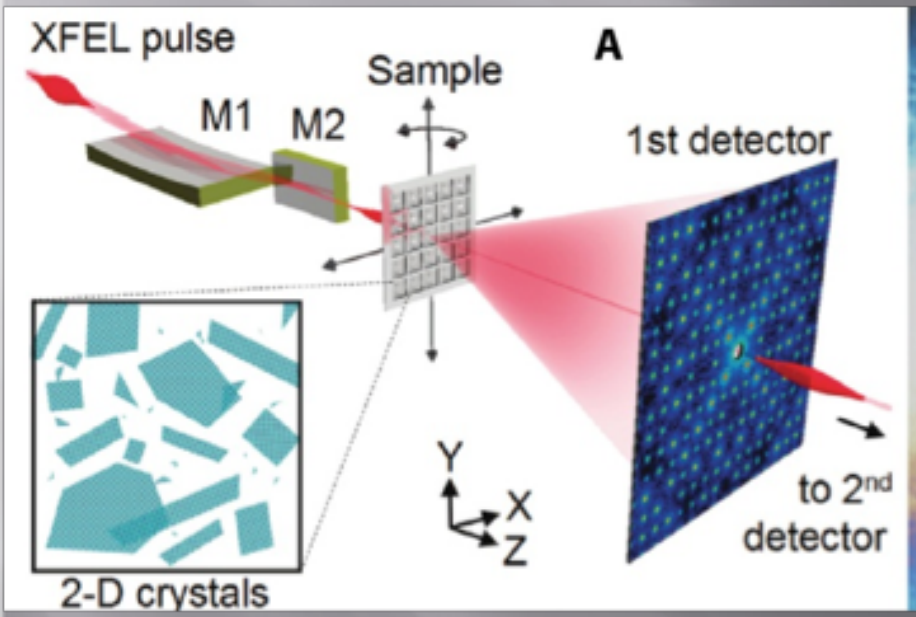

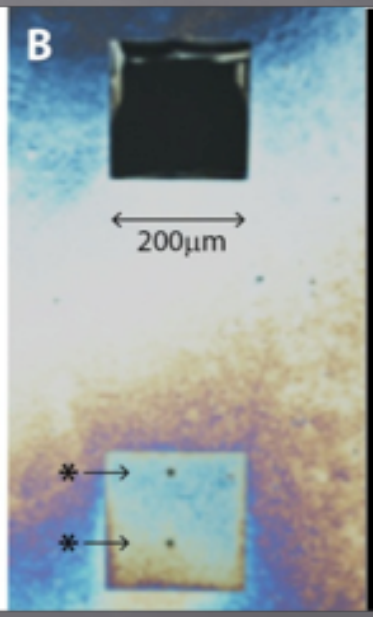

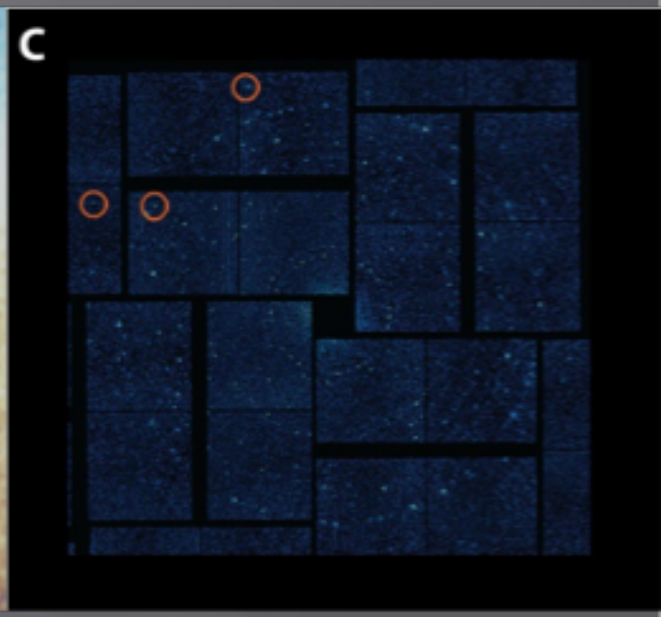

2D crystals of Voltage Gaited Channel

- **3D structure of Channel in 2 Dimensional crystals obtained by cryo-EM**
- Prepared in the Biomolecular Research Laboratory at PSI
- by Ching Ju Tsai with Xiao Dan Li project start 2010

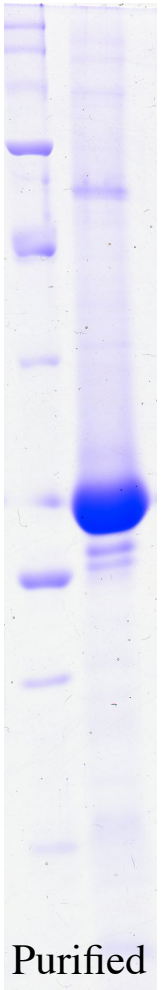

Purified channel

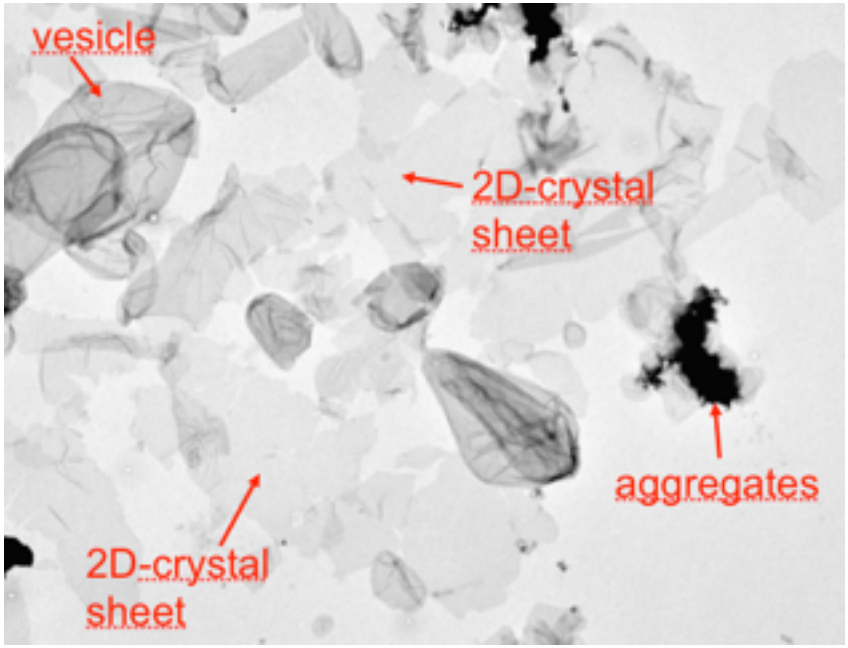

Suspension of 2D crystal on carbon film

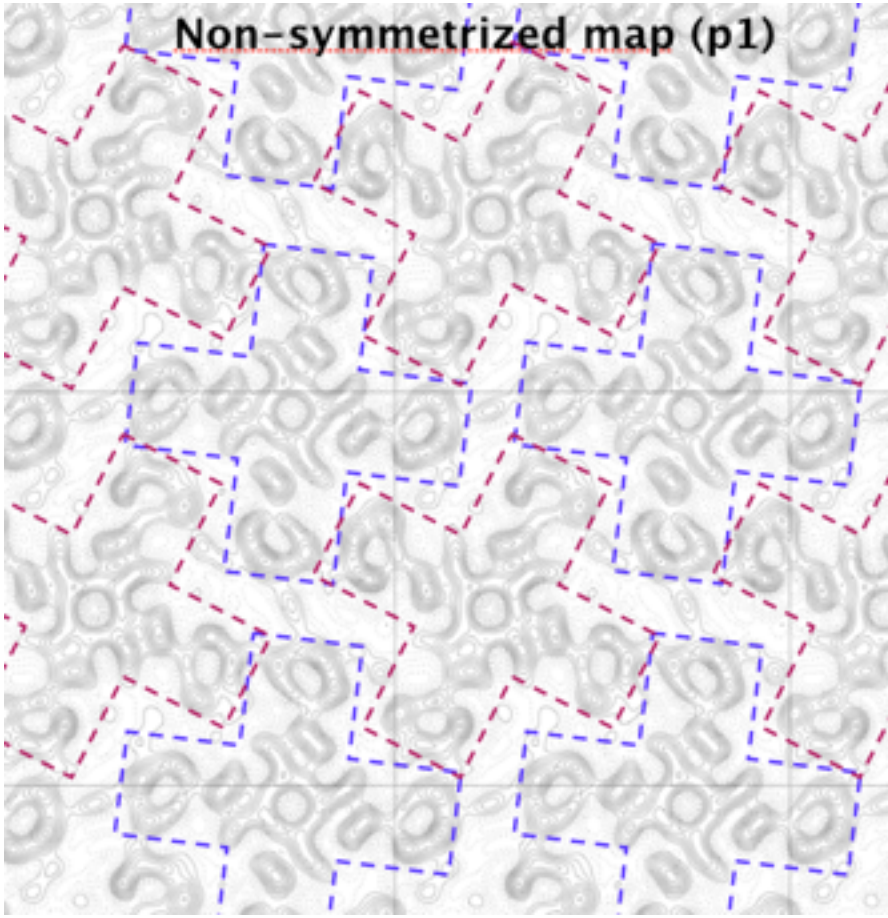

Cryo-EM projection structure of 2D crystal

3D structure of Voltage Gaited Channel

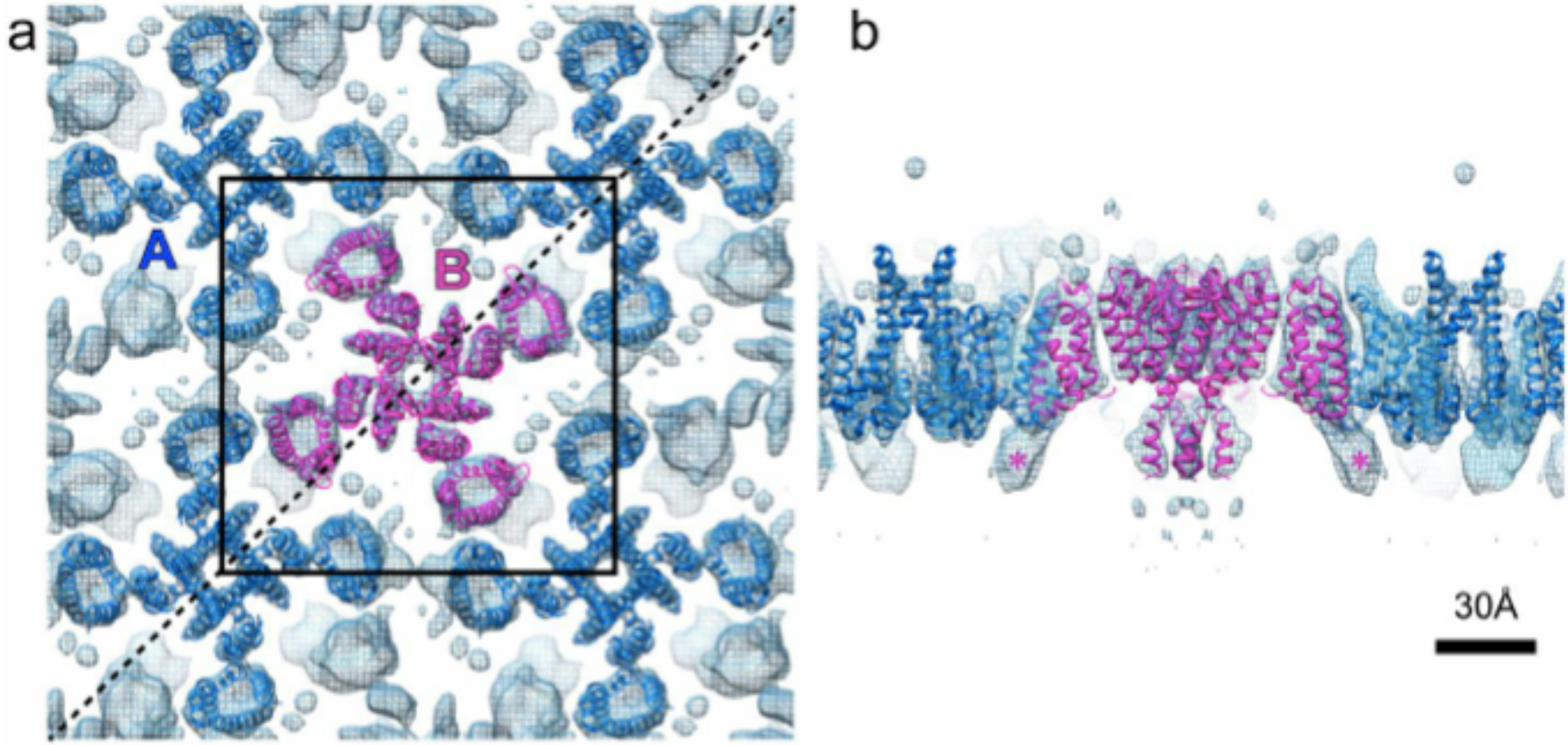

3D Cryo-EM structure from 2D crystal of a channel

Ching Ju Tsai with solid suppor

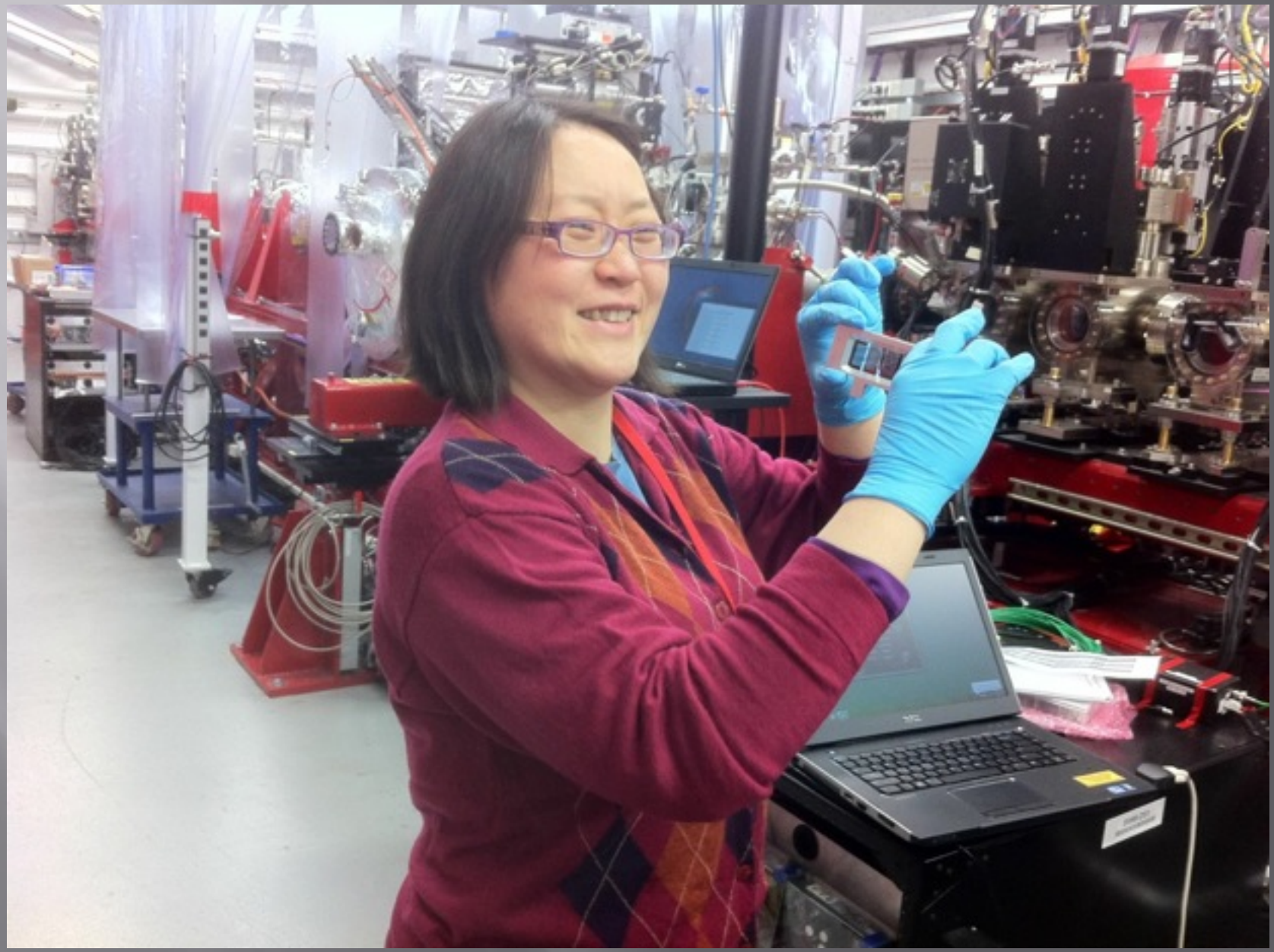

X-ray Free Electron Laser end station

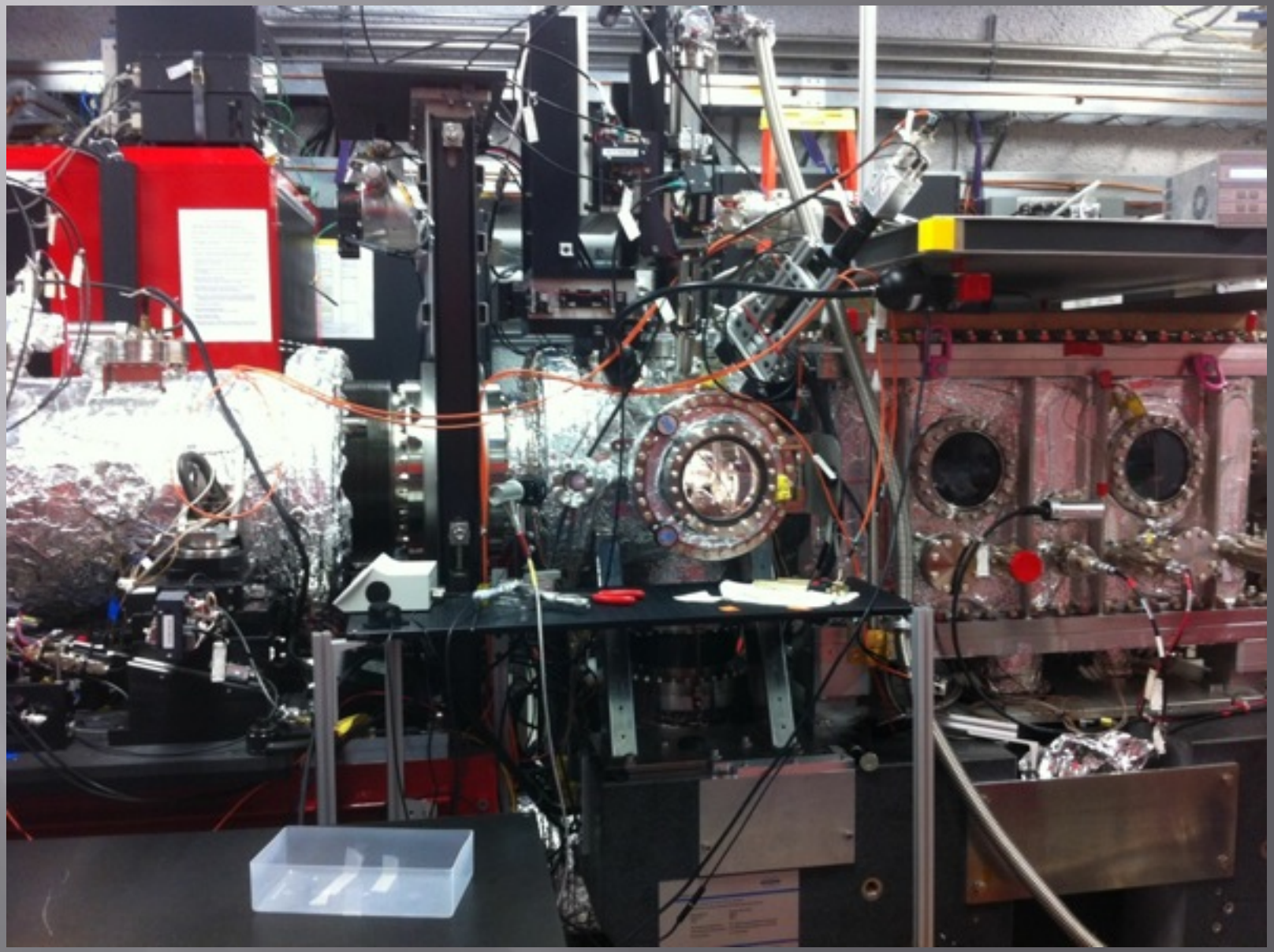

Solid support in vacuum chamber

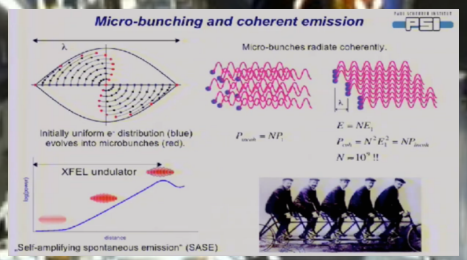

Devastating impact of a X-FEL

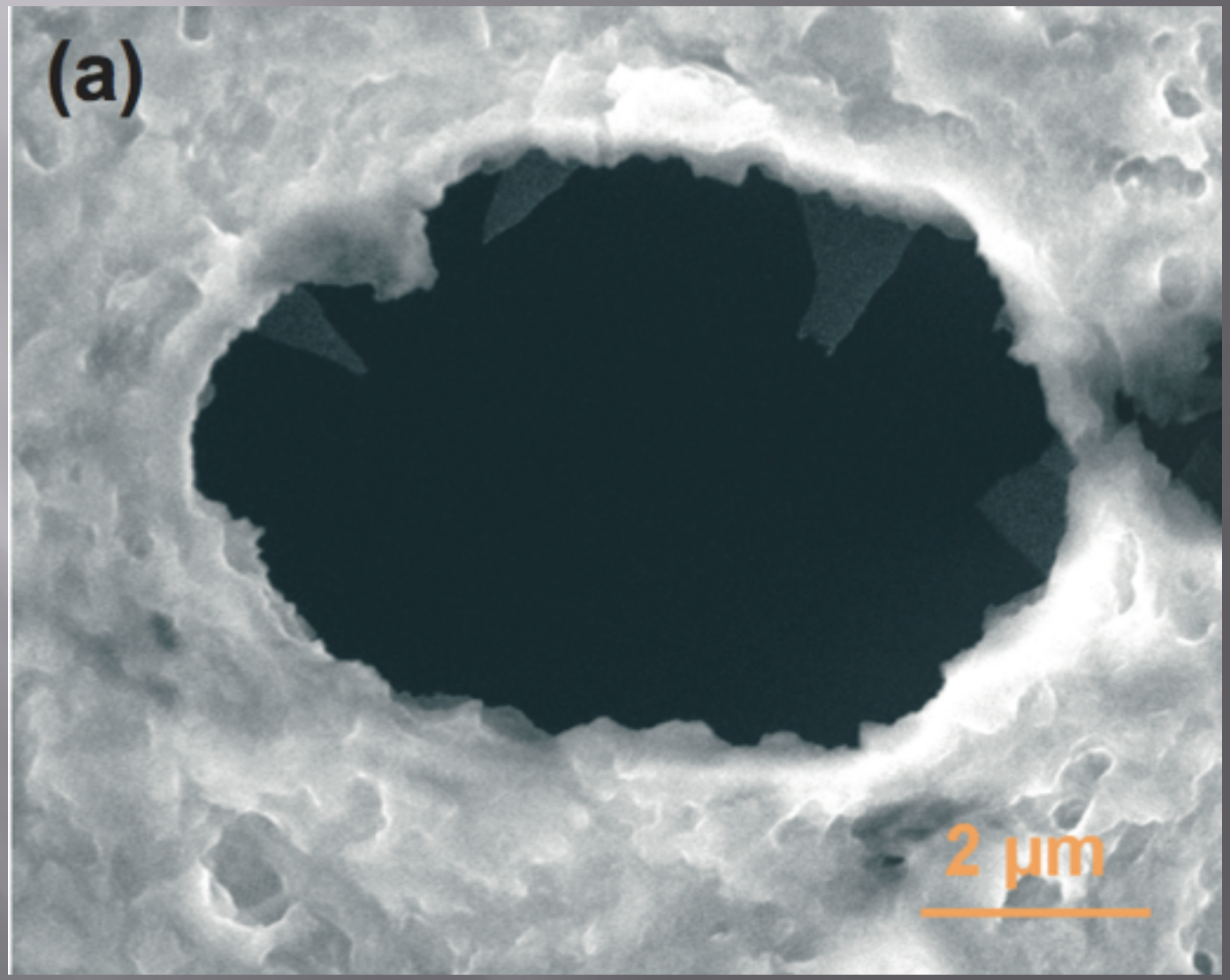

First diffraction pattern of several 2D crystal patches

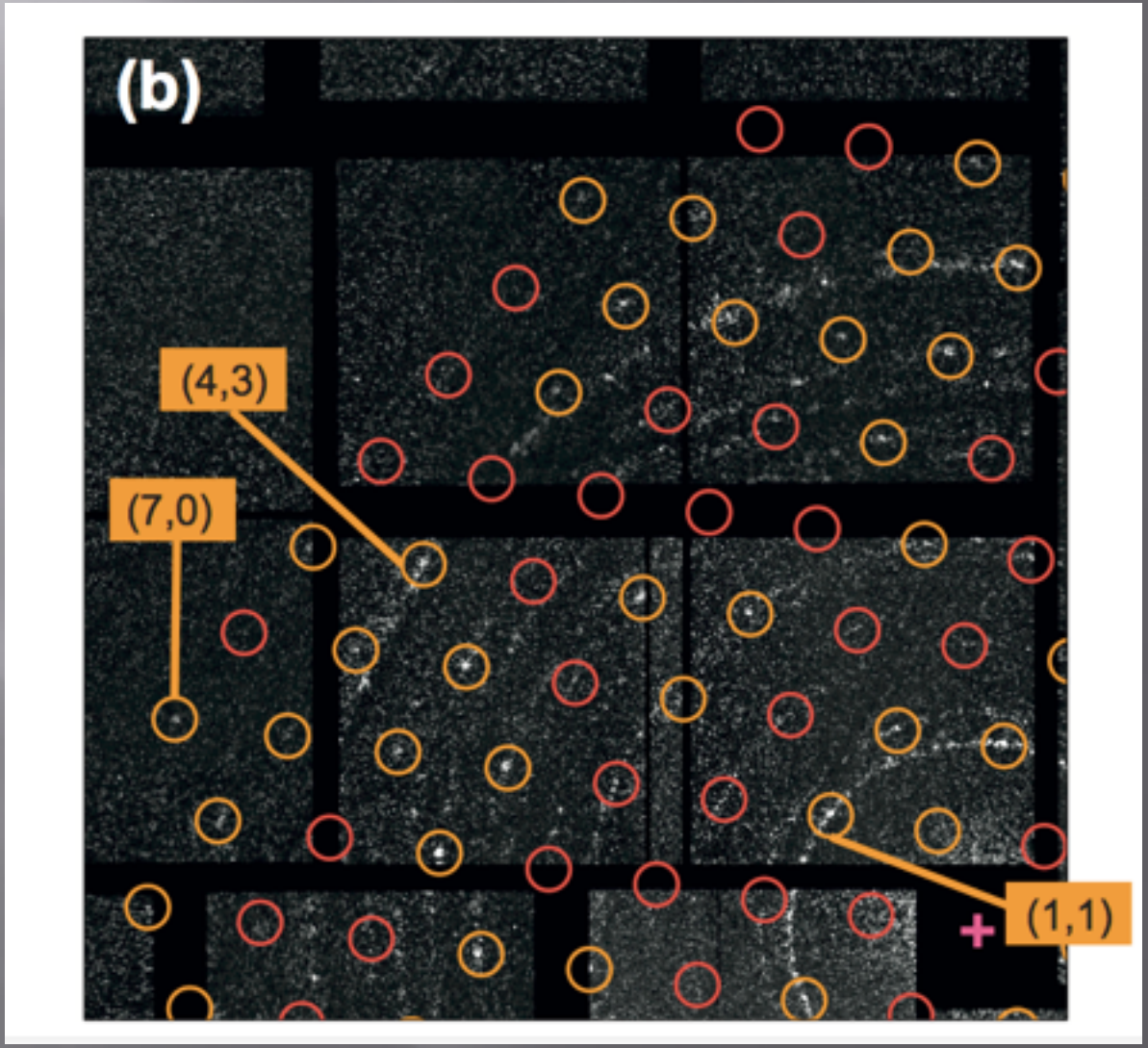

X-Ray diffraction of single 2D crystal

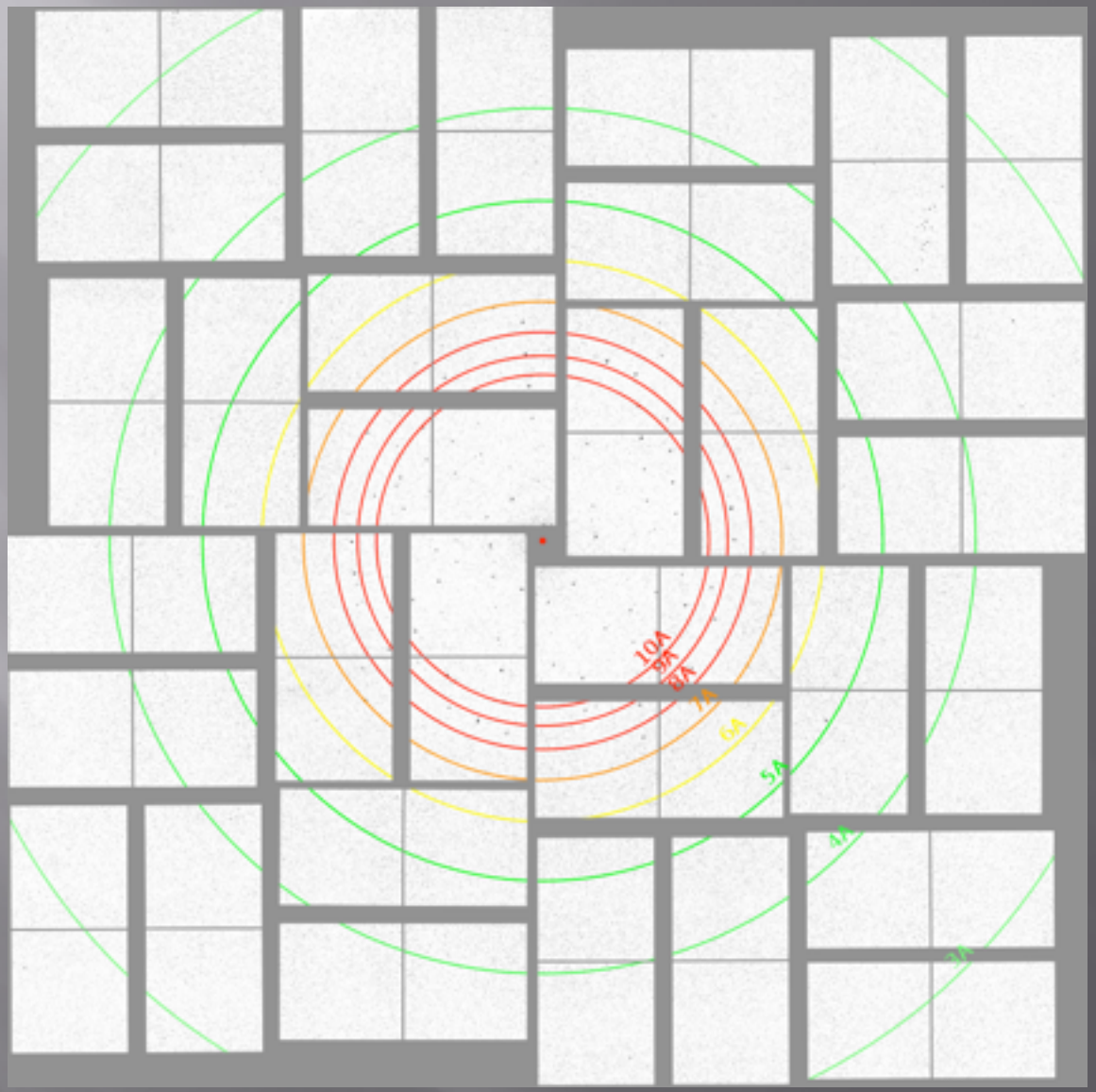

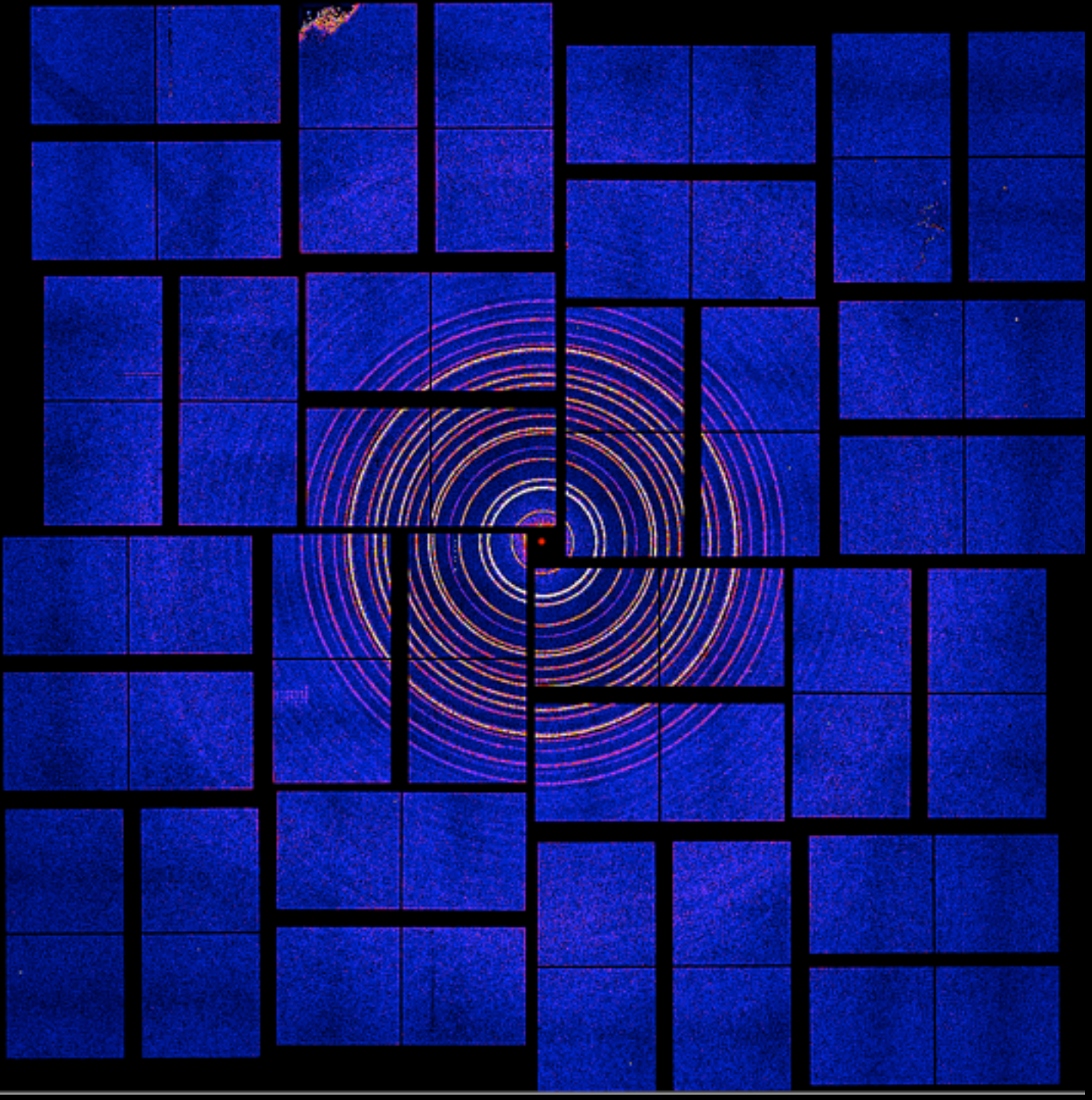

Run 0165
Averaged pattern from 104 images

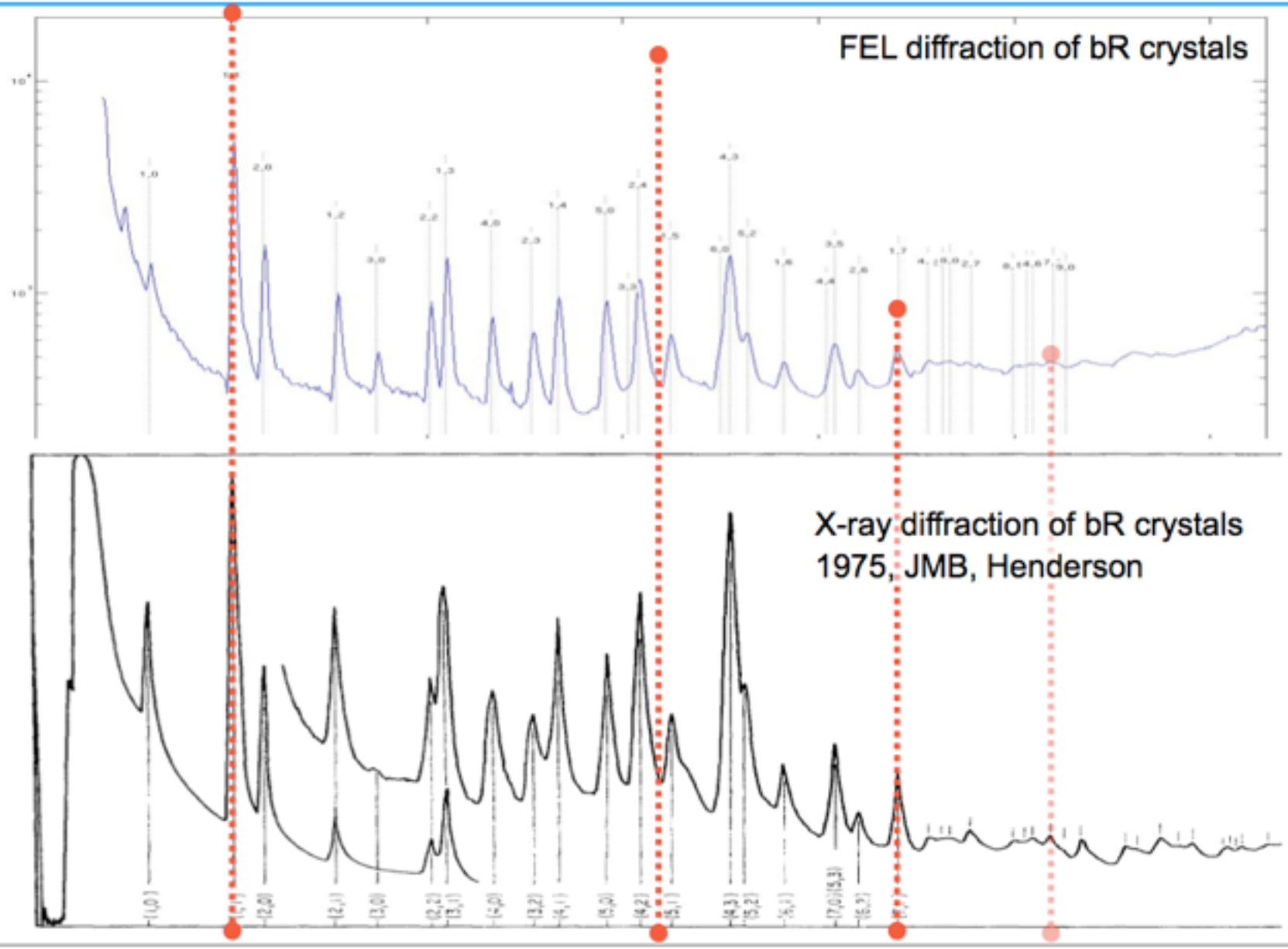
FEL diffraction of bR crystals
X-ray diffraction of bR crystals
1975, JMB, Henderson

Diffraction from 2D crystals on improved

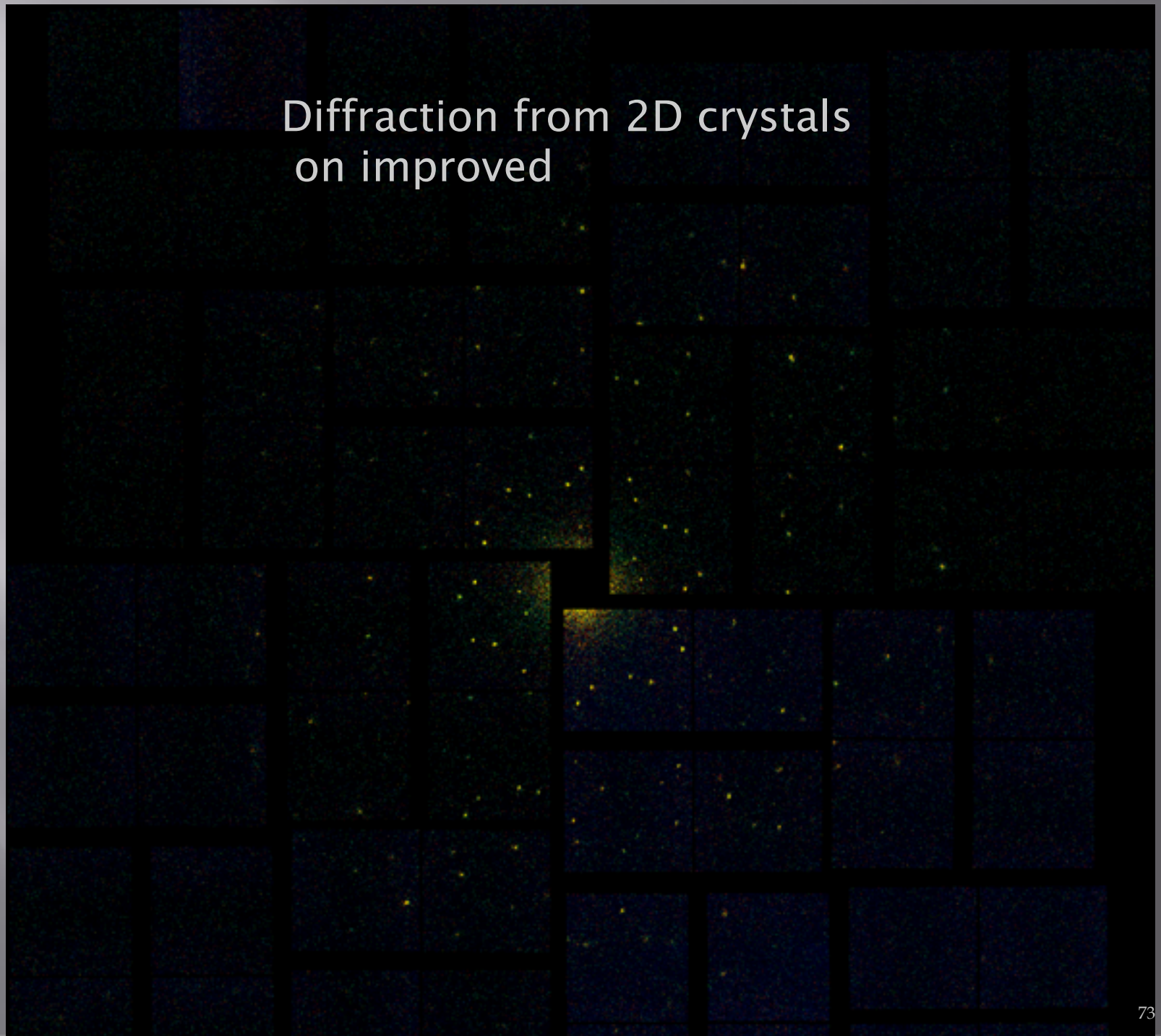

First Publikation on D2 Membrane Protein Crystal X-ray diffraction

IUCrJ
ISSN 2052-2525
BIOLOGY | MEDICINE

Received 21 October 2013
Accepted 21 January 2014

Edited by H. Chapman, DESY/Universität Hamburg, Germany

Keywords: two-dimensional protein crystal; femtosecond crystallography; single layer X-ray diffraction; membrane protein

Femtosecond X-ray diffraction from two-dimensional protein crystals

Matthias Frank,[a]* David B. Carlson,[b] Mark S. Hunter,[a] Garth J. Williams,[c] Marc Messerschmidt,[c] Nadia A. Zatsepin,[d] Anton Barty,[e] W. Henry Benner,[a] Kaiqin Chu,[f] Alexander T. Graf,[a] Stefan P. Hau-Riege,[a] Richard A. Kirian,[e] Celestino Padeste,[g] Tommaso Pardini,[a] Bill Pedrini,[g] Brent Segelke,[a] M. Marvin Seibert,[c] John C. H. Spence,[d] Ching-Ju Tsai,[g] Stephen M. Lane,[f] Xiao-Dan Li,[g] Gebhard Schertler,[g] Sebastien Boutet,[c] Matthew Coleman[a] and James E. Evans[h,b]*

[a]Lawrence Livermore National Laboratory, 7000 East Avenue, Livermore, CA 94550, USA, [b]Department of Molecular and Cellular Biology, University of California, Davis, 1 Shields Avenue, Davis, CA 95616, USA, [c]Linac Coherent Light Source, 2575 Sand Hill Road, Menlo Park, CA 94025, USA, [d]Arizona State University, 300 East University Drive, Tempe, AZ 85287, USA, [e]Center for Free-Electron Laser Science, University of Hamburg, Luruper Chaussee 149, Hamburg 22761, Germany, [f]Center for Biophotonics, 2700 Stockton Boulevard, Sacramento, CA 95817, USA, [g]Paul Scherrer Institute, 5232 Villigen PSI, Switzerland, and [h]Environmental Molecular Sciences Laboratory, Pacific Northwest National Laboratory, 3335 Innovation Boulevard, Richland, WA 99354, USA. *Correspondence e-mail: frank1@llnl.gov, james.evans@pnnl.gov

X-ray diffraction patterns from two-dimensional (2-D) protein crystals obtained using femtosecond X-ray pulses from an X-ray free-electron laser (XFEL) are presented. To date, it has not been possible to acquire transmission X-ray diffraction patterns from individual 2-D protein crystals due to radiation damage. However, the intense and ultrafast pulses generated by an XFEL permit a new method of collecting diffraction data before the sample is destroyed. Utilizing a diffract-before-destroy approach at the Linac Coherent Light Source, Bragg diffraction was acquired to better than 8.5 Å resolution for two different 2-D protein crystal samples each less than 10 nm thick and maintained at room temperature. These proof-of-principle results show promise for structural analysis of both soluble and membrane proteins arranged as 2-D crystals without requiring cryogenic conditions or the formation of three-dimensional crystals.

First Publikation on D2 Membrane Protein Crystal X-ray diffraction

Submitted to Phil. Trans. R. Soc. B - Issue

7 Å resolution in protein 2D-crystal X-ray diffraction at LCLS

Bill Pedrini*[1], Ching-Ju Tsai[1], Guido Capitani[1], Celestino Padeste[1], Mark S. Hunter[2], Nadia A. Zatsepin[4], Anton Barty[5], W. Henry Benner[2], Sébastien Boutet[6], Geoffrey K. Feld[2], Stefan P. Hau-Riege[2], Richard A. Kirian[5], Christopher Kupitz[4], Marc Messerschmitt[6], John I. Ogren[7], Tommaso Pardini[2], Brent Segelke[2], Garth J. Williams[6], John C. H. Spence[4], Rafael Abela[1], Matthew Coleman[2], James E. Evans[3], Gebhard Schertler[1], Matthias Frank†[2], and Xiao-Dan Li‡[1]

[1]Paul Scherrer Institute, 5232 Villigen PSI, Switzerland
[2]Lawrence Livermore National Laboratory, 7000 East Avenue, Livermore, CA, 94550, USA
[3]Environmental Molecular Sciences Laboratory, Pacific Northwest National Laboratory, 3335 Innovation Blvd., Richland, WA, 99354, USA
[4]Arizona State University, 300 E. University Dr., Tempe, AZ, 85287, USA
[5]Center for Free-Electron Laser Science, DESY, Notkestrasse 85, 22607 Hamburg, Germany
[6]Linac Coherent Light Source, 2575 Sand Hill Road, Menlo Park, CA, 94025, USA
[7]Physiscs Departement, Boston University, 590 Commonwealth Ave, Boston, MA, 02215, USA

January 22, 2014

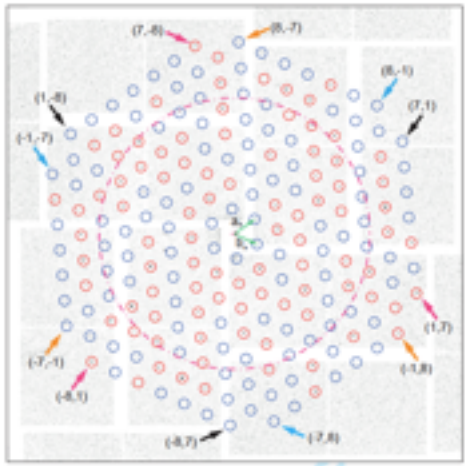

Figure 1: Example of a diffraction image from a single bR 2D crystal. The dashed ring corresponds to 10 Å resolution. The circles mark the positions of expected diffraction peaks at lower than 7 Ångström. The precise orientation of the peak lattice was derived from the positions of the prominent, easily identifiable peaks encircled in red. The basis vectors (a_r, b_r) of the 2D reciprocal space lattice are shown as green arrows. The small arrows mark the position of peaks in the classes ((7, 1)) (black), ((3, 7)) (magenta), ((−7, −1)) (orange) and ((−1, −7)) (cyan), each class consisting of three equivalent peaks.

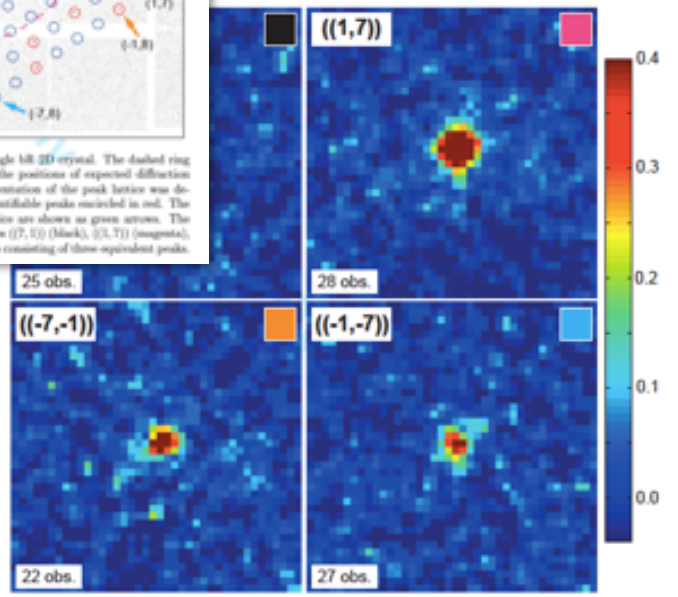

Figure 3: Examples of "image sector sums" (see text) for the four peak classes ((7, 1)), ((−7, −1)), ((1, 7)) and ((−1, −7)), all at 7.2 Å resolution. For each peak, the number of observations is indicated, and the color in the small box at the top right of each panel corresponds to that of the arrows in Figure 1. The intensity color scale is the same for all four panels. Maximum intensity is about 40 times the background noise, calculated as the average on all image sector sums of the local noise level measured away from the central peak region.

Lipidic Cubic Phase Crystallization

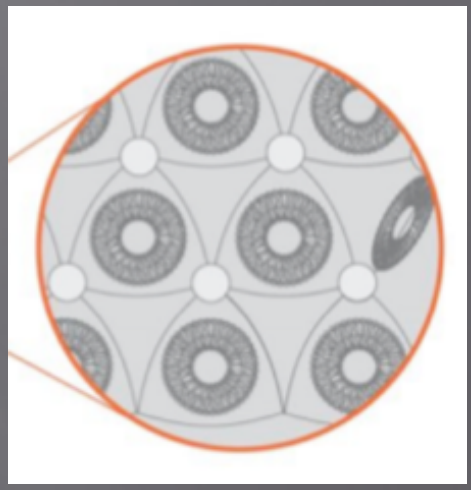

- Our membrane protein structures have often moderate resolution
- Lipidic Cubic Phase (LCP) crystallization produces often membrane protein crystals with Type I packing of molecules
- The new crystal forms can show increased order
- This way can get better resolution membrane protein structures
- Still a number of technical issues in practice

MRC Robotic Cubic Lipidic Phase Dispendser

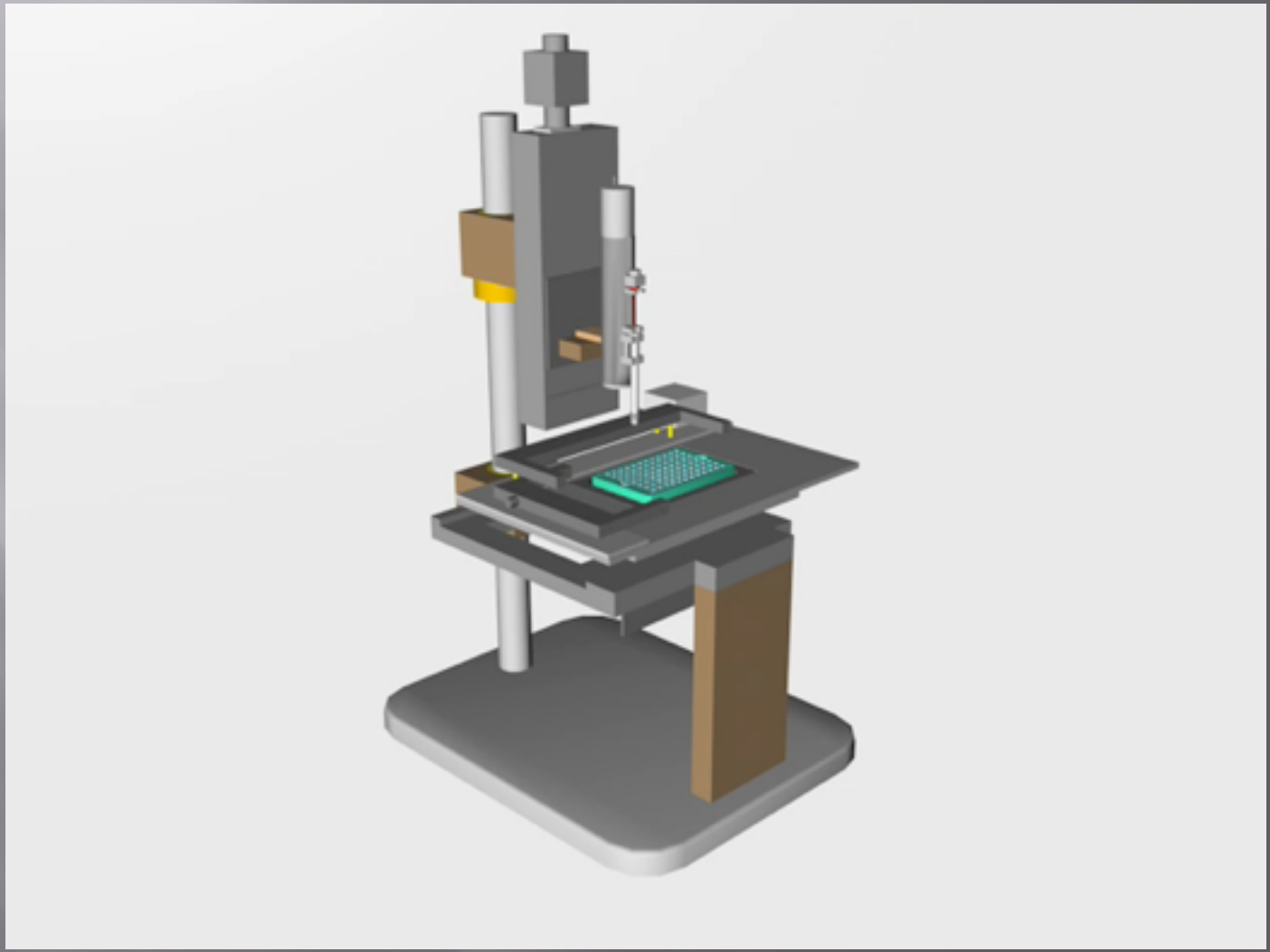

100nL dispense on UV transparent 96 well plate

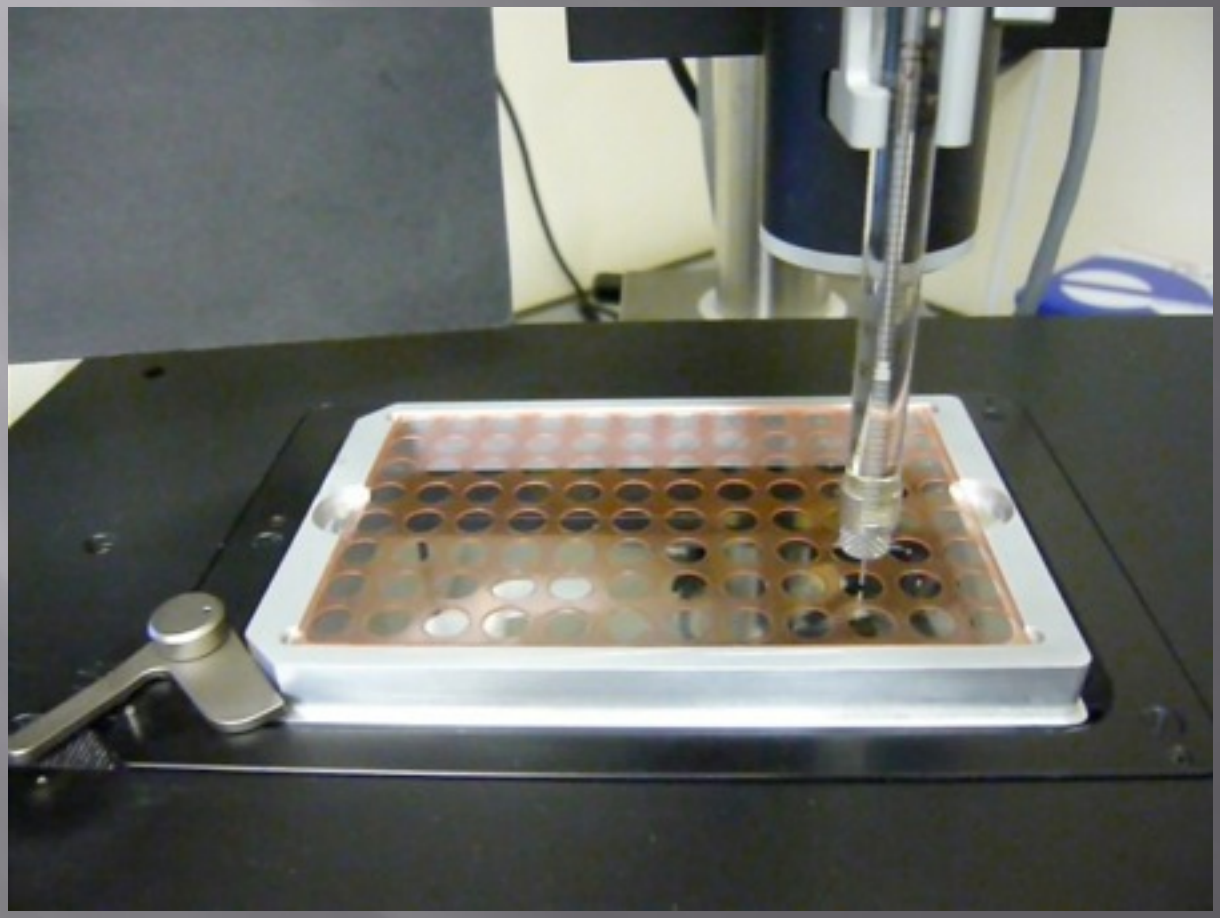

LCP crystals of stabilised beta 1 adrenergic receptor

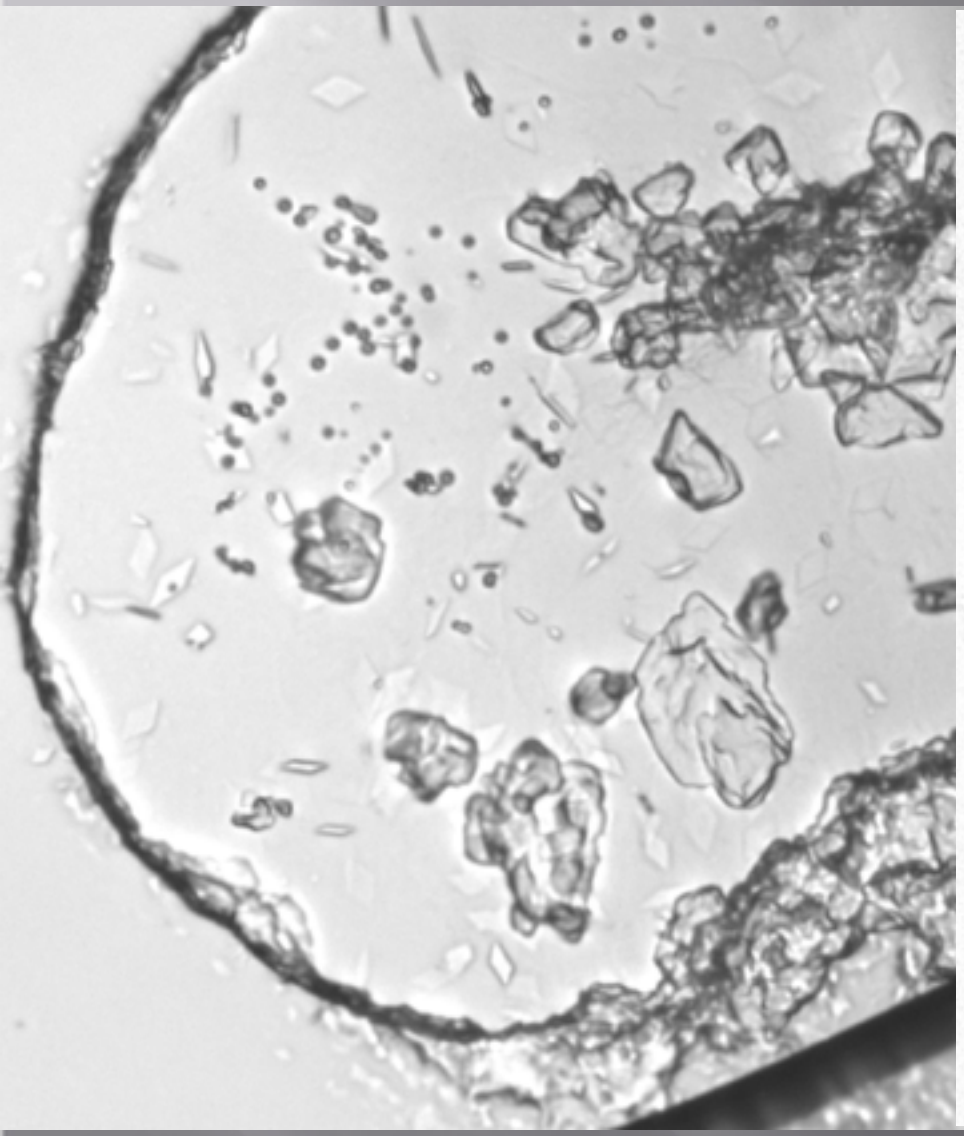

Visible light

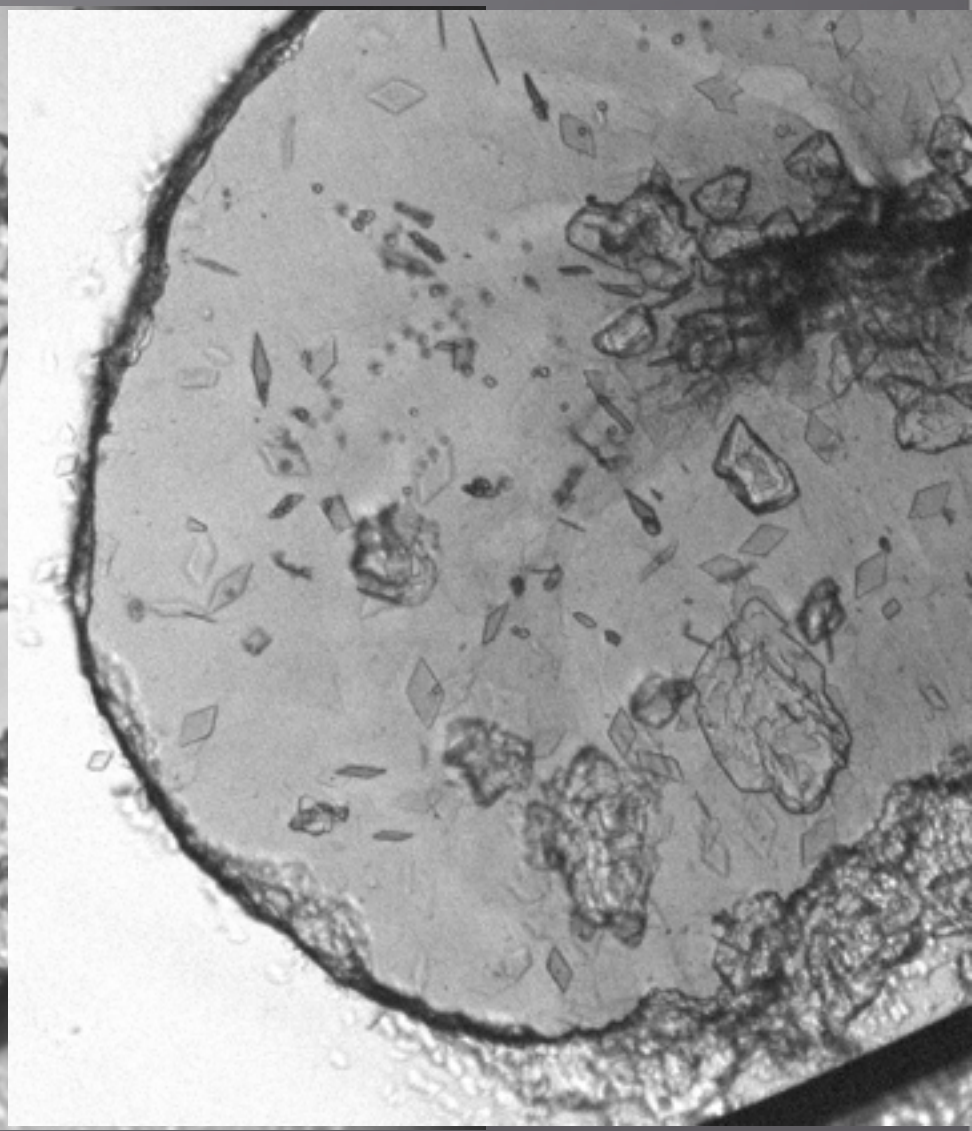

UV image 280 nm

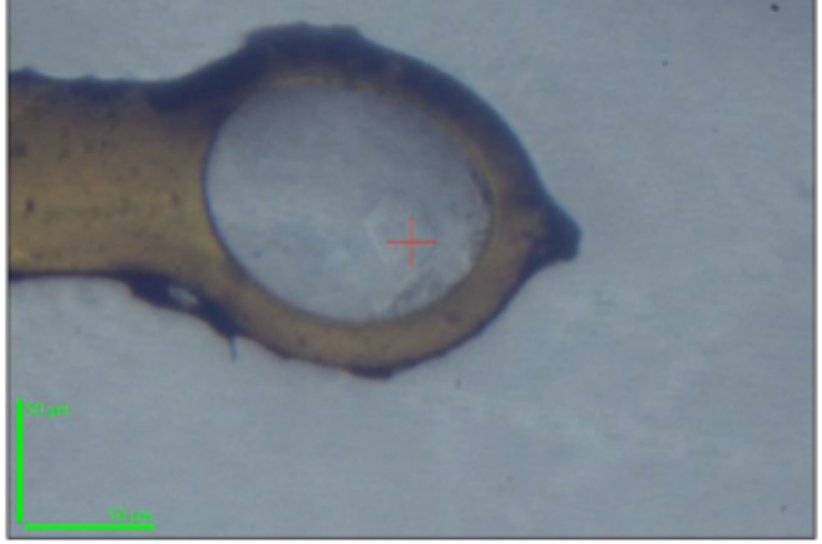

X-Ray Source Brilliance

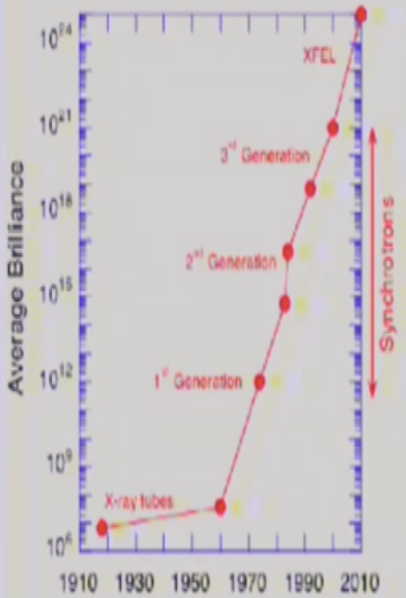

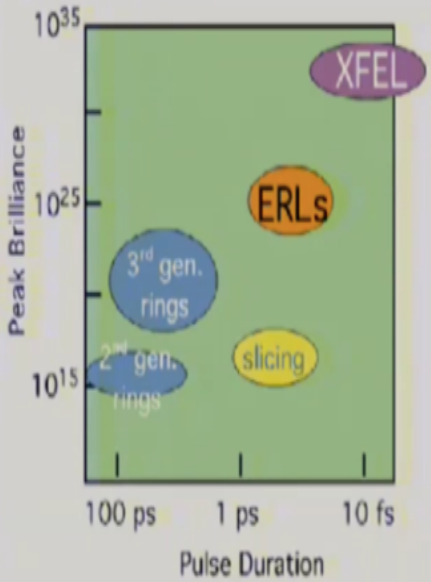

brilliance =

photons / time / area / solid-angle / energy-bandwidth

2.4 Å

Stabilisd beta 1 adrenergic receptor
Type I membrane protein crystal packing

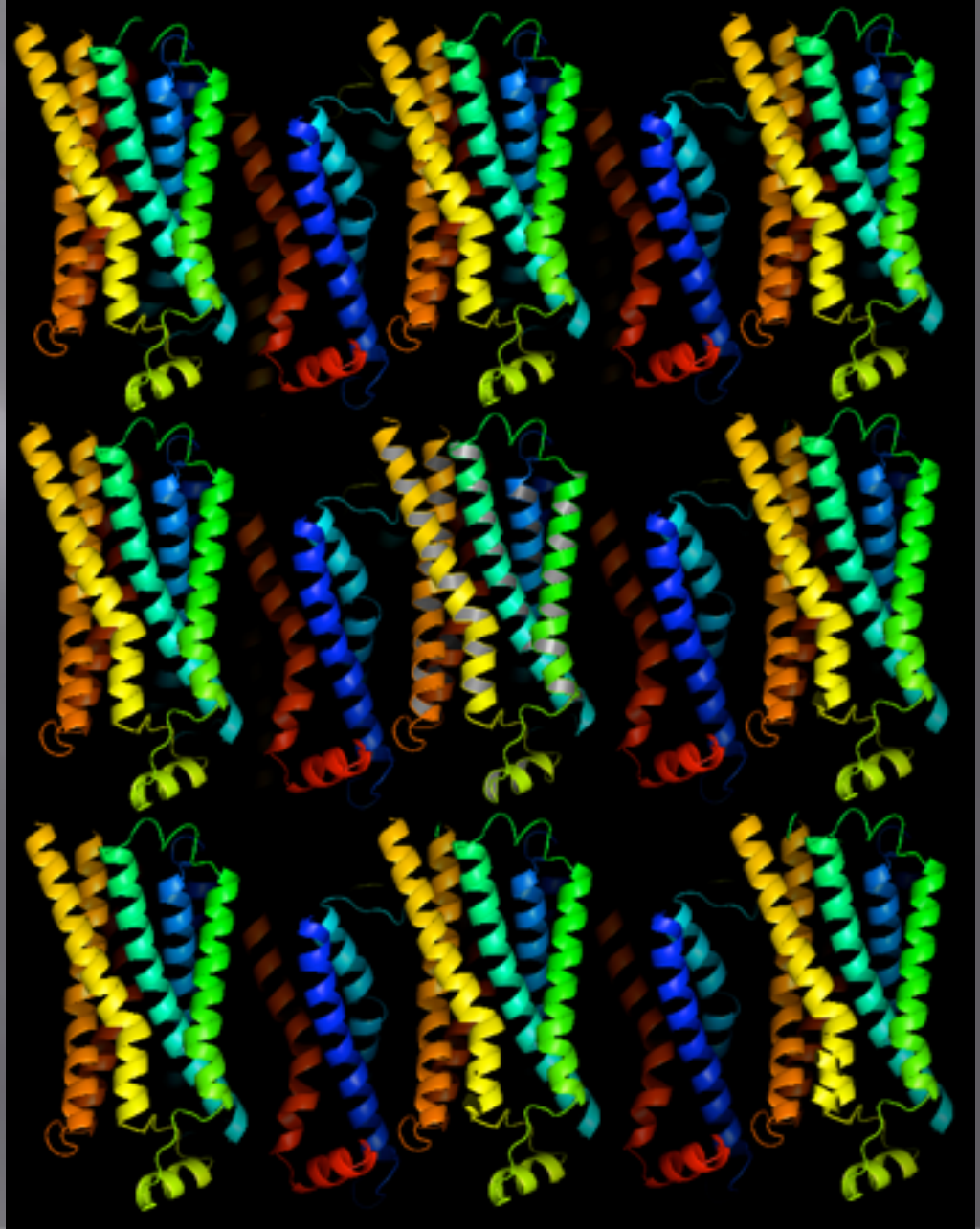

$\beta_1$adrenergic receptor LCP crystals

Spacegroup: P 2_1 2 2_1

Cell: a=54.4Å b=61.6Å c=94.3Å

$\alpha = \beta = \gamma = 90°$

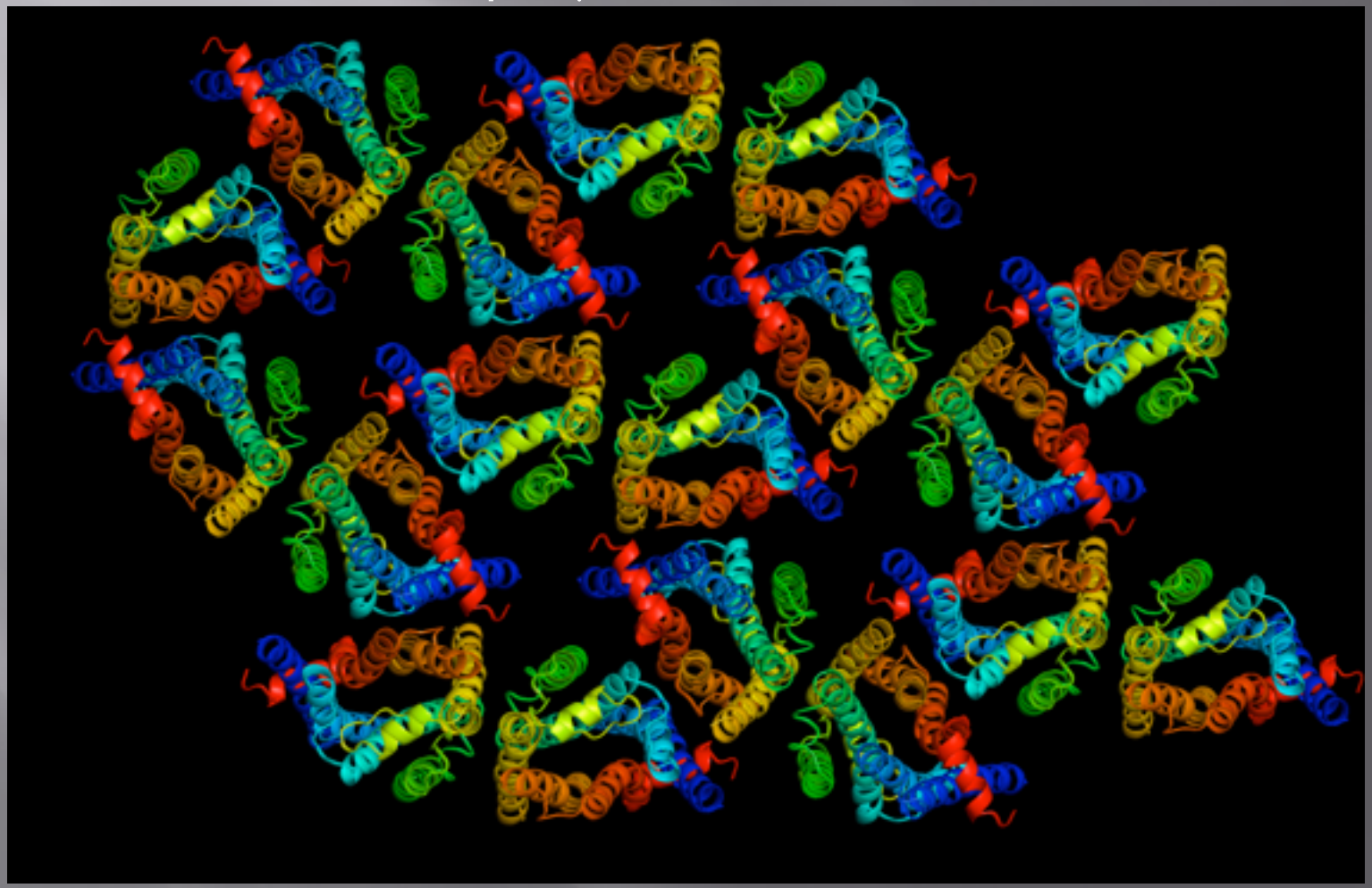

100nL dispense on UV transparent 96 well plate

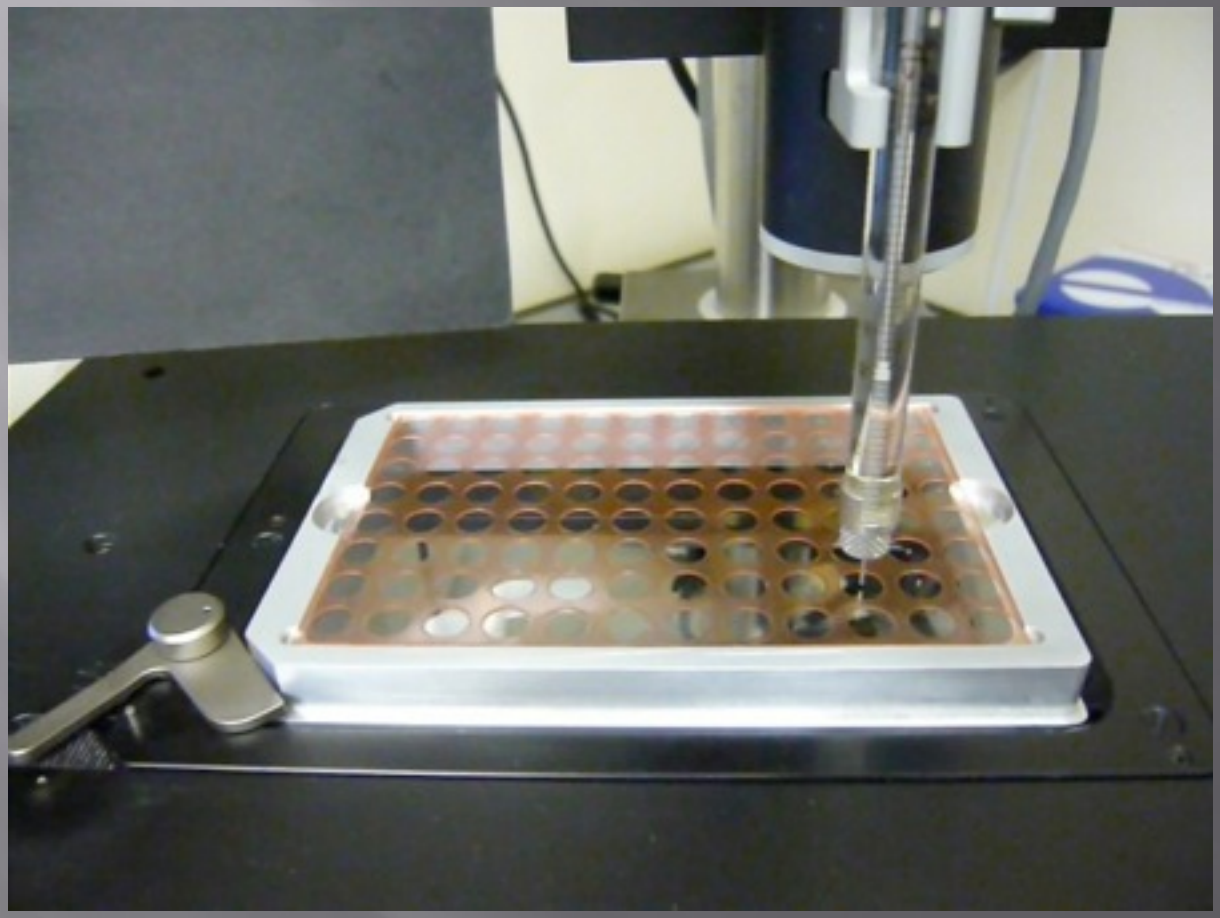

TTP LabTech launches dedicated instrument for lipidic cubic phase screening

TTP LabTech are pleased to announce the launch of mosquito® LCP. Developed in collaboration with senior researchers from the MRC, UK (Gebhard Schertler and Pat Edwards), this instrument facilitates the automation and increased throughput of lipidic cubic phase (LCP) crystallisation set-ups. This novel automation system enables LCP screening to be performed accurately and with ease.

The LCP technique for crystallising membrane proteins can be difficult and time-consuming to set up by hand as it utilises highly viscous lipid mesophases to reconstitute proteins. TTP LabTech has overcome these problems with mosquito® LCP, a dedicated pipetting instrument for automated LCP screening set-up. This new product boasts the full functionality of the renowned mosquito product, whilst incorporating technical innovations specific for LCP techniques.

Using a positive displacement syringe with automated tip positioning, mosquito LCP provides accurate and repeatable dispensing of the LCP drops. The precise positioning of the LCP material also facilitates automated imaging of membrane protein crystals in a range of high density plate types. Mosquito® LCP provides significant benefits over manual processes due to the use of its unique disposable tip technology. For the precipitant additions step, this not only guarantees zero cross-contamination, but negates the need for time-consuming tip washing. Subsequently, high throughput rates of more than eight 96- well plates per hour are easily achieved and evaporation of the dispensed LCP is minimised.

'The mosquito® is already being used extensively for automated, high throughput protein crystallisation in sitting drop, hanging drop and micro batch applications,' commented Gebhard Schertler from the MRC 'This new instrument now extends the applications of the mosquito® to the LCP technique. The mosquito® LCP will be an invaluable addition to any membrane protein crystallisation laboratory.'

www.ttplabtech.com

european pharmaceutical review digital

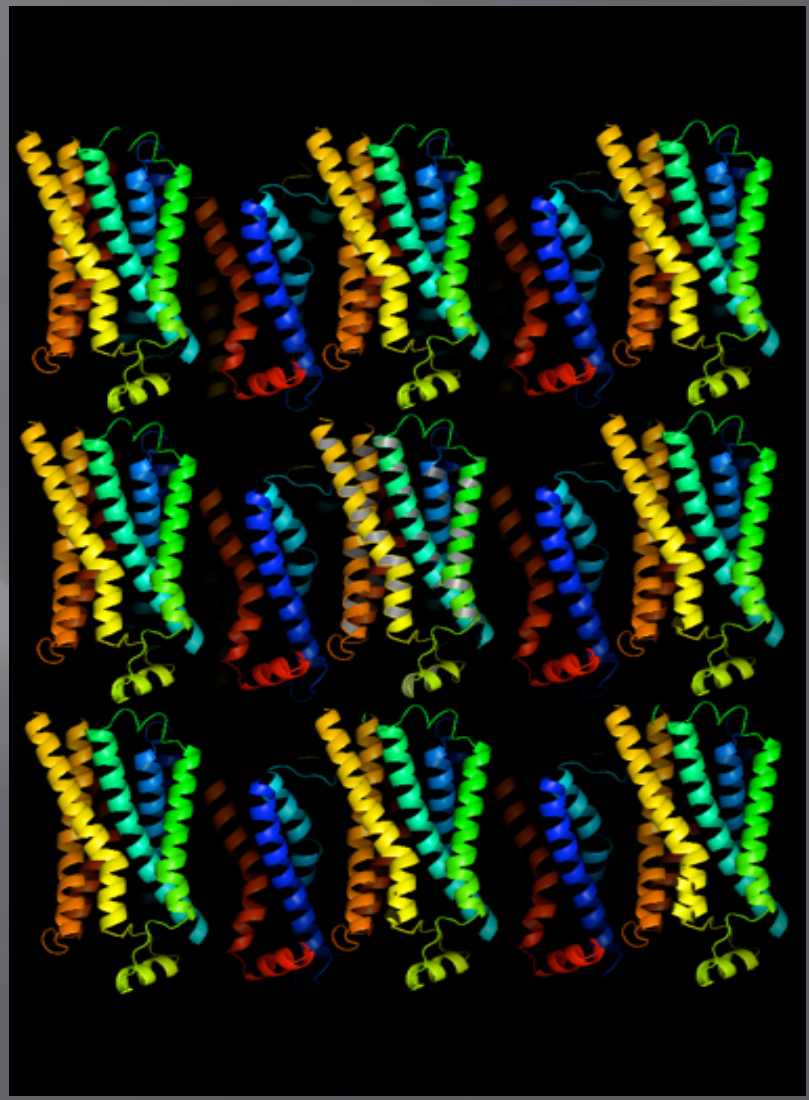

LCP crystals of stabilized beta 1 adrenergic receptor

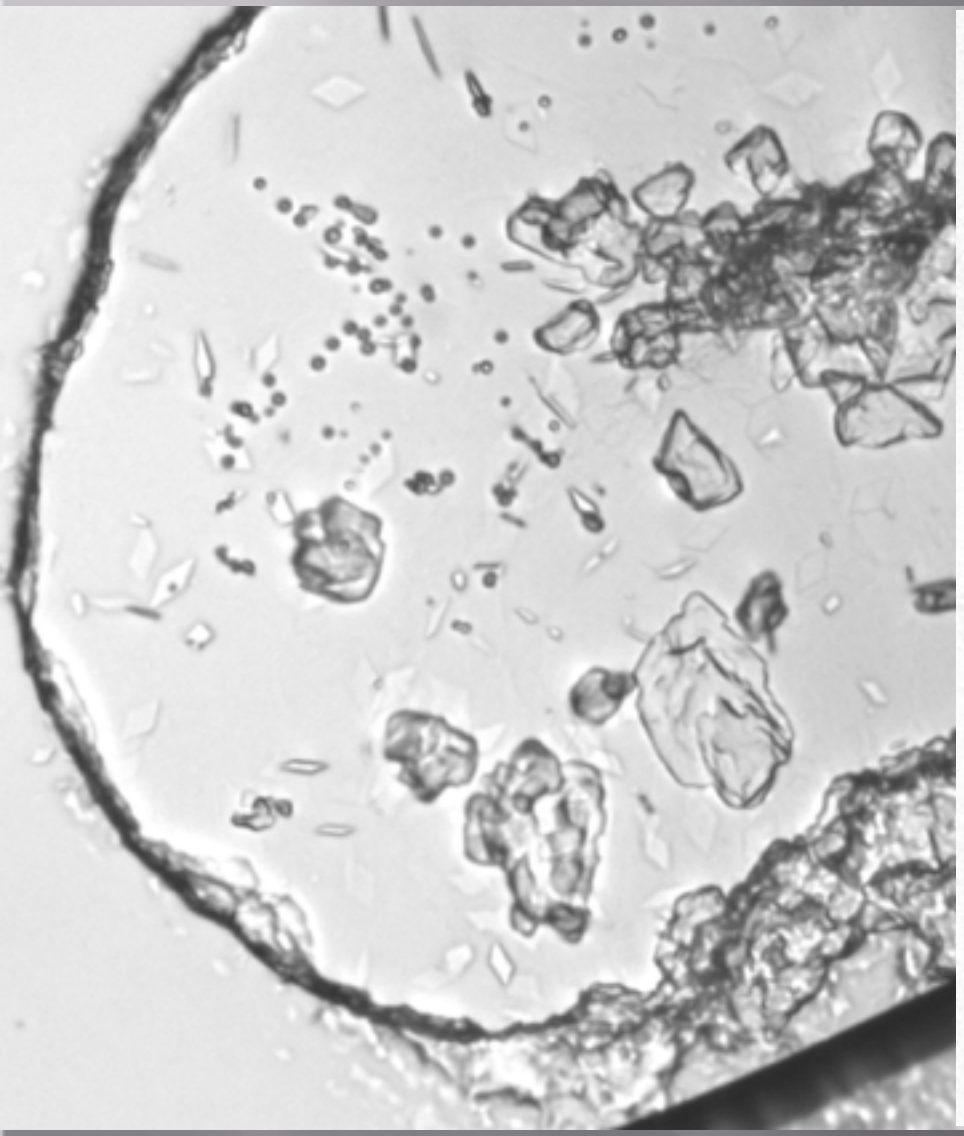

Visible light

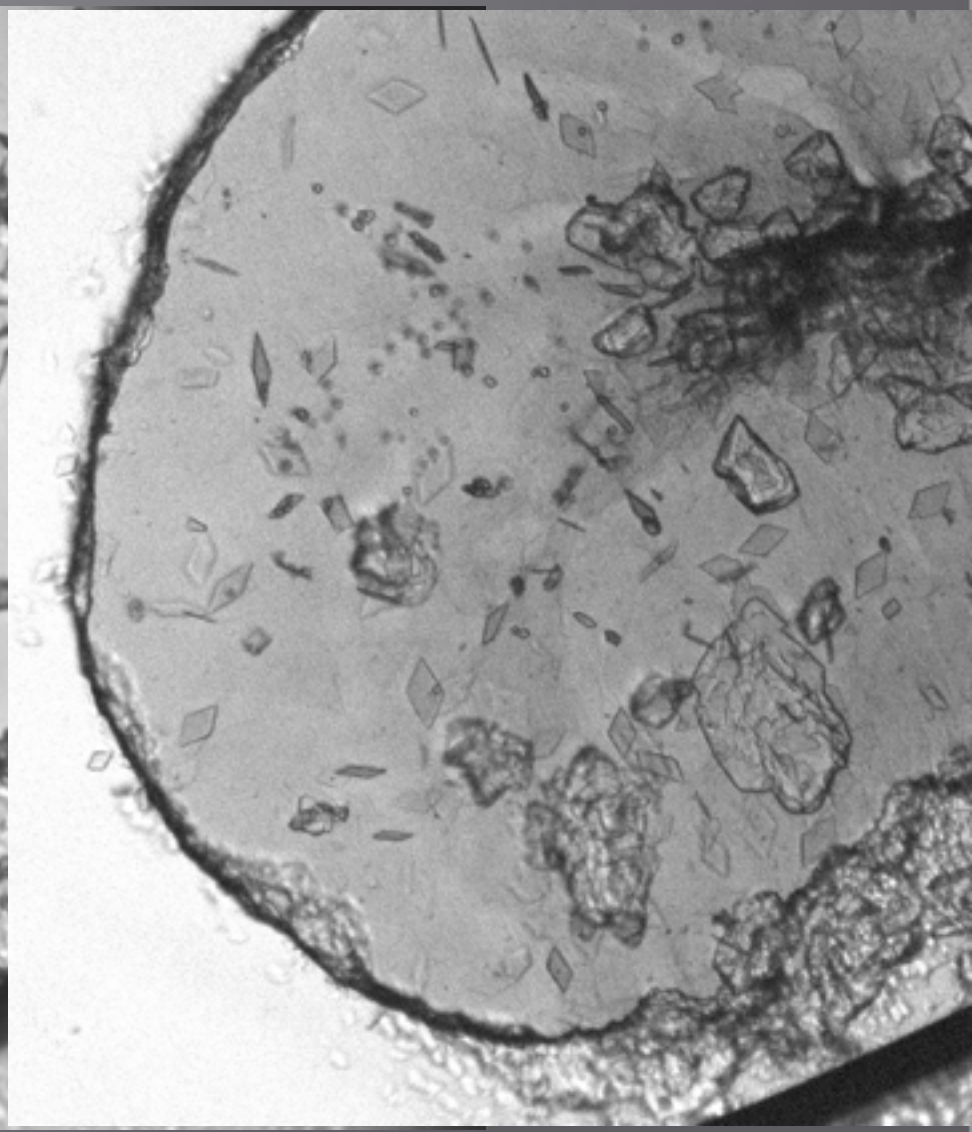

UV image 280 nm

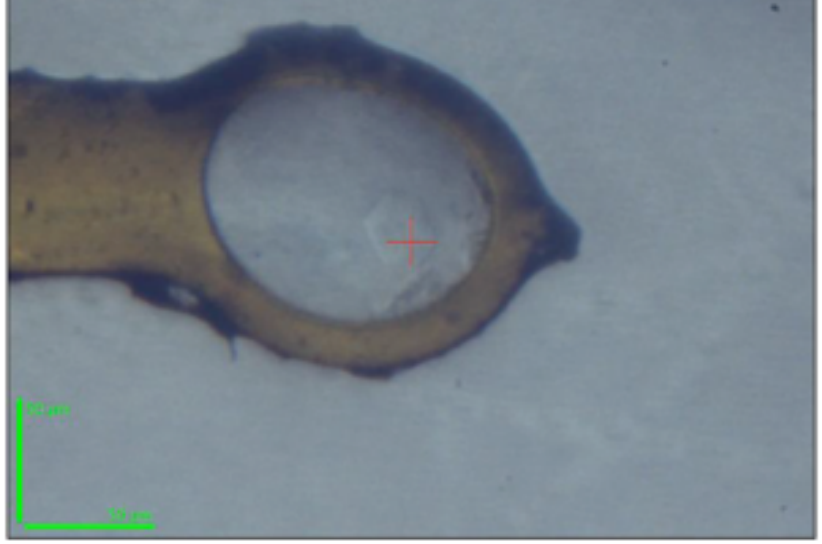

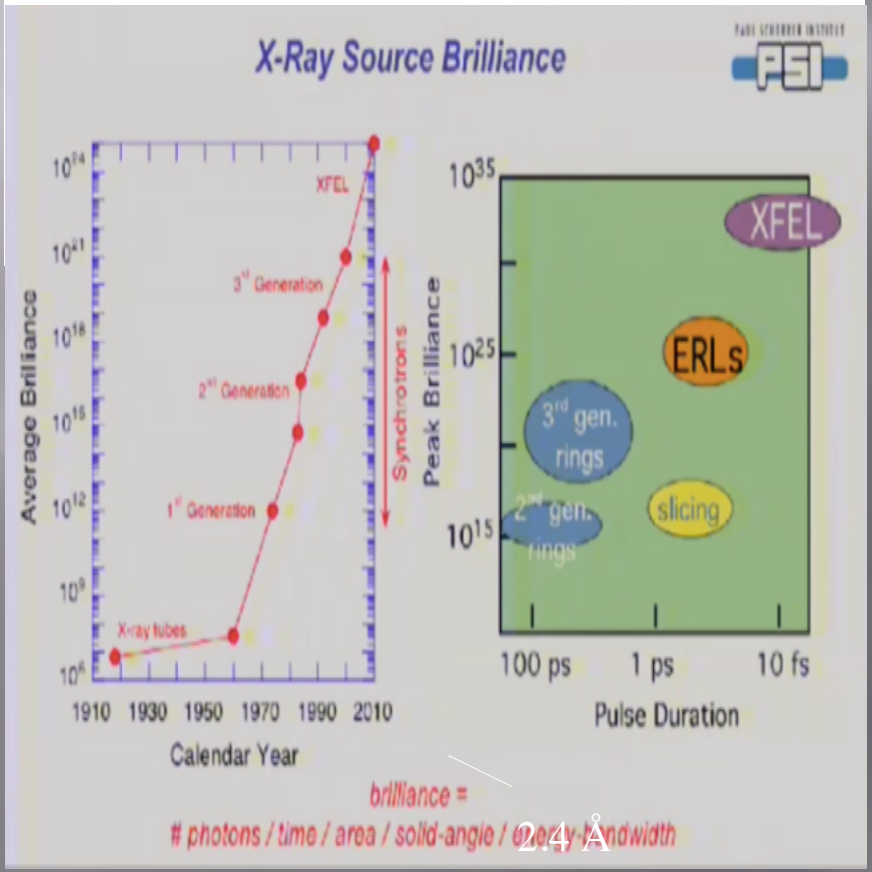

Stabilisd beta 1 adrenergic receptor
Type I membrane protein crystal packing

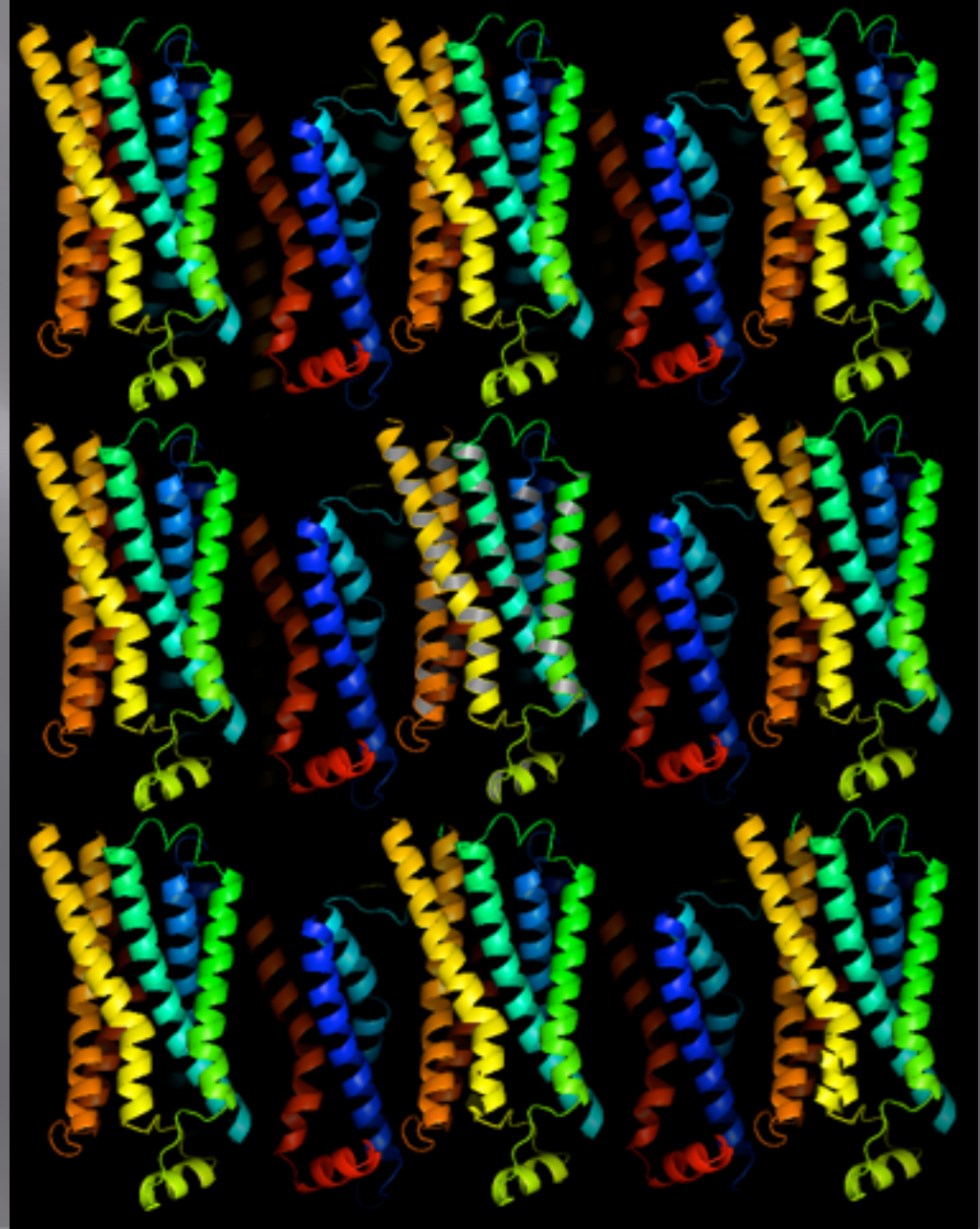

2.4 Å

PAUL SCHERRER INSTITUTE

Basic XFEL design

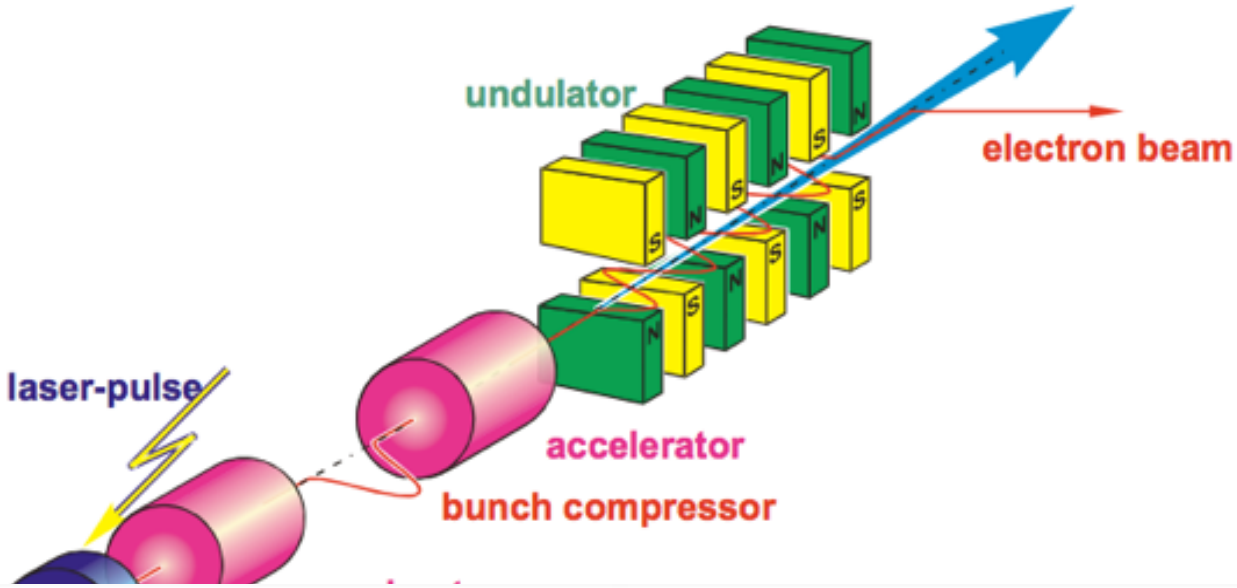

The 2.1 Å Resolution Structure of Cyanopindolol-Bound β_1-Adrenoceptor Identifies an Intramembrane Na^+ Ion that Stabilises the Ligand-Free Receptor

Jennifer L. Miller-Gallacher[¤a], Rony Nehmé[], Tony Warne, Patricia C. Edwards, Gebhard F. X. Schertler[¤b¤c], Andrew G. W. Leslie, Christopher G. Tate*

Structural Studies Division, MRC Laboratory of Molecular Biology, Cambridge, Cambridgeshire, United Kingdom

Lipidic Cubic Phase crystallization for SFX

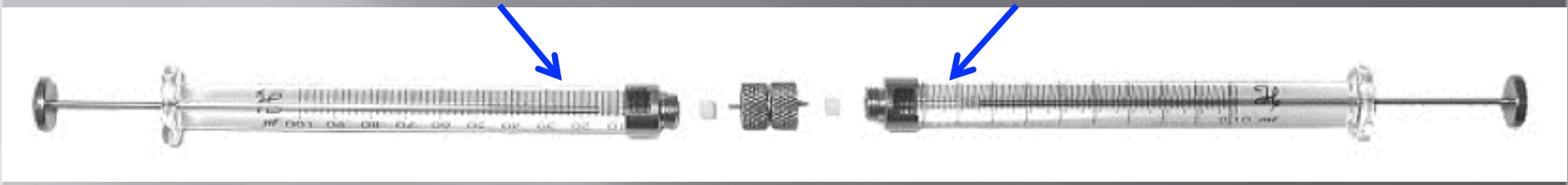

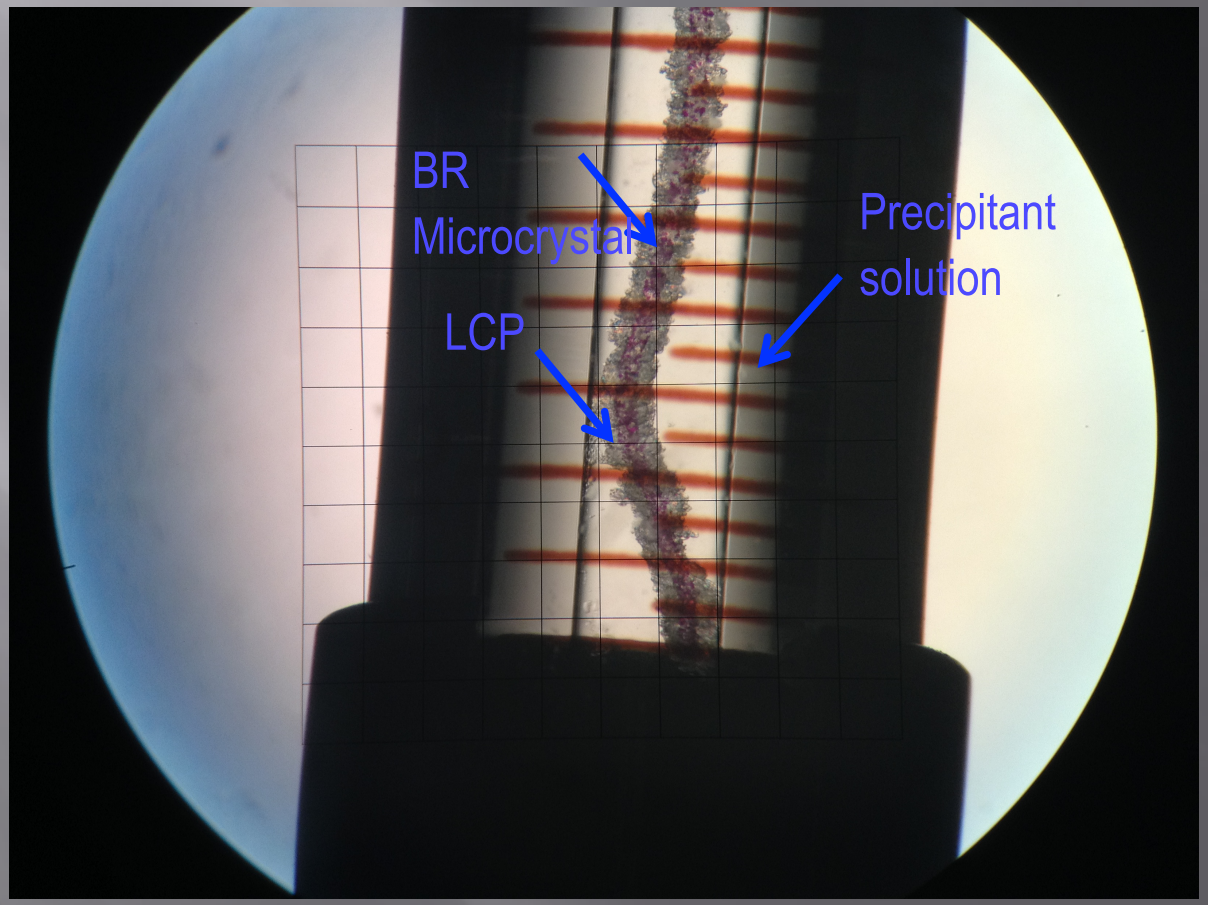

Lipidic cubic phase (LCP) Jet injector

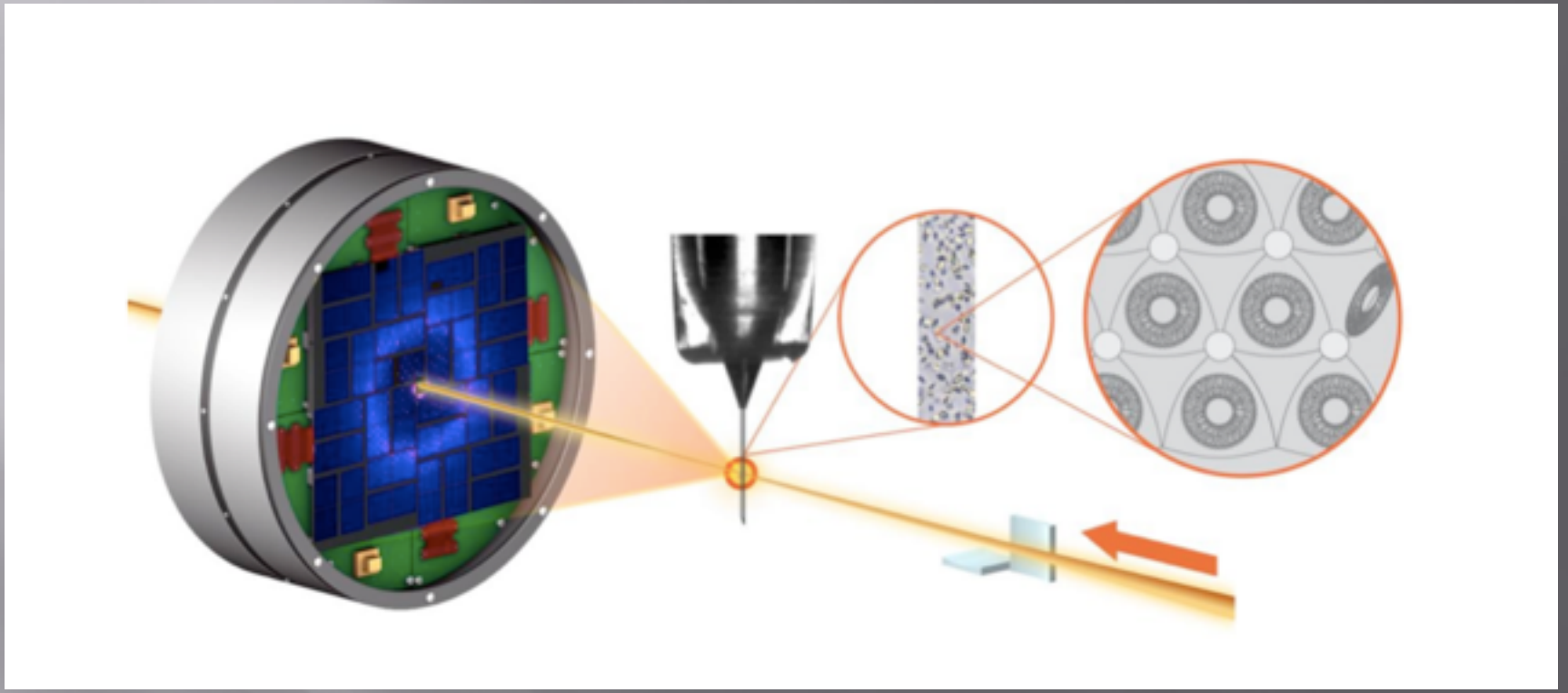

Experimental setup for SFX data collection using an LCP injector

AIP | Review of Scientific Instruments

Injector for scattering measurements on fully solvated biospecies

U. Weierstall, J. C. H. Spence, and R. B. Doak

LCP Jet

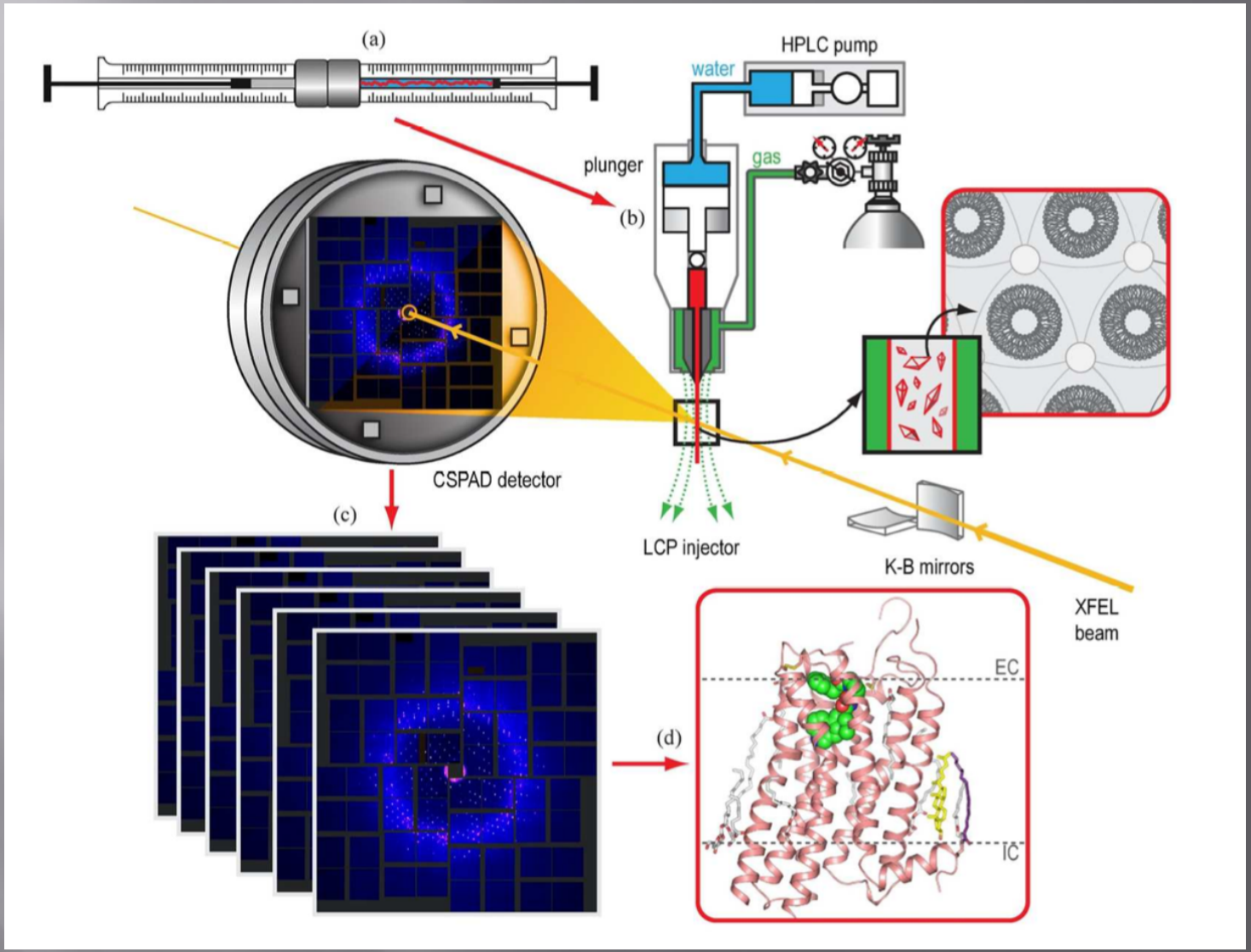

AIP Review of Scientific Instruments

Injector for scattering measurements on fully solvated biospecies

U. Weierstall, J. C. H. Spence, and R. B. Doak

LCP Jet

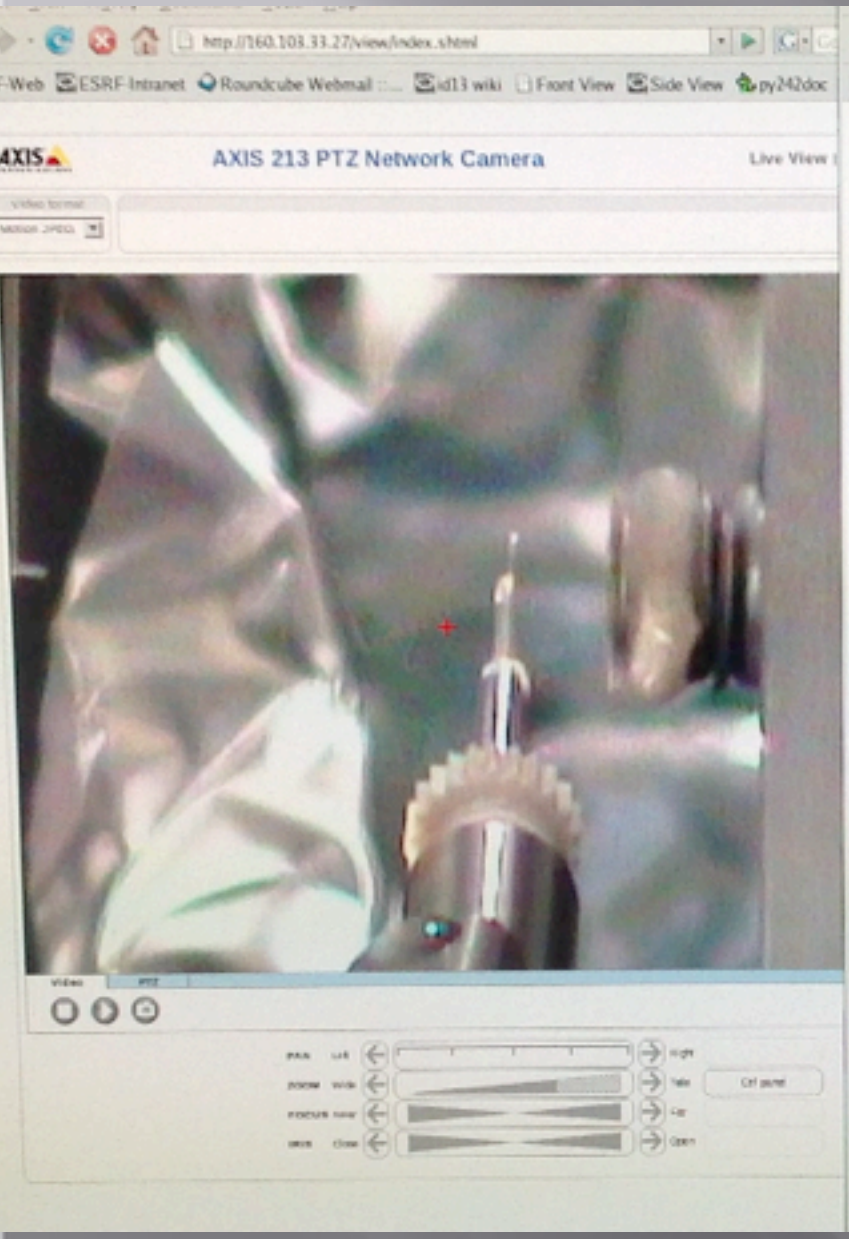
AXIS 213 PTZ Network Camera
Live View

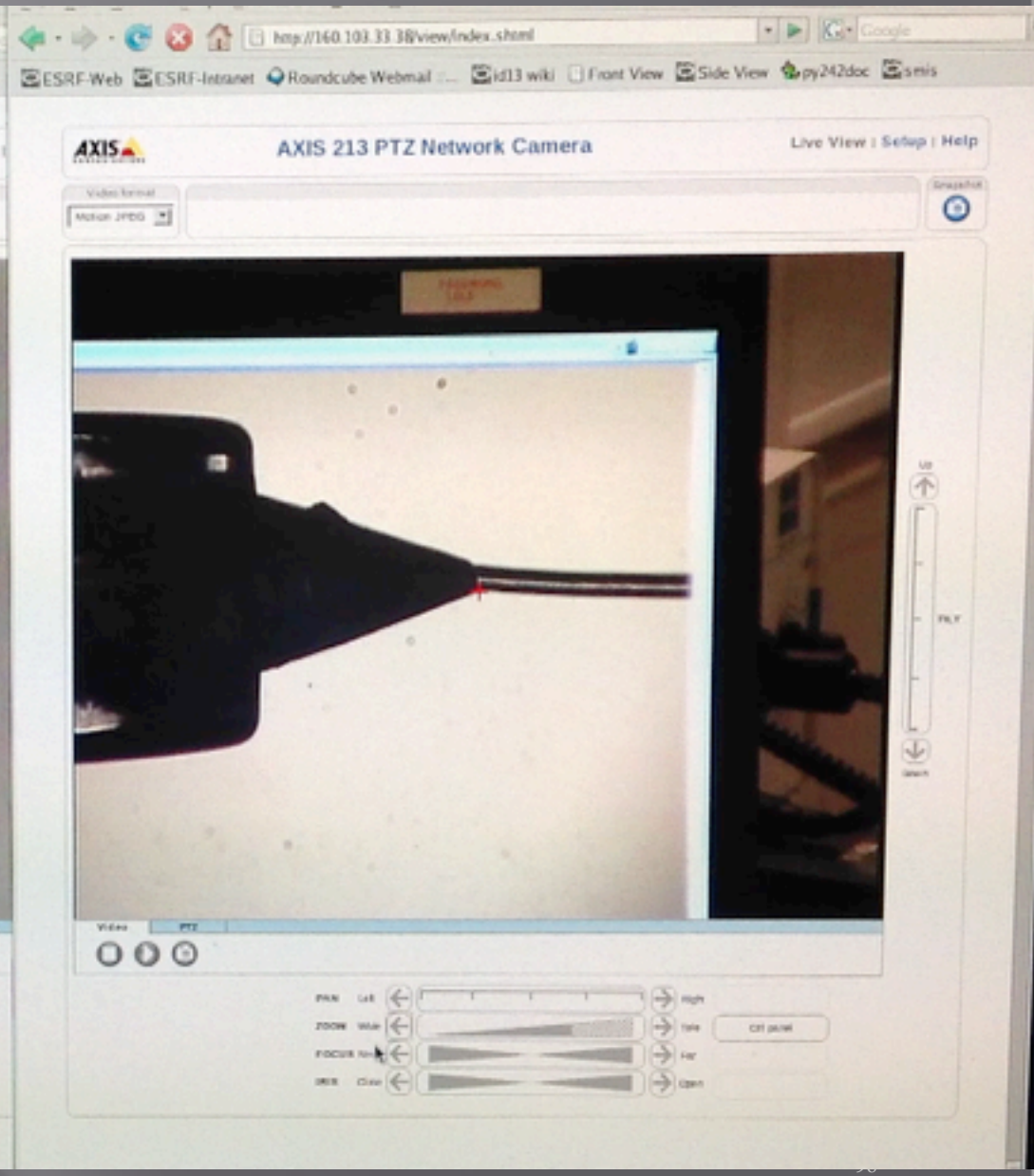
AXIS 213 PTZ Network Camera
Live View | Setup | Help

Data collection with LCP Jet
NANOMEM consortium

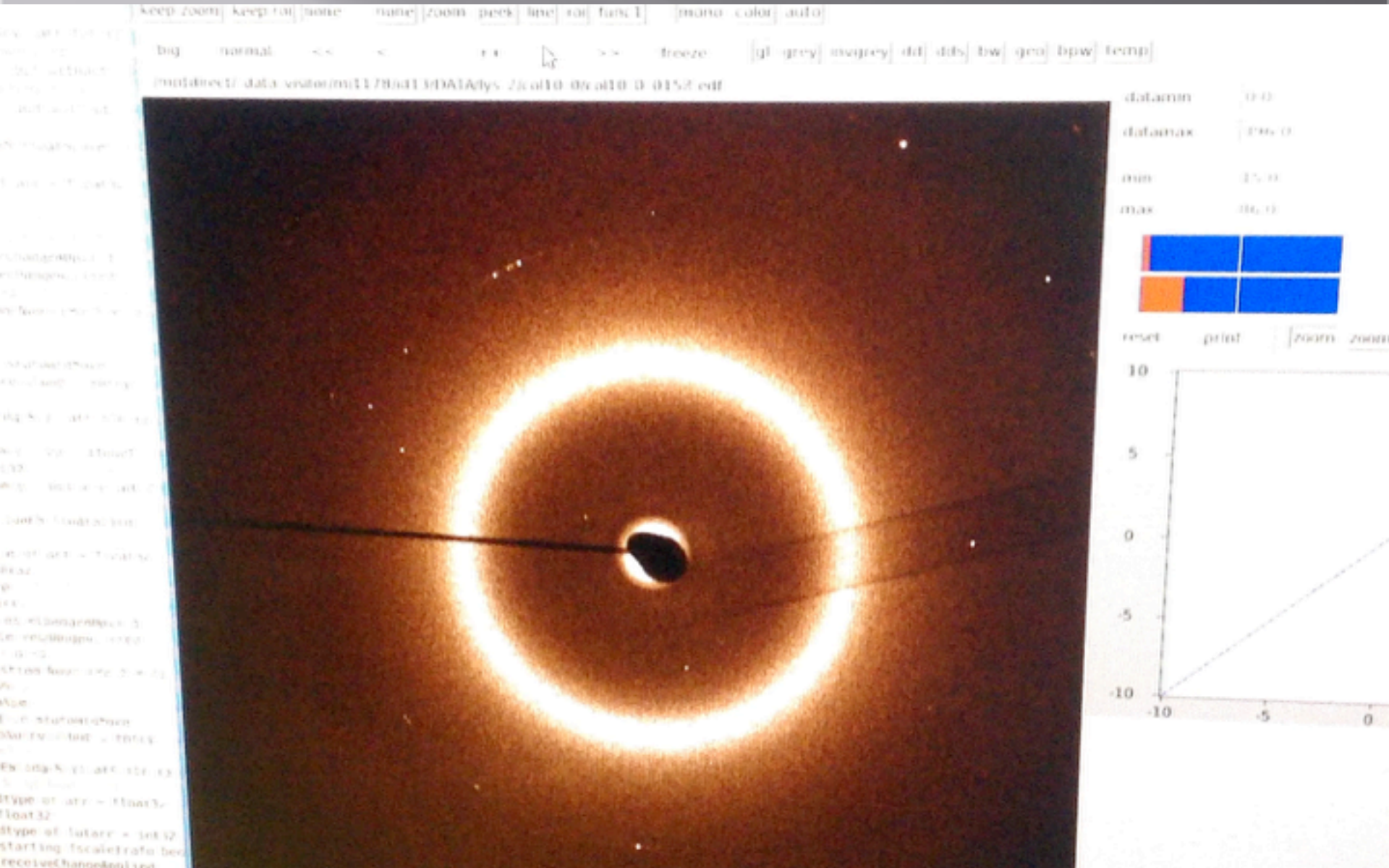

Bacteriorhodopsin structure assembled from single shot diffraction

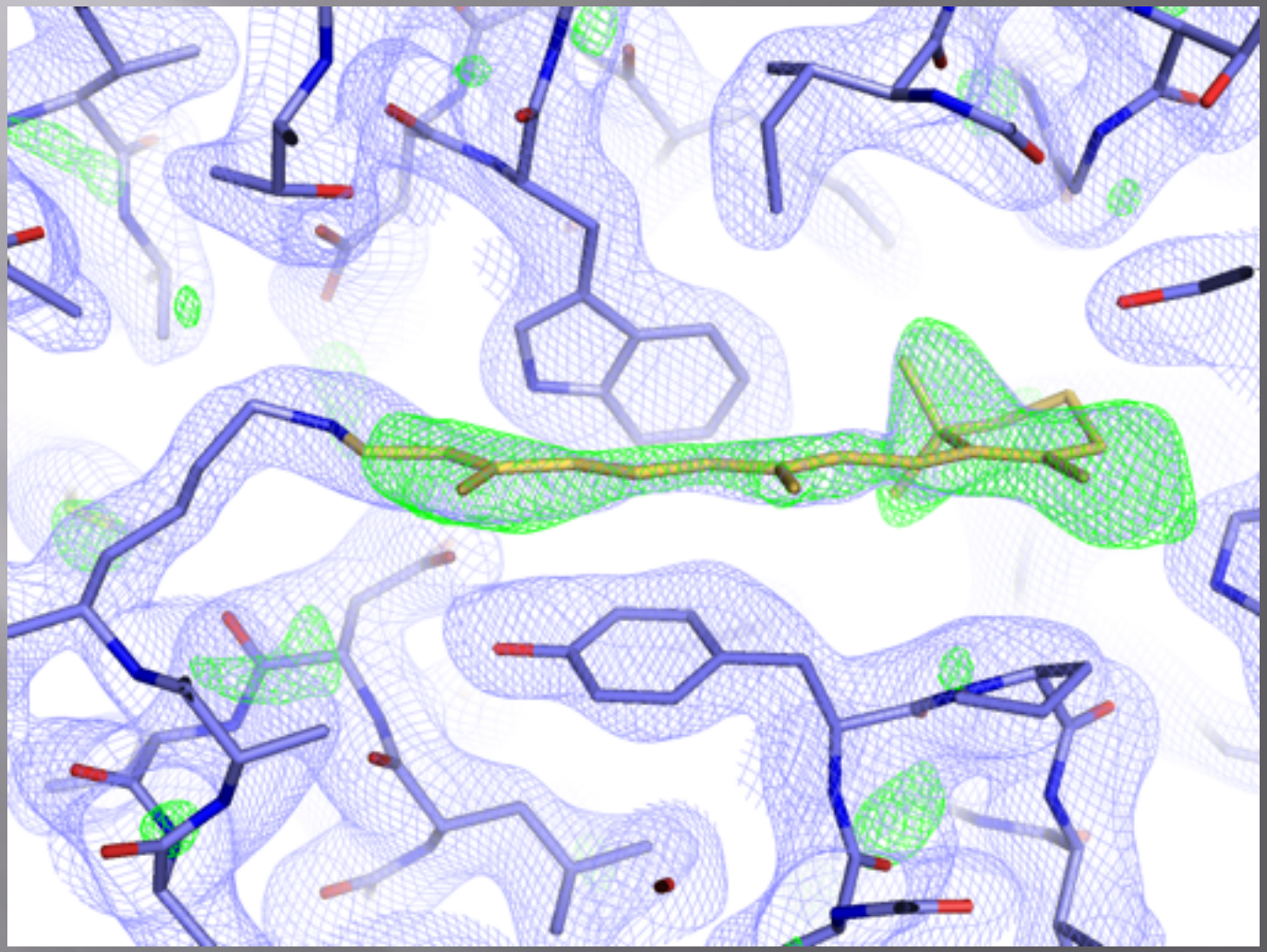

NANOMEM Consortium

Bacteriorhodopsin diffraction in LCP at LCLS Stanford

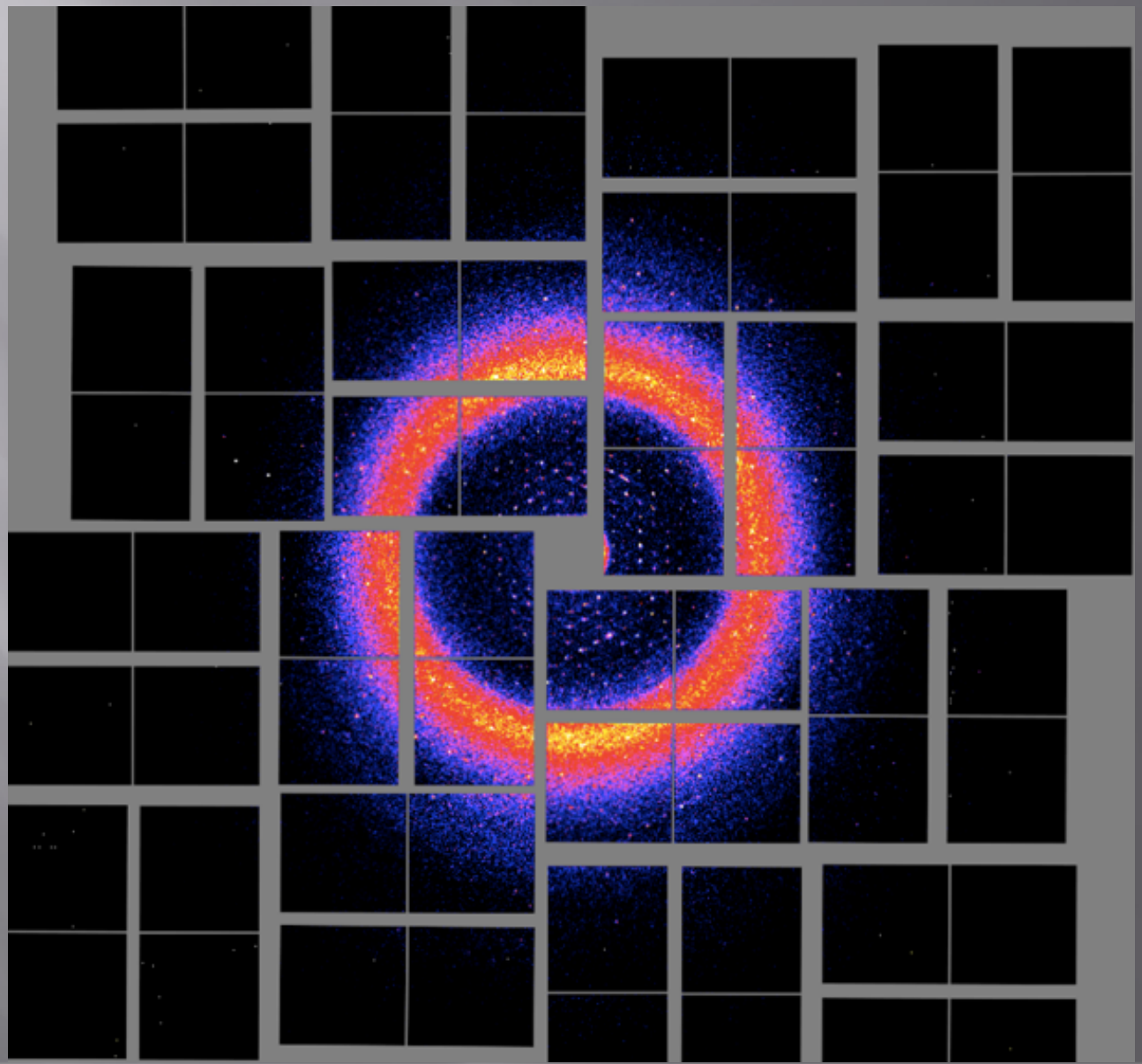

Example for XFEL data collection using a LCP jet

Courtesy of Dianfan Li, Caffrey Lab
Data from LCLS

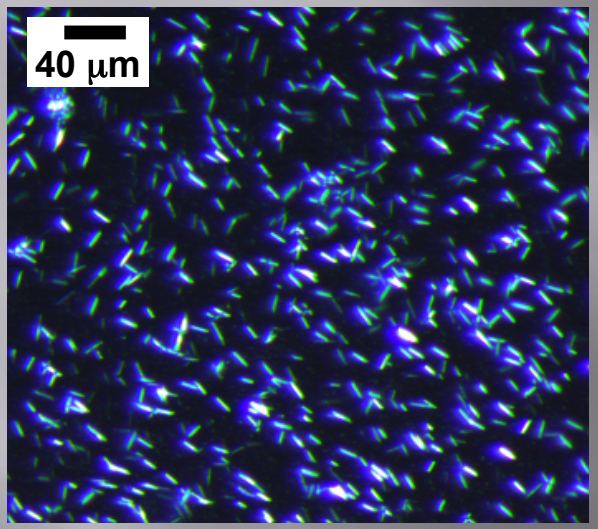

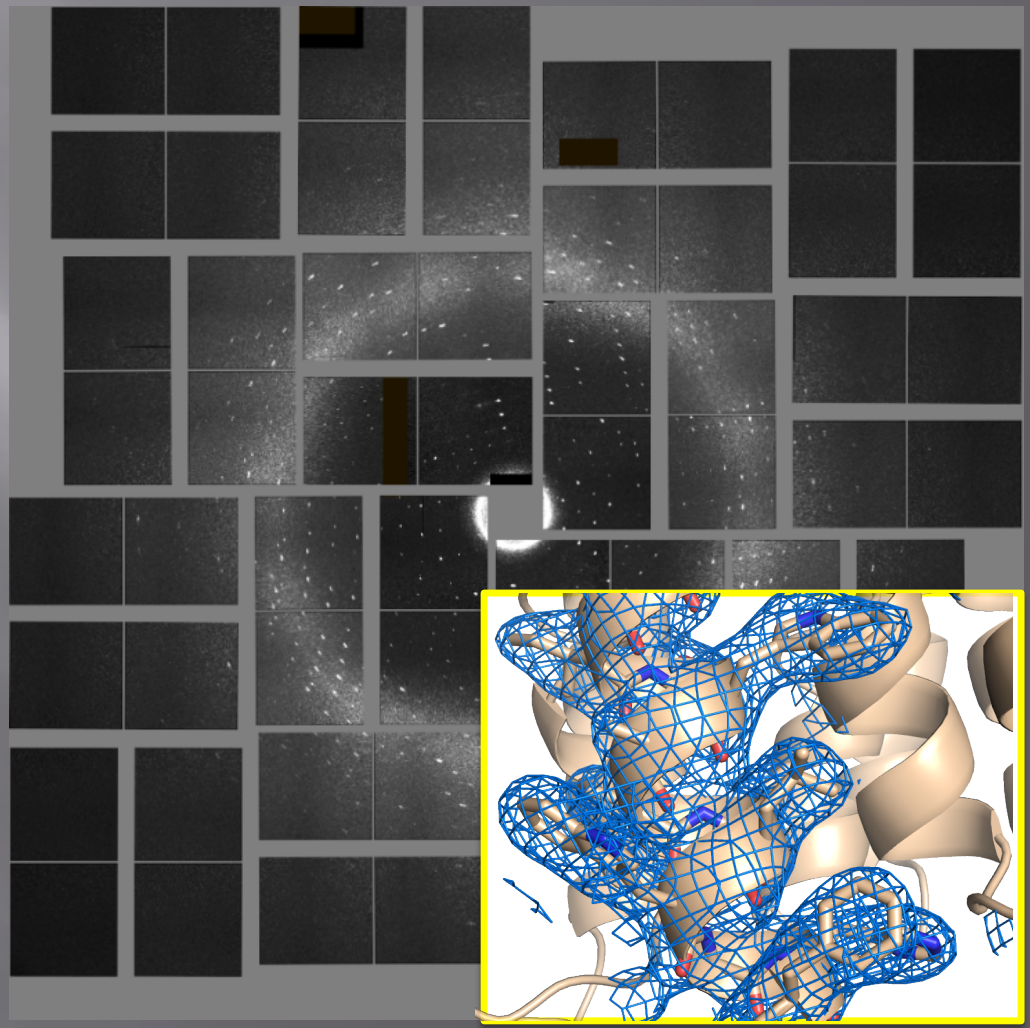

- 0.2 mg protein,
- 14 % hit rate @ 120 Hz
- 2.8 Å resolution
- 1,000 x data redundancy

Femtosecond photo isomerization in Rhodopsin crystals

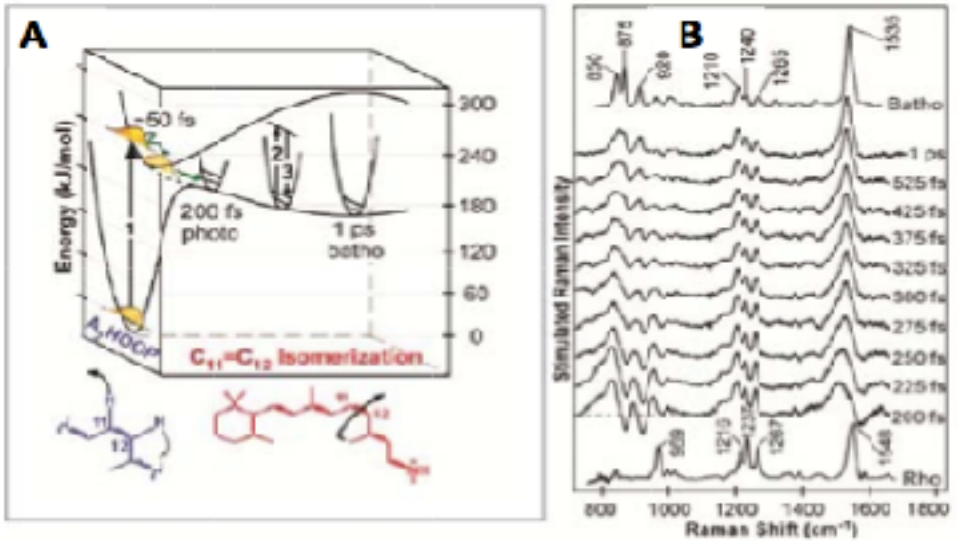

Fig.1. Femtosecond photoisomerisation of retinal during the first event of vision. **A.** Multidimensional representation of the isomerization coordinate of retinal analyzed by coherent Raman vibrational spectroscopy[17]. The cis-retinal photo-rhodopsin and the all-trans retinal bathorhodopsin states are reached after 200fs and 1ps, respectively. **B.** Time-resolved femtosecond stimulated Raman spectra of rhodopsin[17] in the ground-state (Rho) and in the trapped bathorhodopsin (Batho) state.

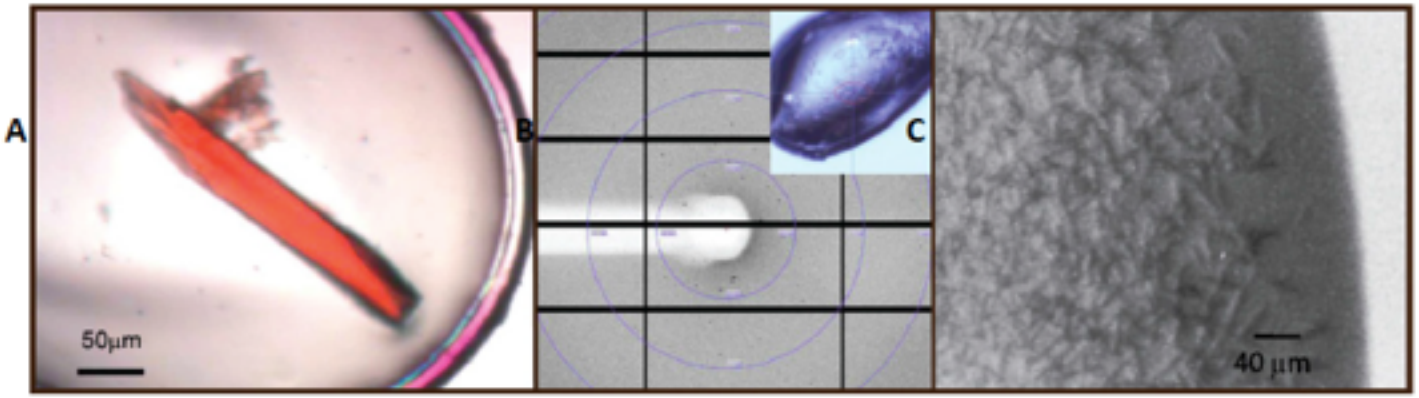

X-ray Free Electron Laser Pump probe experiment

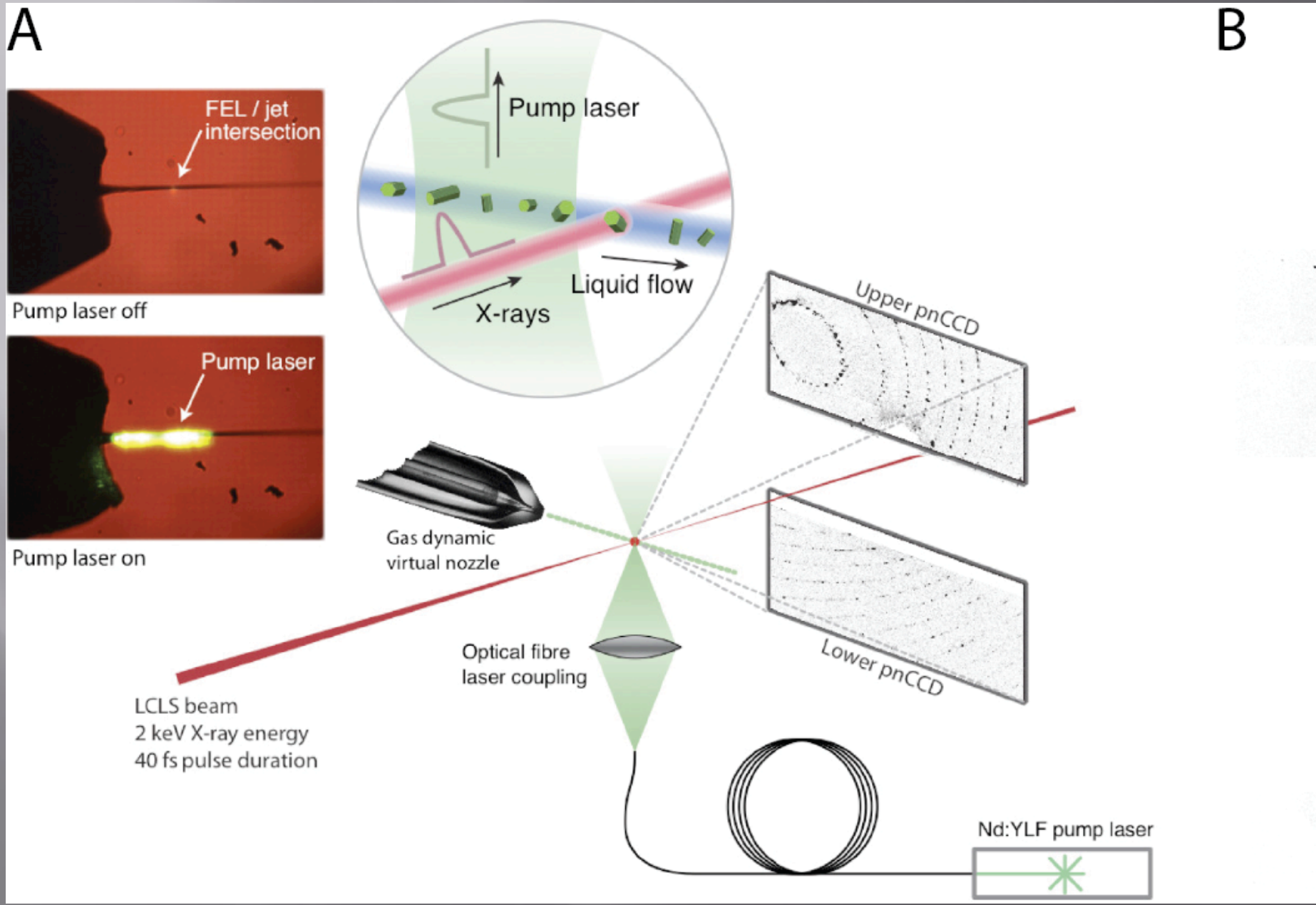

The catalytic step in vision

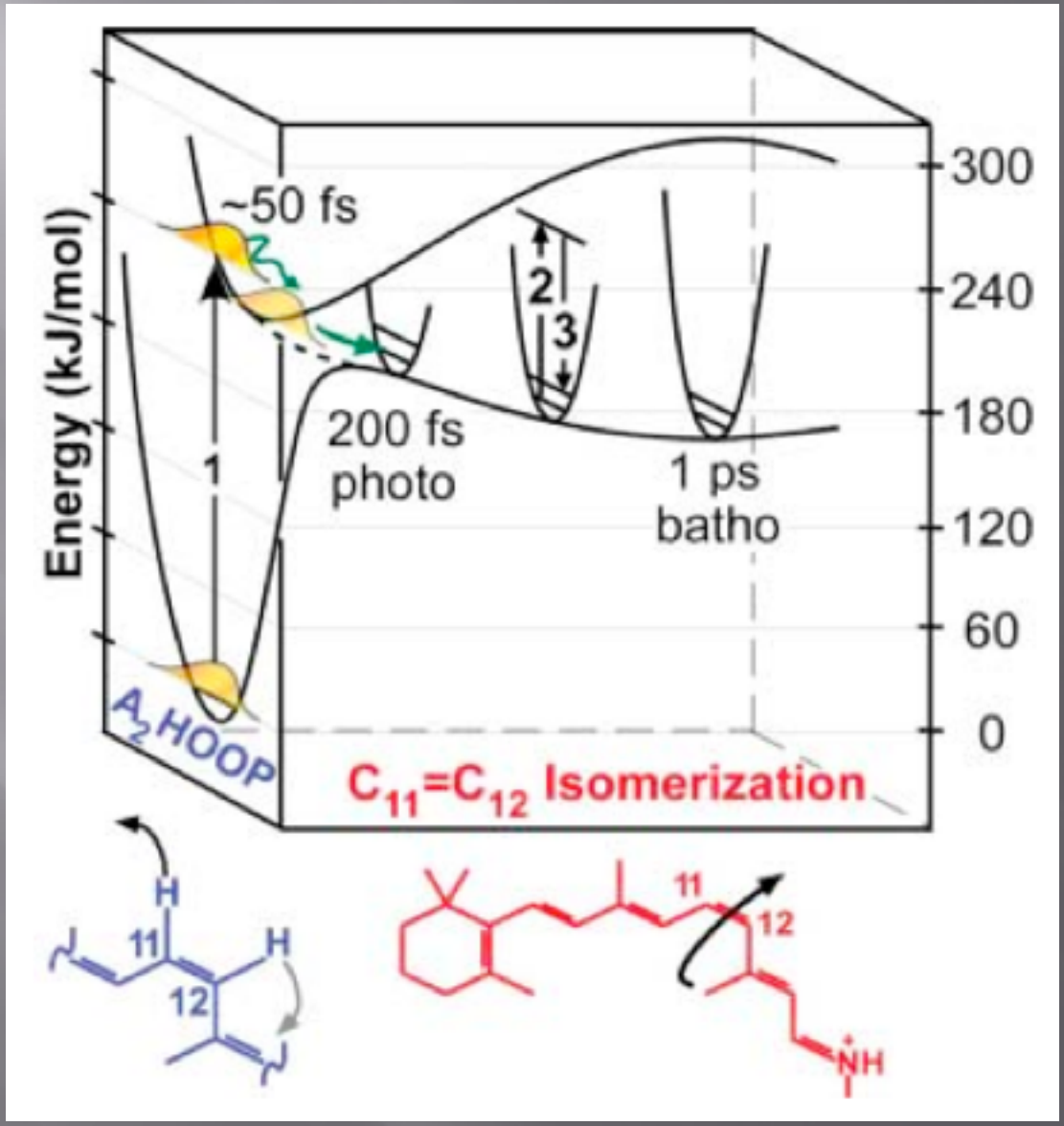

The Future of Structural Biology

Micro and nano- diffraction with micro focus beam lines will stay important

Dynamic of biological structures is essential

X-ray Free Electron Lasers will change the way we work also on synchrotrons

Joerg Standfuss
Project leader

Daniel Mattle
Postdoctoral researcher

Przemek Nogly
Postdoctoral researcher

Martin Ostermaier
Ph.D. student

Xavier Deupi
Project leader

Chayne Piscitelli
Postdoctoral researcher

Milos Matkovic
Ph.D. student

Ankita Singhal
Ph.D. student

Christian Peterhans
Ph.D. student

Kathrin Jaeger
Ph.D. student

Prof. Gebhard F.X. Schertler
Group Leader

Dr. Valerie Panneels
Lab Manager

Jan Rheinberger
Ph.D. Student

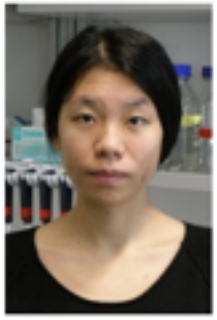

Wenging Wu
Ph.D. Student

Guido Capitani
Project Leader

Dr. Ching-Ju Tsai
Research scientist

Dr. Xiaodan Li
Project Leader

Part of the LB 32 Team at LCLS CXI

Richar Neutze and the part of the measuring team
from PSI, Arrizona, and Hamburg and Goeteborg

Dark Complications

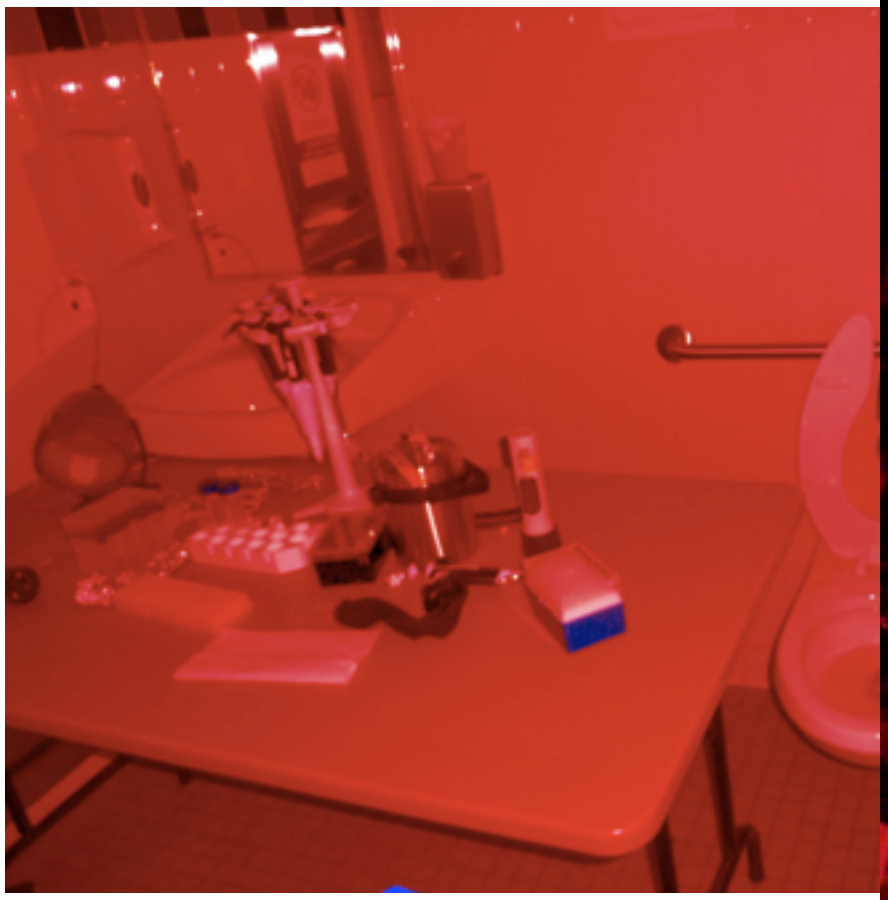

Pluming Experince: in dim red light

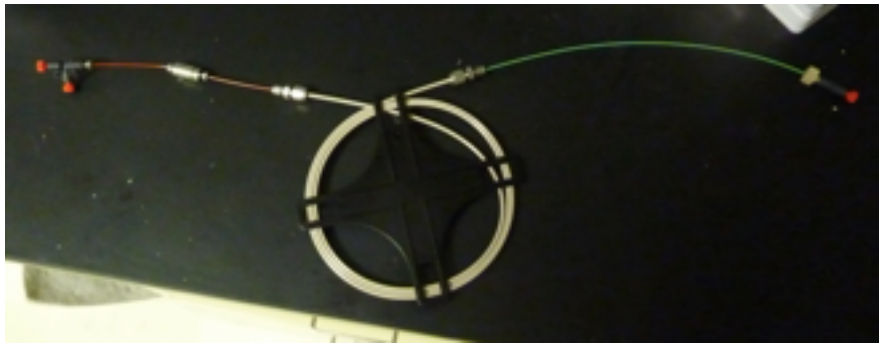

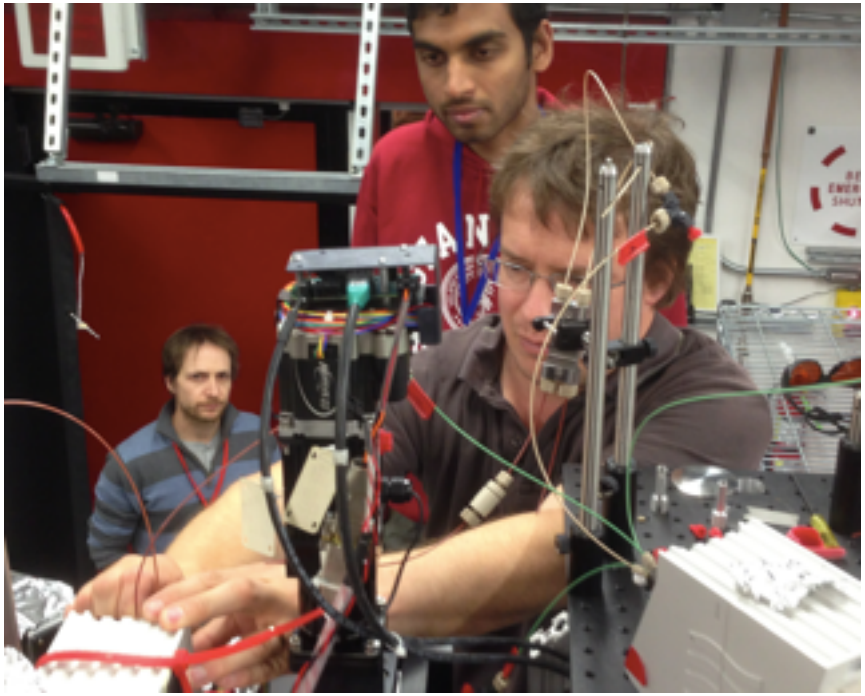

Jet Control: Flying a Jet at 10m / sec

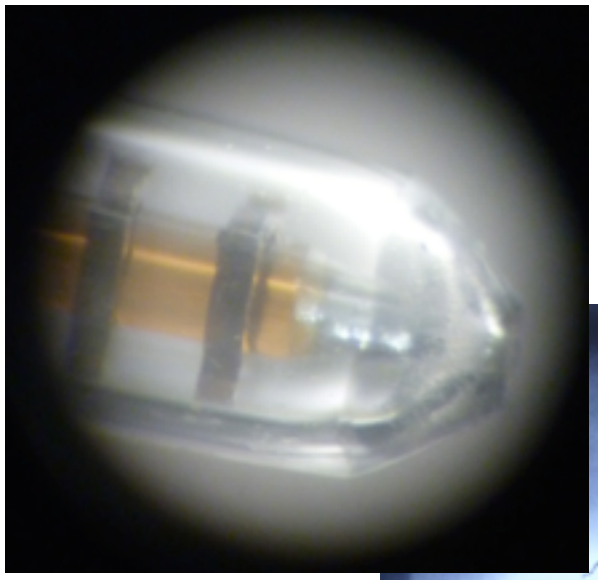

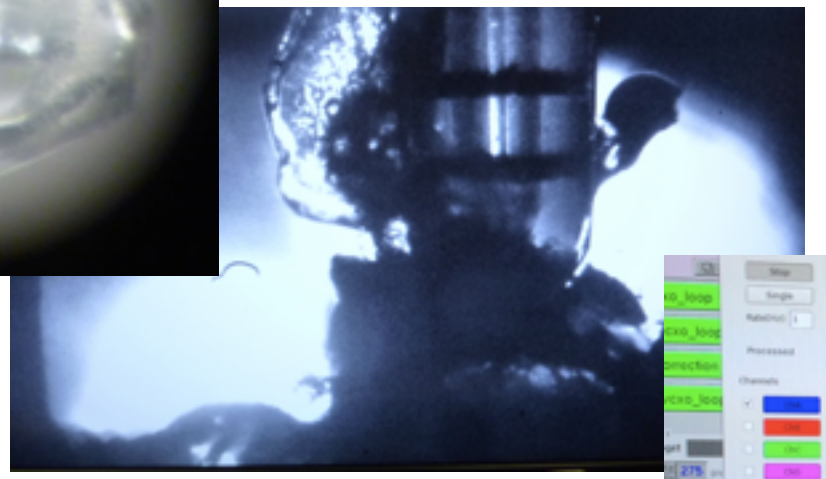

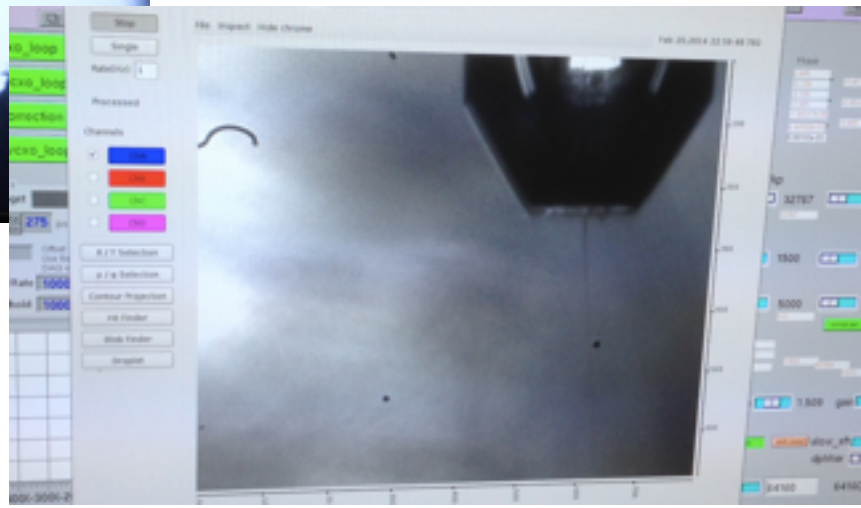

Laser alignment and timing tool

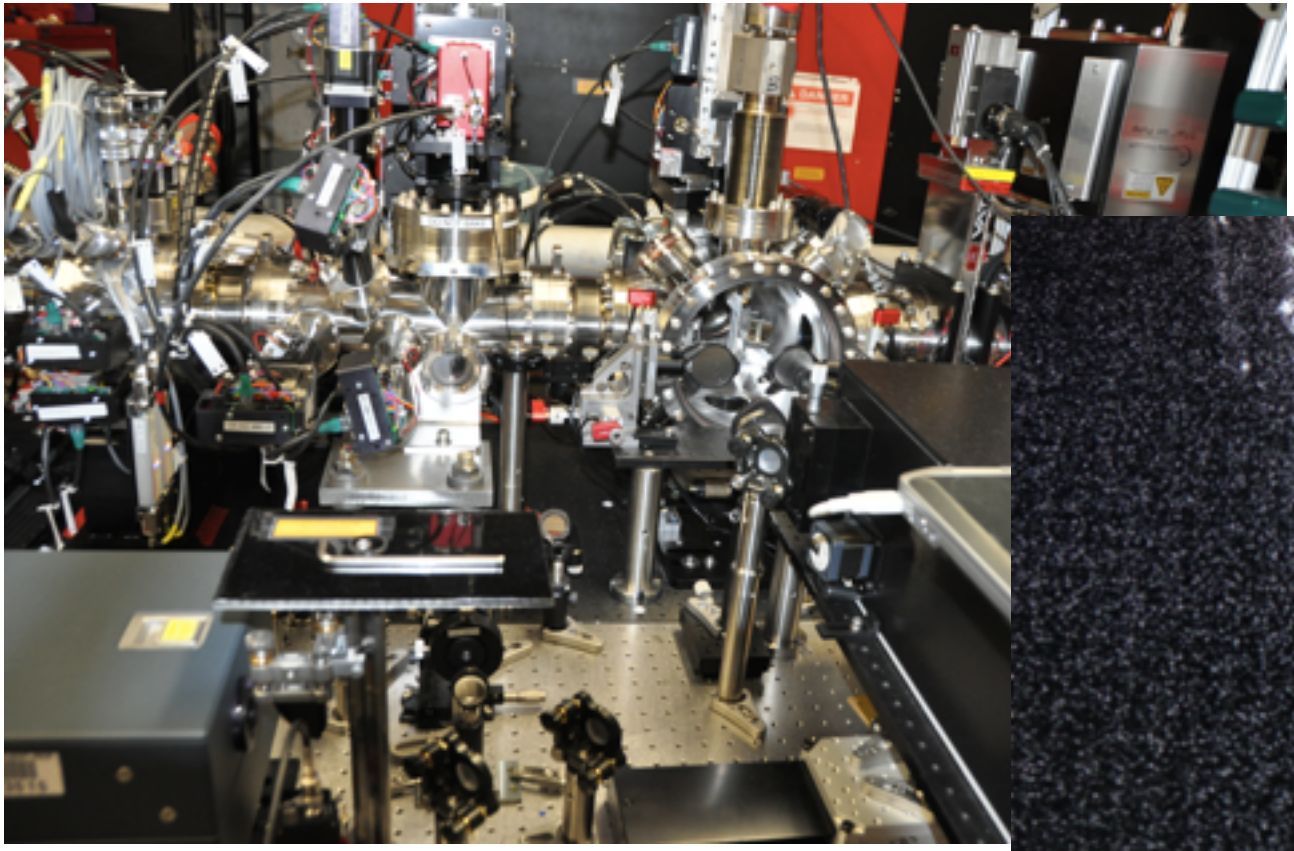

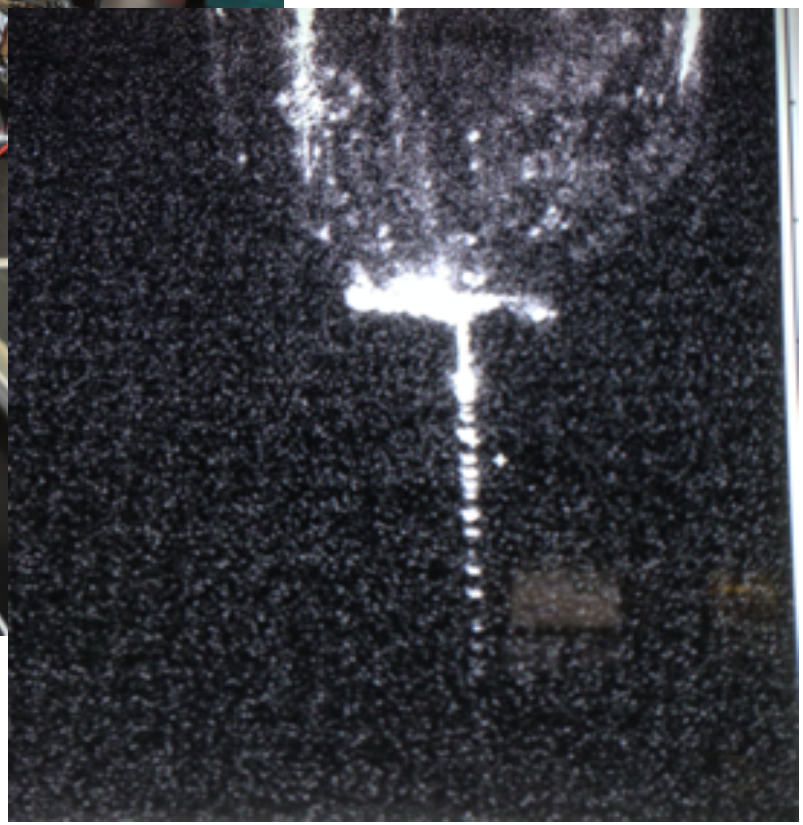

g nice signals measurments going

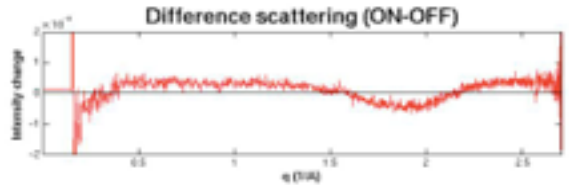

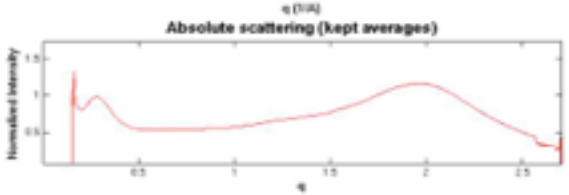

Run number: r0216
Run length: 291/112 sec
Time delay: 1e-06 sec
Laser intensity: 22 uJ
Normalization range: 2.1-2.2
Dark kept: 30.03%
Light kept: 30.03%
Intensity capped: 29.35%

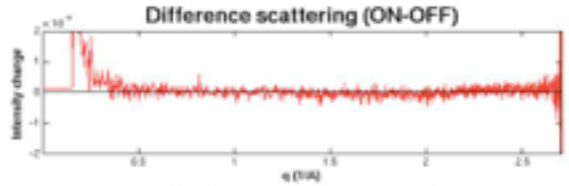

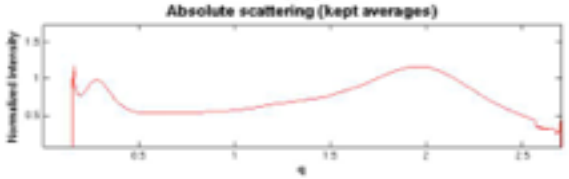

Run number: r0219
Run length: 146/75 sec
Time delay: -5e-12 sec
Laser intensity: 22 uJ
Normalization range: 2.1-2.2
Dark kept: 35.23%
Light kept: 35.23%
Intensity capped: 12.65%

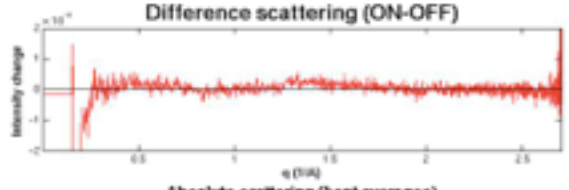

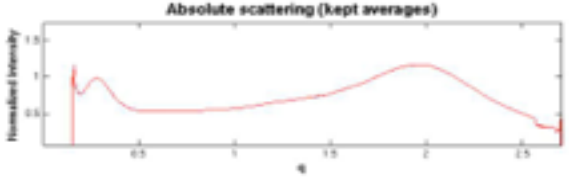

Run number: r0218
Run length: 162/66 sec
Time delay: 2e-11 sec
Laser intensity: 22 uJ
Normalization range: 2.1-2.2
Dark kept: 28.1%
Light kept: 28.1%
Intensity capped: 23.2%

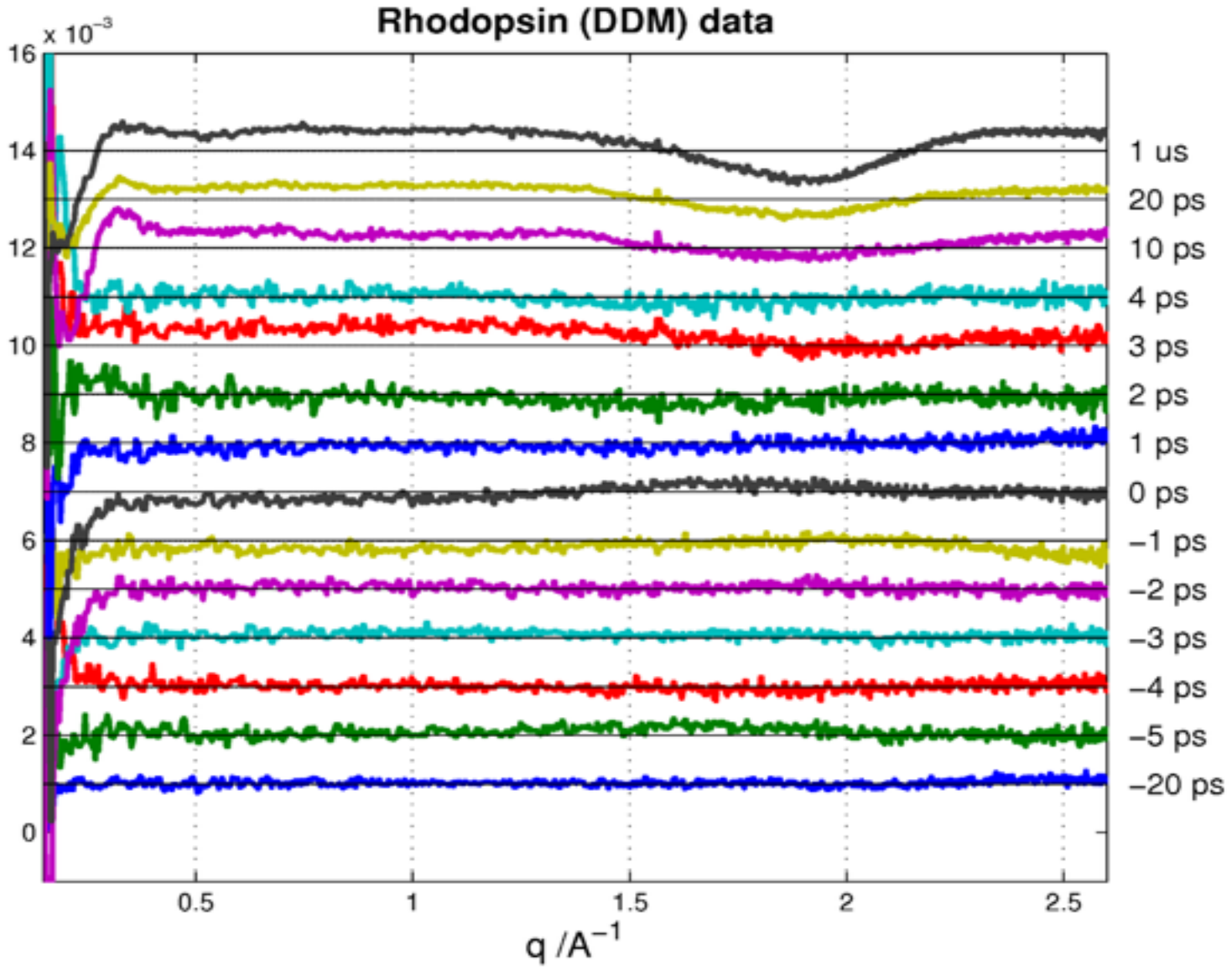

-20ps, 10ps, 20ps and 1us consists of three merged curves, illustrating the improvement one gets to the signal to noise ratio with redundancy in data on same timepoint

Delay line for x-ray pump-probe experiments

Conventional pump-probe experiments are limited to *reversible processes* as only one delay can be probed at a time.

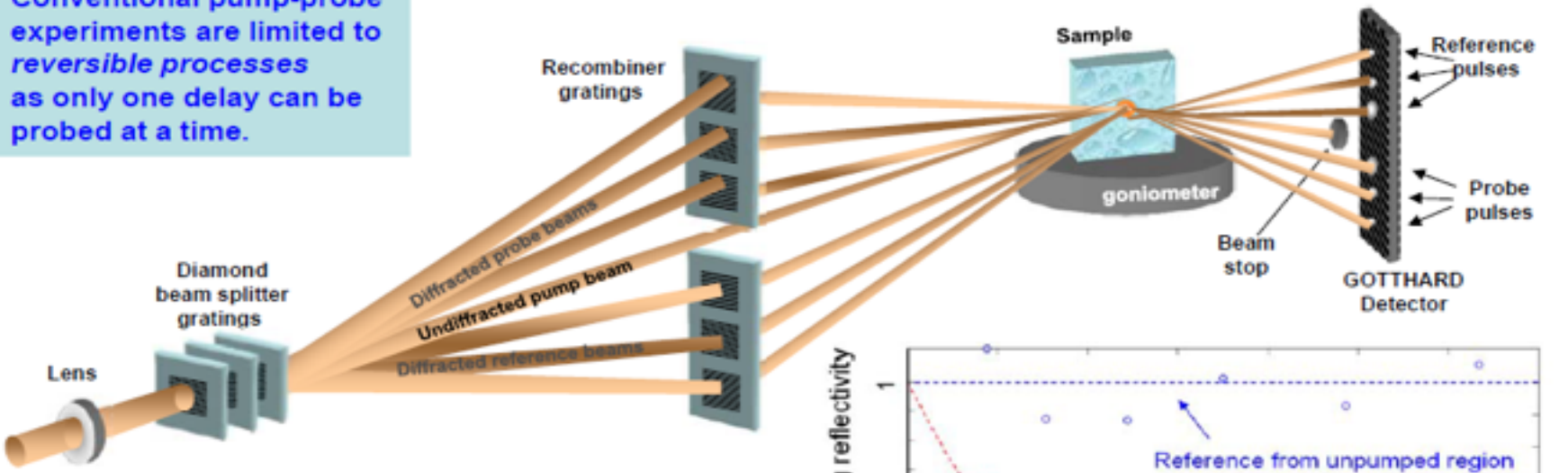

A novel x-ray delay line based on diffraction gratings creates *several probe beams* with different delays.

Allows for observation of *irreversible processes* with femtosecond resolution.

First *„single-pump multi-probe"* measurements demonstrated at LCLS.

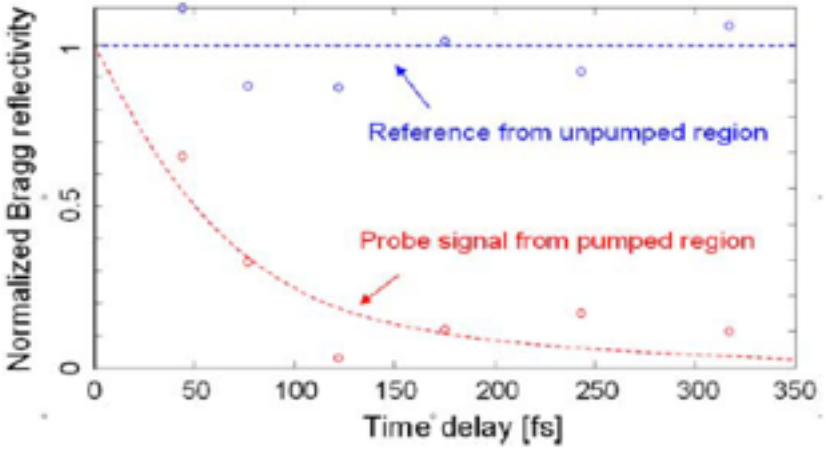

Bi <111> Bragg reflectivity measured with XFEL radiation at 4.5 keV photon energy .

Ch. David et. al.

Thank you for your attention!!

SwissFEL fein **und** schnell
bei extrem hoher Intensität

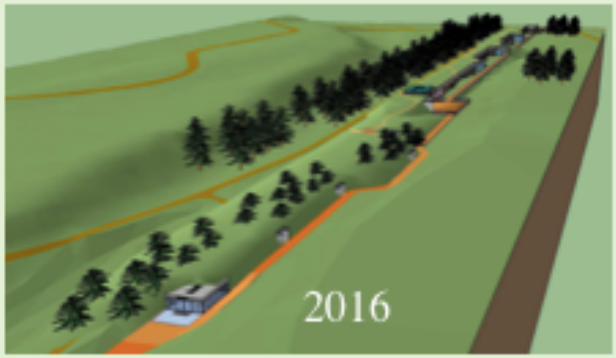

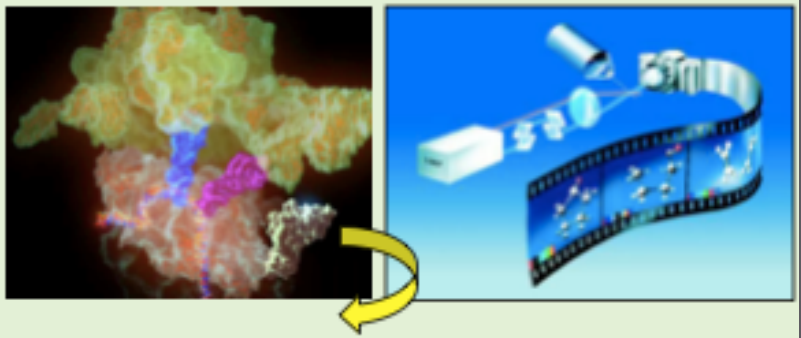

neue, direkte Einblicke in physikalische, chemische und biologische Prozesse unseres Alltags

ein Freier-Elektronen-Röntgen-Laser für die Schweiz